

# Weak Lensing

Yannick Mellier

IAP and Obs. de Paris / LERMA

## II. Cosmic Shear

# The Universe in one slide

## (for those who are not familiar with cosmology)

- Looks homogeneous and isotropic on very large scales (cosmological principle)
- Is flat (almost null curvature)
- Is expanding, with accelerating expansion
- Is composed of 70% of (unknown) dark energy, 25% of (unknown) dark matter, and 4% of ordinary (baryonic) matter
- Its present-day structuration results from gravitational instability
- The growth rate of structure depends on both its dark matter and dark energy content
- Its cosmic history is visible through its matter distribution: the dark matter power spectrum
- The evolution of the dark matter power spectrum can be recovered from observation of the high redshift universe (i.e. look-back time)
- Cosmologists characterise the universe by a series of cosmological parameters:
  - $H_0$  = expansion (Hubble constant)
  - $\Omega_m$  = amount of matter
  - $\Omega_X$  = amount of dark energy (could be a cosmological constant  $\Lambda$ )
  - $w$  = property of dark energy  $P=w\rho$  (i.e. equation of state of dark energy)
  - $\sigma_8$  = normalisation of the dark matter power spectrum; initial  $P(k) = \sigma_8 k^n$  (but  $P(k)$  changes with time;  $n$  is the spectral index)

# Look-back time (redshift)

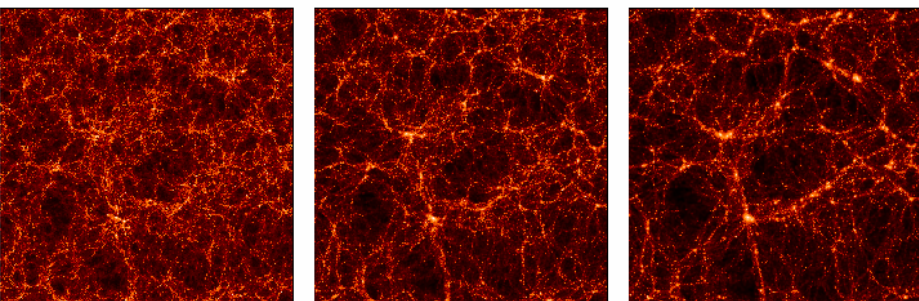
$H_0 = 70$

$\Omega_m = 0.3, \Omega_\chi = 0.7$

$\Lambda\text{CDM}$

$W = -1 (\Lambda),$

$\sigma_8 = 0.9$

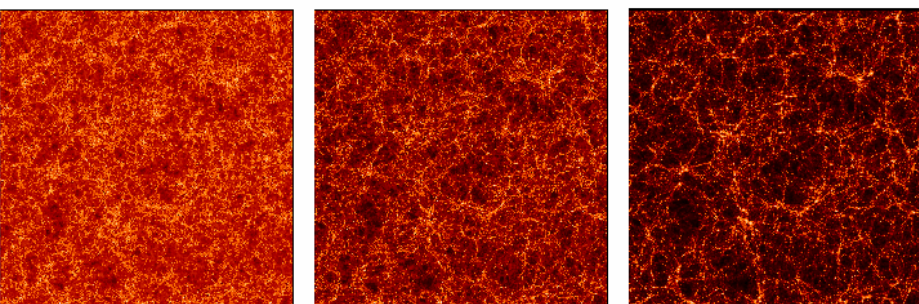


$H_0 = 50$

$\Omega_m = 1.0, \Omega_\chi = 0.0$

$\text{SCDM}$

$\sigma_8 = 0.51$

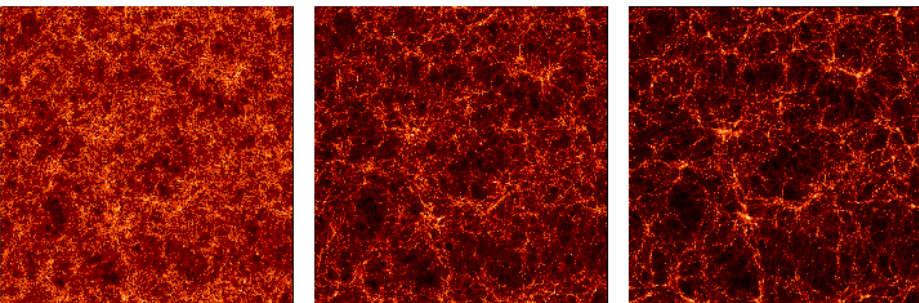


$H_0 = 70$

$\Omega_m = 1.0, \Omega_\chi = 0.0$

$\tau\text{CDM}$

$\sigma_8 = 0.51$



$H_0 = 70$

$\Omega_m = 0.3, \Omega_\chi = 0.7$

$\text{OCDM}$

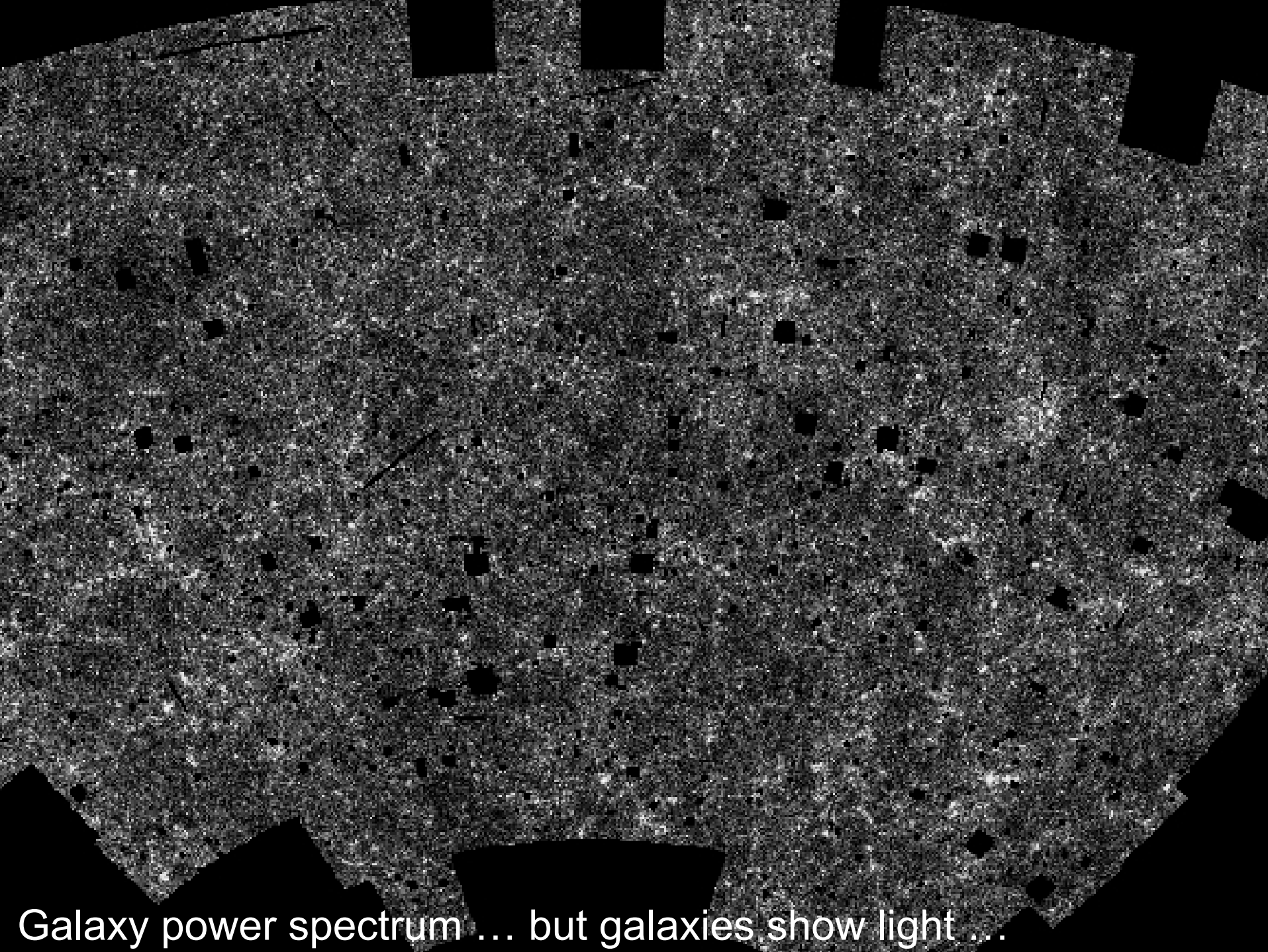
$\sigma_8 = 0.85$

Structure formation  
as function of the  
dark matter and dark  
energy content



Dark energy and dark  
matter are revealed by  
the properties of the  
dark matter power  
spectrum

# How can we observe the dark matter power spectrum ?



Galaxy power spectrum ... but galaxies show light ...

# Using gravitational lensing to observe the dark matter power spectrum

# Structure Formation Theory

# Structure Formation Theory

## Overview

- Very small perturbations are assumed to exist at high redshift (whatever their origin)
- Perturbations then grow from gravity (gravitational instability)
- The growth of perturbation will be modified by other physical effects : free streaming, pressure
- Because of pressure and free streaming,
  - . baryonic and non-baryonic matter grow differently
  - . Hot, warm and cold dark matter grow differently
- All components have their own equations, but they are coupled

# Structure Formation

## Fluid equations

Continuity equation

$$\frac{\partial \rho(\vec{r}; t)}{\partial t} + \nabla_r \cdot [\rho \vec{u}(\vec{r}; t)] = 0 \quad (1)$$

Euler equation

$$\frac{\partial \vec{u}}{\partial t} + (\vec{u} \cdot \nabla_r) \vec{u} = -\nabla_r \varphi \quad (2)$$

Poisson equation

$$\nabla_r^2 \varphi = 4\pi G \rho - \Lambda \quad (3)$$

# Structure Formation in comoving coordinates

Euler equation becomes

$$\frac{\partial \vec{v}}{\partial t} + \frac{\dot{a}}{a} \vec{v} + \frac{1}{a} (\vec{v} \cdot \nabla_x) \vec{v} = -\frac{1}{a} \nabla_x \Phi \quad (1)$$

Defining the density contrast:

$$\delta(\vec{x}; t) = \frac{\rho(\vec{x}; t) - \bar{\rho}(t)}{\bar{\rho}(t)}$$

Continuity  $\rightarrow$  
$$\frac{\partial \delta}{\partial t} + \frac{1}{a} \nabla_x \cdot [(1 + \delta) \vec{v}] = 0 \quad (4)$$

And the Poisson equation writes:

$$\nabla_x^2 \Phi = \frac{3H_0^2}{2a} \Omega_m \delta \quad (5)$$

# Structure Formation

## Linear perturbation equations

If we only consider terms linear in  $v$  and  $\delta$

$$\frac{\partial \delta}{\partial t} + \frac{1}{a} \nabla_x \cdot \vec{v} = 0 \quad (3)$$

$$\frac{\partial \vec{v}}{\partial t} + \frac{\dot{a}}{a} \vec{v} = -\frac{1}{a} \nabla_x \Phi \quad (4)$$

# Structure Formation

## Linear perturbation equations

Fourier decomposition

$$\delta(\vec{x}; t) = \int \frac{d^3 k}{(2\pi)^2} \tilde{\delta}(\vec{k}; t) e^{i\vec{k}\cdot\vec{x}} \quad (1)$$

$$\rightarrow \boxed{\frac{\partial^2 \delta}{\partial t^2} + \frac{2\dot{a}}{a} \frac{\partial \delta}{\partial t} - \frac{3H_0^2}{2a^3} \Omega_m \delta = 0} \quad (2)$$

Usually written as

$$\ddot{D} + \frac{2\dot{a}}{a} \dot{D} = \frac{3H_0^2}{2a^3} \Omega_m D \quad (3)$$

The growing modes,  $D_+$ , imply that  $\delta$  grow as

$$\delta(\vec{x}; t) = D_+(t) \delta_0(\vec{x}) \quad (4)$$

and it can be shown that

$$D_+(t) = D_{in} H(a) \int_0^a \frac{da'}{[a' H(a')]^3} \quad (5)$$

where  $D_{in}$  is such that  $D_+(t_0) = D_+(a=1) = 1$ .

$D_+$  is called the growth factor

# Structure Formation

## Including pressure perturbation

$$\frac{\partial \vec{U}}{\partial t} + 2\frac{\dot{a}}{a}\vec{U} = -\frac{1}{a^2}\nabla_x \Phi - \frac{\nabla \delta p}{\bar{\rho}} \quad (1)$$

Using the same equations as before and Fourier-transform them lead to

$$\ddot{\delta} + 2\frac{\dot{a}}{a}\dot{\delta} = \left(4\pi G\bar{\rho} - c_s^2 \frac{k^2}{a^2}\right) \delta \quad (2)$$

where

$$c_s = \left(\frac{\partial p}{\partial \rho}\right)^{1/2} \quad (3)$$

The behavior of perturbations depends on the scale  $k$ :

- for small  $k$ , perturbation grow
- for large  $k$ , perturbations oscillate

# Summary: Linear Structure Growth

---

- Relation to horizon scale

- Comoving horizon size:

$$d_H = \frac{c}{H_0} \Omega_m^{-1/2} a^{1/2} \left(1 + \frac{a_{eq}}{a}\right)^{-1/2} \quad (266)$$

- If perturbation enters the horizon during the radiation dominated (R) period then:

The expansion timescale  $\sim (G\rho_R)^{-1/2}$  < collapse time scale  
 $\sim (G\rho_{DM})^{-1/2}$

→ Radiation prevents growth of perturbation

# Summary: Linear Structure Growth

---

- Relation to horizon scale

- Comoving horizon size:

$$d_H = \frac{c}{H_0} \Omega_m^{-1/2} a^{1/2} \left(1 + \frac{a_{eq}}{a}\right)^{-1/2}$$

- If  $\lambda = 2\pi/k \gg d_H$  then

- \*  $\delta \propto a^2$  if  $a \ll a_{eq}$

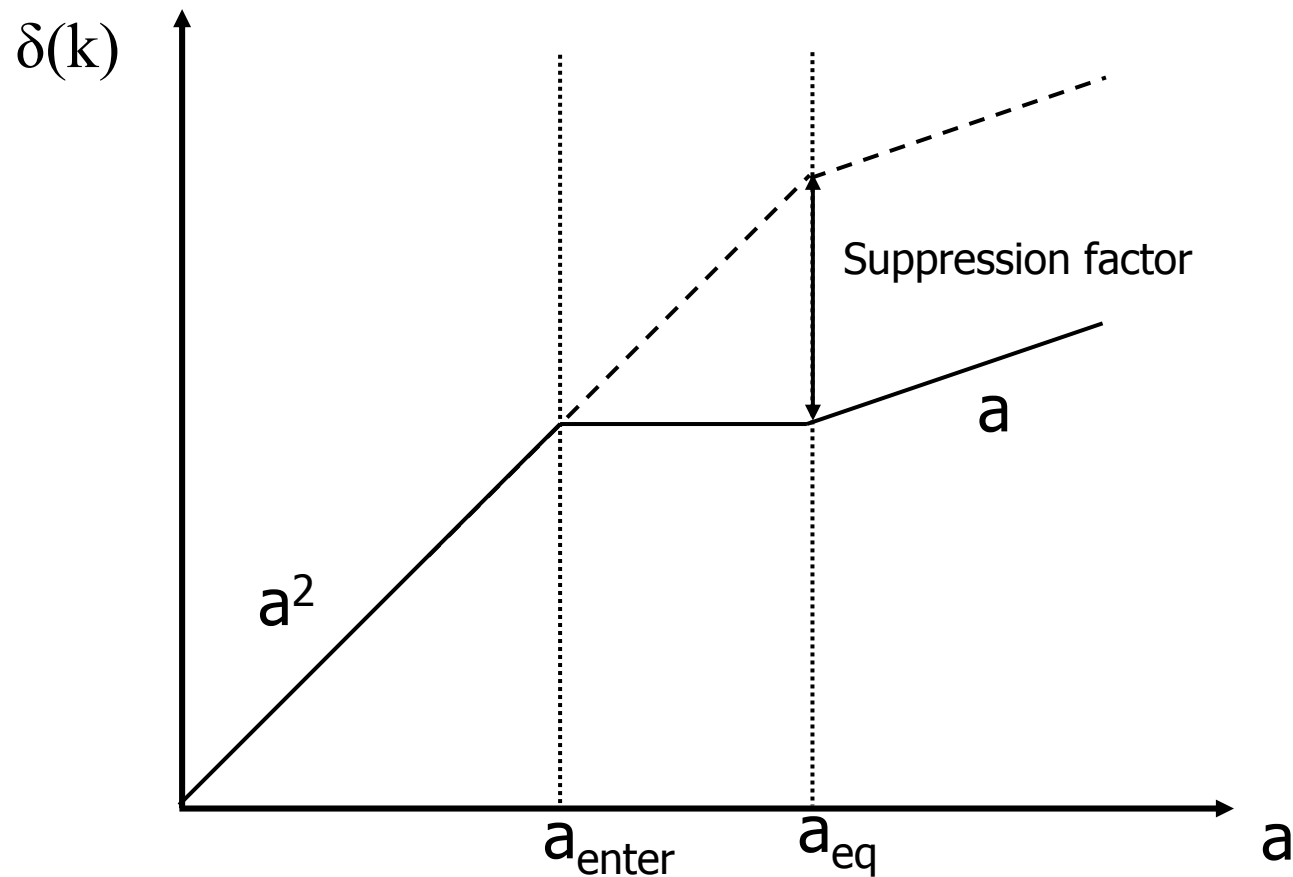
- \*  $\delta \propto a$  if  $a \gg a_{eq}$

- If  $\lambda = 2\pi/k \ll d_H$  then

- \* no growth if  $a \ll a_{eq}$

- \*  $\delta \propto a$  if  $a \gg a_{eq}$

# Summary: Linear Structure Growth



# The Transfer Function

---

In the linear regime, for sub-horizon matter-dominated universe, we have

$$\delta_k(z) = D_+(z) \delta_k(z=0)$$

The transfer function is a way to account for deviation from the simple linear evolution.

$$T_k = \frac{D_+(z) \delta_k(z=0)}{\delta_k(z)}$$

Since at  $z \gg 1$ , almost no scale of interest entered the horizon yet, in absence of any alteration,  $T_k = 1$  at all  $z$

However pressure and free streaming produce modifications. They are modeled using fitting formula:

- For a CDM model:

$$T_k = \frac{\ln(1 + 2.34q)}{2.34q} [1 + 3.89q + (16.1q)^2 + (5.46q)^3 + (6.71q)^4]^{-1/4}$$

- For a HDM model

$$T_k = \exp(-3.9q - 2.1q^2)$$

where

$$q = \frac{k}{\Omega_m h^2 \text{Mpc}^{-1}} = \frac{k / (h \text{ Mpc}^{-1})}{\Gamma}$$

and

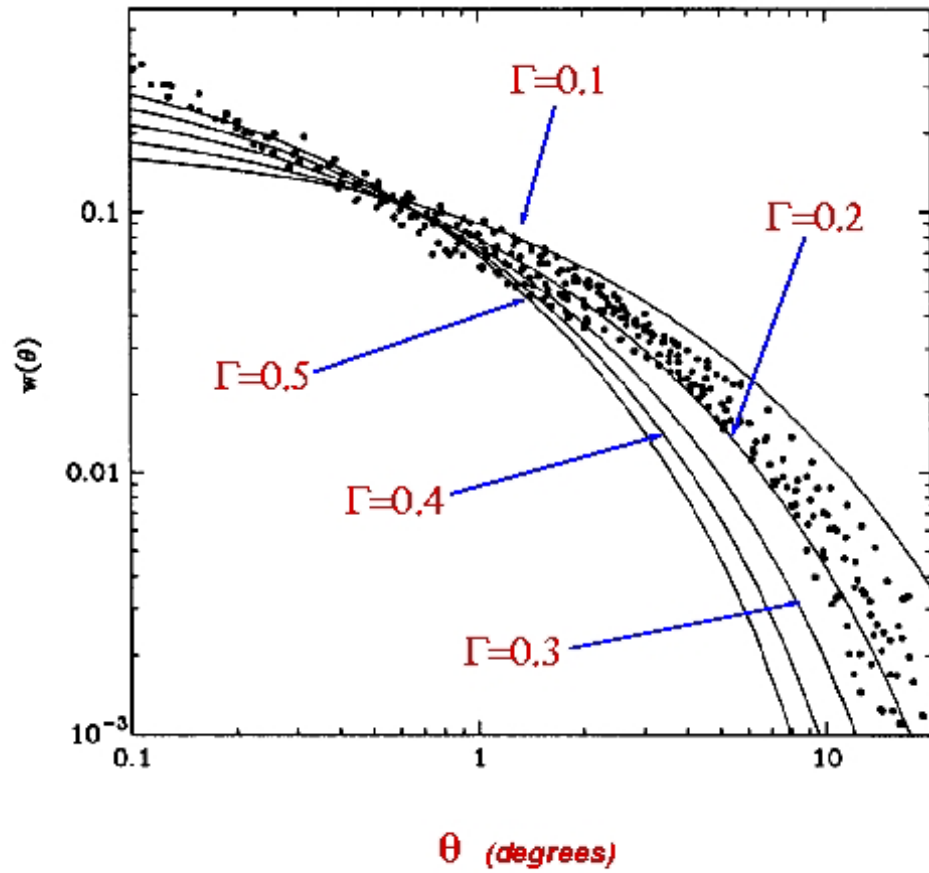
$$\Gamma = \Omega_m h$$

is the *shape parameter*

It seems  $\Gamma \simeq 0.2$

Note that for a CDM  $T_k \propto k^{-2}$  for large  $k$ ; while for a HDM  $T_k$  decreases exponentially with  $k$ .

# Structure Formation



Shape  
parameter

# The Power Spectrum

The power spectrum of the density fluctuation,  $P_\delta$ , is defined as

$$\langle \delta_{\vec{k}} \delta_{\vec{k}}^* \rangle = (2\pi)^3 \delta_D(\vec{k} - \vec{k}') P_\delta(k)$$

The power spectrum at any time,  $P_\delta(k, z)$  can be derived from the initial power spectrum  $P(k) = P_i(k, z_i)$  using the transfer function

$$P_\delta(k, z) = P_i(k) \frac{D_+^2(z)}{D_+^2(z_i)} T_k^2$$

# The Power Spectrum

---

For a simple power law,  $P_i(k) \propto k^n$ , with  $n = 1$  the asymptotic behavior of the power spectrum is

$$P_\delta(k) \propto k \text{ for small } k$$

$$P_\delta(k) \propto k^{-3} \text{ for large } k$$

- The steep decrease at large  $k$  is due to the suppression of small scale perturbations which entered the horizon before matter-radiation equality.
- The turn over depends on  $d_h(a_{eq})$ . It is the most characteristic scale in the dark matter power spectrum

# The Power Spectrum... in Summary

---

In summary the power spectrum

- is determined with the spectral index,  $n$ , and
- the shape parameter,  $\Gamma$ .
- But the normalisation is missing...
- The non-linear evolution is not described (numerical simulation, relation between the linearly evolved power spectrum to the fully non linear power spectrum, use halo models..)

# Structure Formation

Normalisation of the power spectrum

3 ways of measuring it:

- Normalisation from CMB anisotropy on large scale

Degree of anisotropy=fluctuation spectrum:  
direct measure of normalisation

- Density fluctuation inside a sphere

- Local abundance of clusters of galaxies

# Structure Formation

## Normalisation of the power spectrum

The observed variance of galaxy counts in a sphere of 8 Mpc  
Dispersion of the smoothed density field:

$$\sigma^2(R) = \langle \delta_R^2(\vec{x}) \rangle = \int \frac{d^3k}{(2\pi)^3} |\hat{W}_R(k)|^2 P(k)$$

The normalisation of the power spectrum can in principle be measured from observations.

From galaxies. Inside a sphere of radius  $8 h^{-1}$  Mpc, galaxy catalogues show that

$$\frac{\Delta N}{N} = \frac{\langle (N - \langle N \rangle)^2 \rangle}{\langle N \rangle^2} = 1 \quad (3)$$

Dispersion of a smooth density field

$$\sigma^2(R) = \langle \delta_R^2(\vec{x}) \rangle = \int W_R(|\vec{x} - \vec{y}|) \delta(\vec{y}) d^3y \quad (4)$$

If the galaxies follow the dark matter then

$$\sigma_8 = \sigma^2(8h^{-1}\text{Mpc}) = \frac{\Delta N}{N} = 1 \quad (5)$$

# Structure Formation Theory

## Normalisation of the power spectrum

BUT: galaxies may not trace the dark matter very well. However, one can assume that, to first order, there is a simple linear relation between the fluctuation of the number of galaxies and the mass density contrast:

$$\frac{\Delta n}{n} = b \frac{\Delta \rho}{\rho} \quad (1)$$

and  $b$  is the *bias factor*. In that case:

$$\sigma_8 = \frac{1}{b} \quad (2)$$

# Structure Formation

## Normalisation of the power spectrum

A structure with density contrast that reaches  $\sigma_8 = 1$  enters into the non-linear regime. Today, it corresponds to mass such that:

$$M = \frac{4\pi}{3}\bar{\rho} [8 h^{-1} Mpc]^3 \quad (3)$$

$$M = \frac{4\pi}{3}\Omega_m \frac{3H_0^2}{8\pi G} [8 h^{-1} Mpc]^3 \quad (4)$$

that is

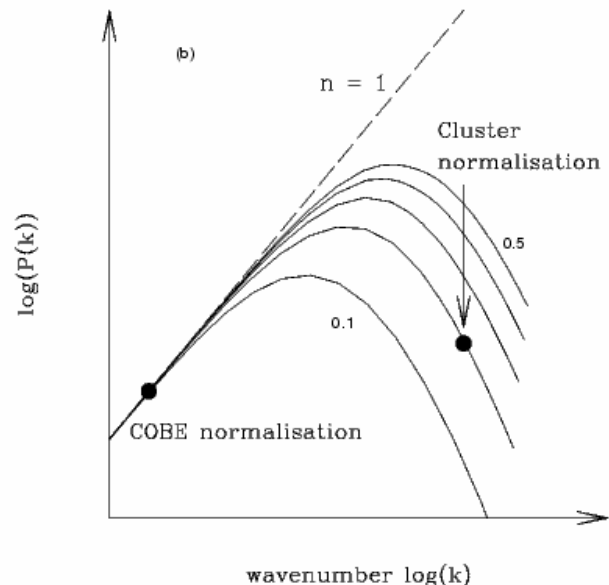
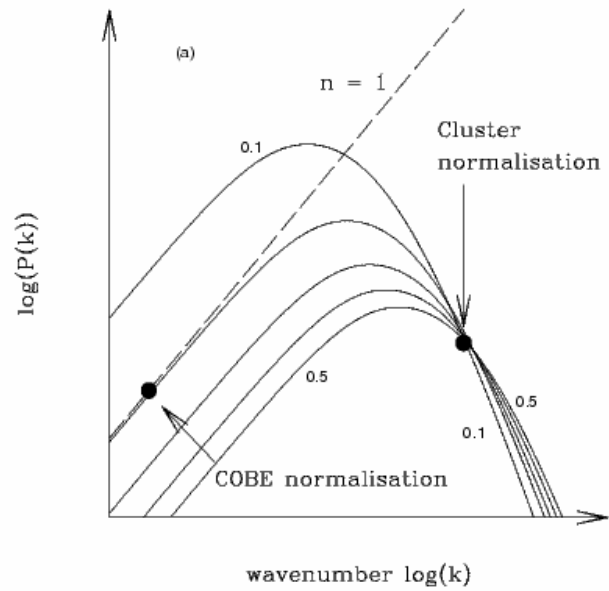
$$M = 5 \times 10^{14} \Omega_m h^{-1} M_\odot \quad (5)$$

which corresponds to clusters of galaxies.

# Structure Formation

Pure CDM spectra, with different shape parameters (0.1-0.5 with step 0.1).

When the shape parameter is 0.2 it match both constraints



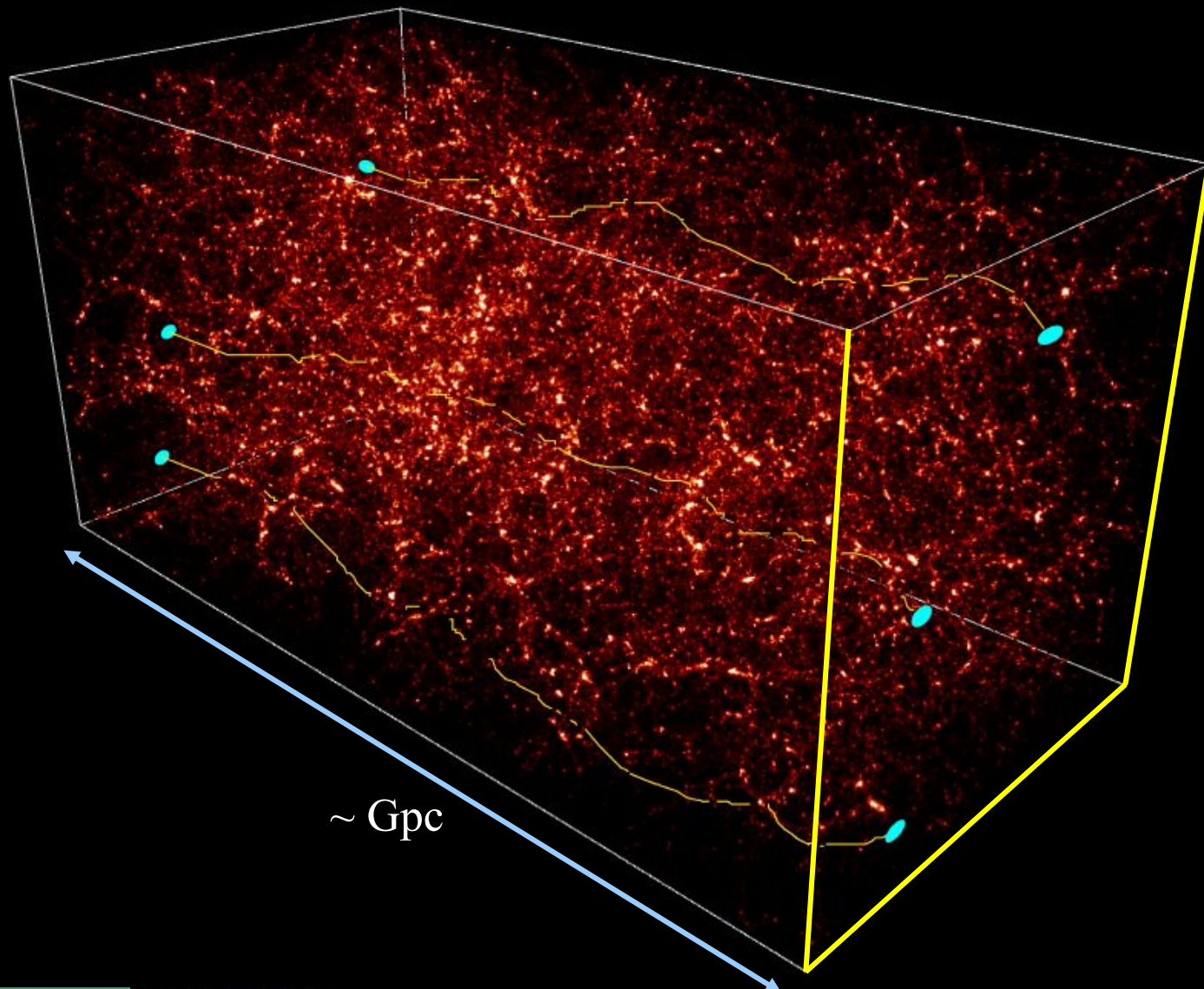
# Structure Formation

## Non linear evolution

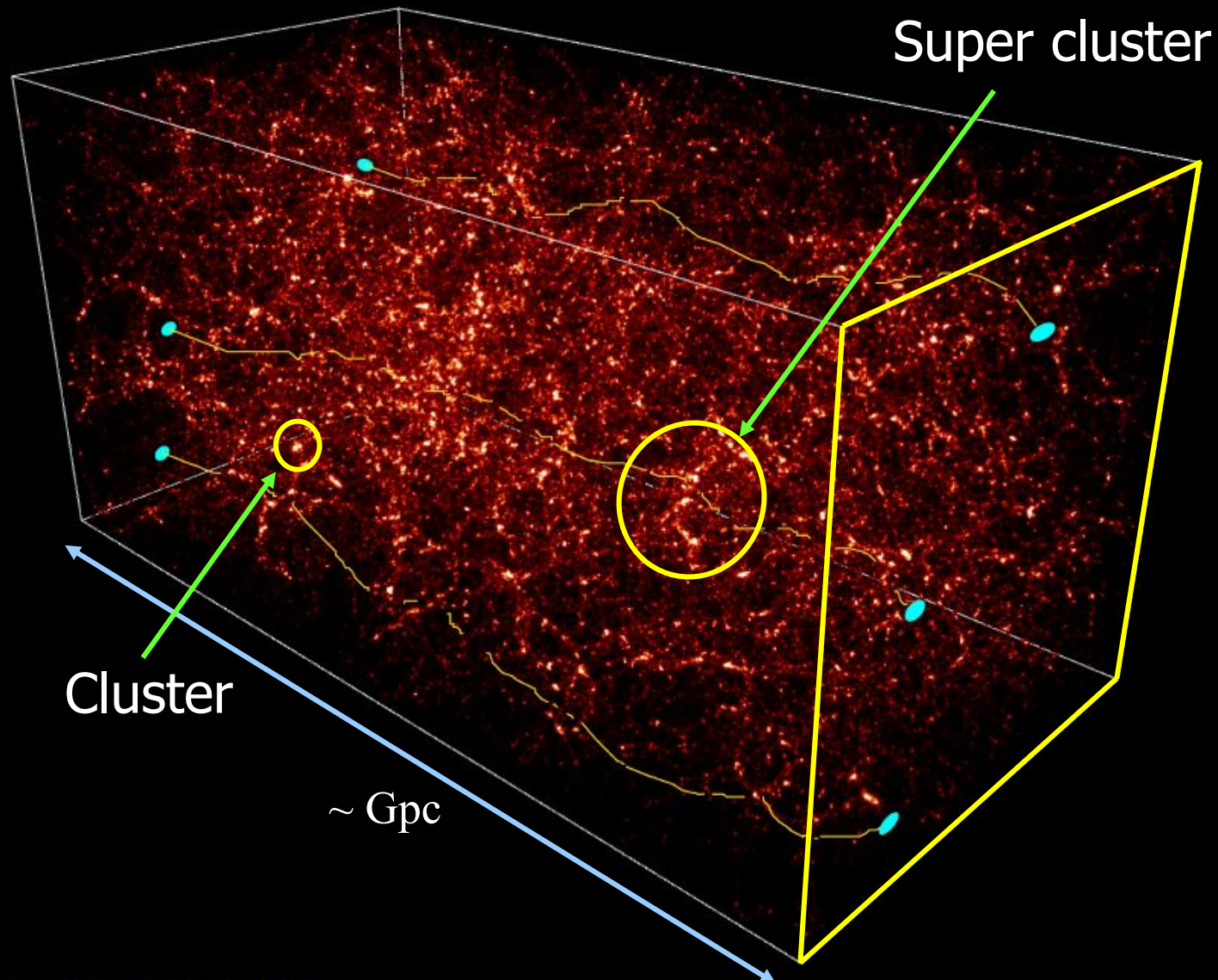
- On very small scale, linear approximation breaks down  
Structures are no longer described analytically
- Non linear models:
  - Assume the non-linear spectrum is a universal function of the linear spectrum
  - Establish relation between the linear and non linear spectra (based on specific ansatz and numerical simulations):
    - Peacock and Dodds
    - Halo models
  - Work well; but approximations

# Cosmological Weak Lensing: Theory

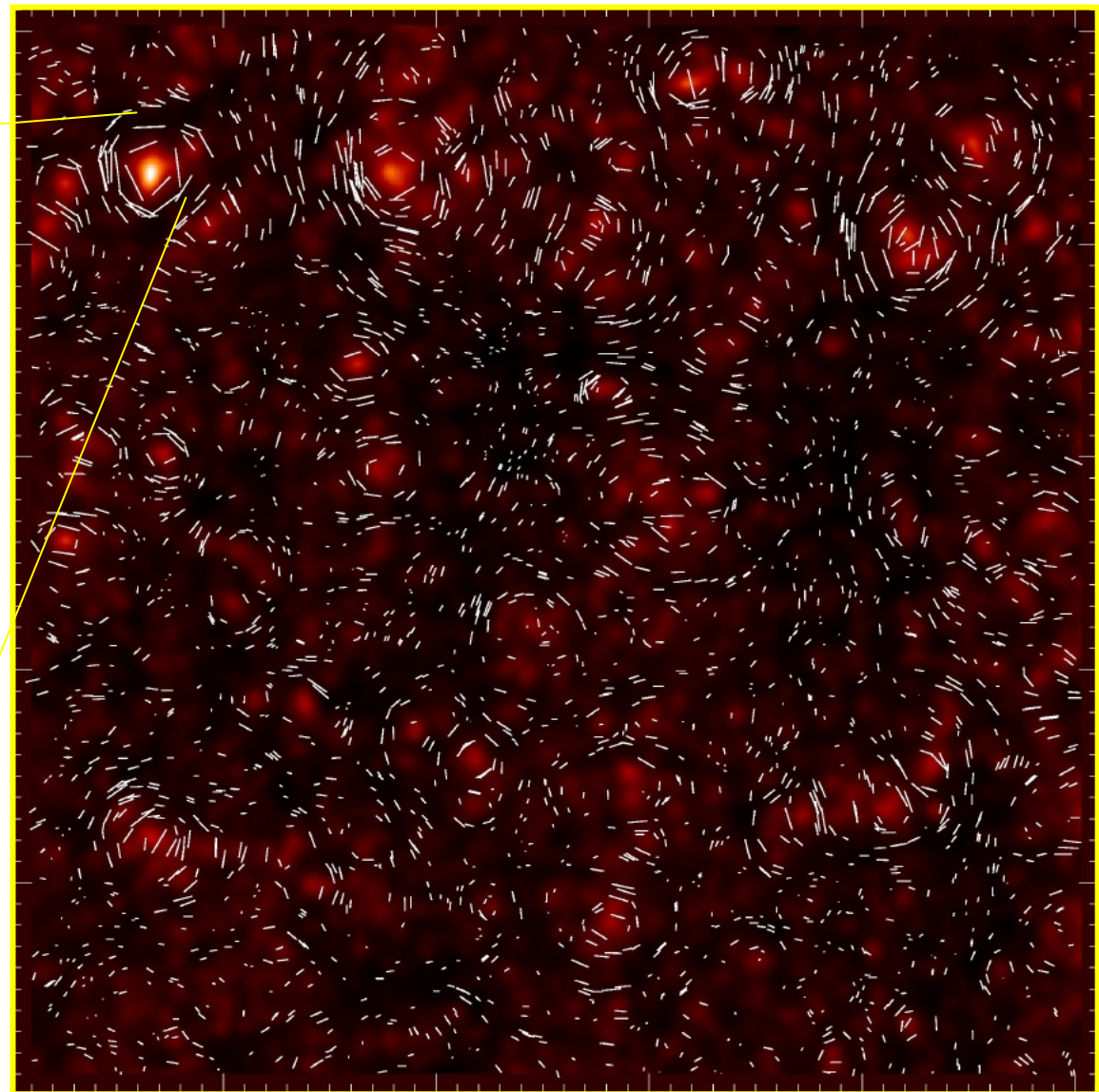
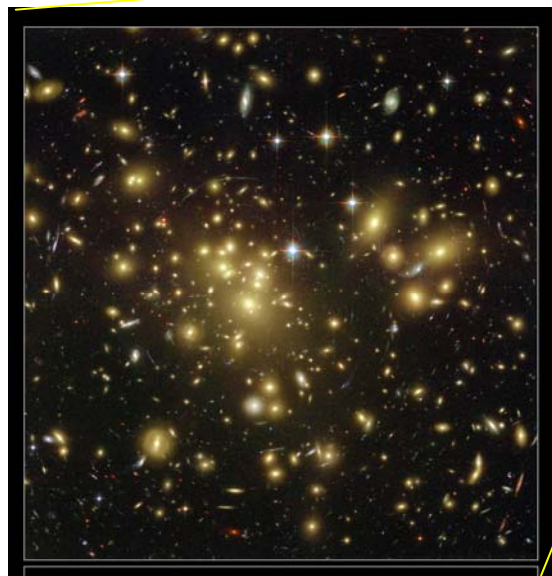
# *Cosmic shear* : propagation of light through the cosmic web



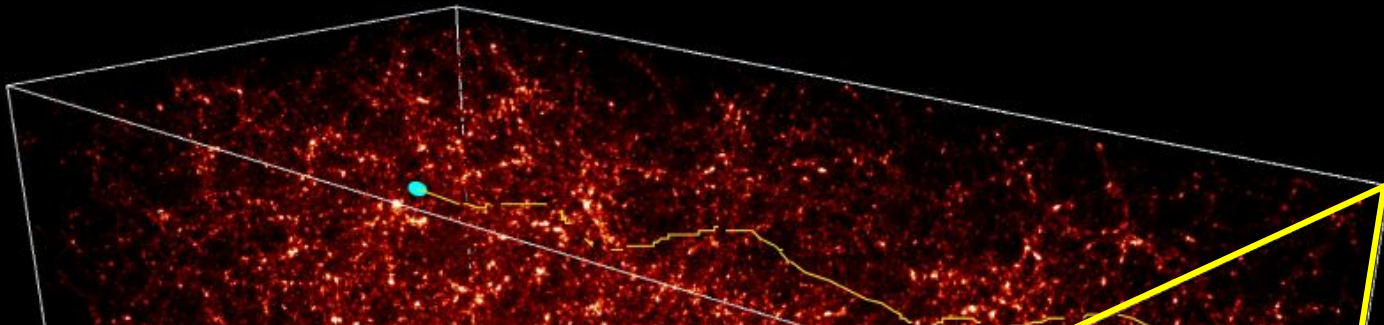
# *Cosmic shear* : propagation of light through the cosmic web



# Cosmological distortion field projected on the sky



## *Cosmic shear* : propagation of light through the cosmic web

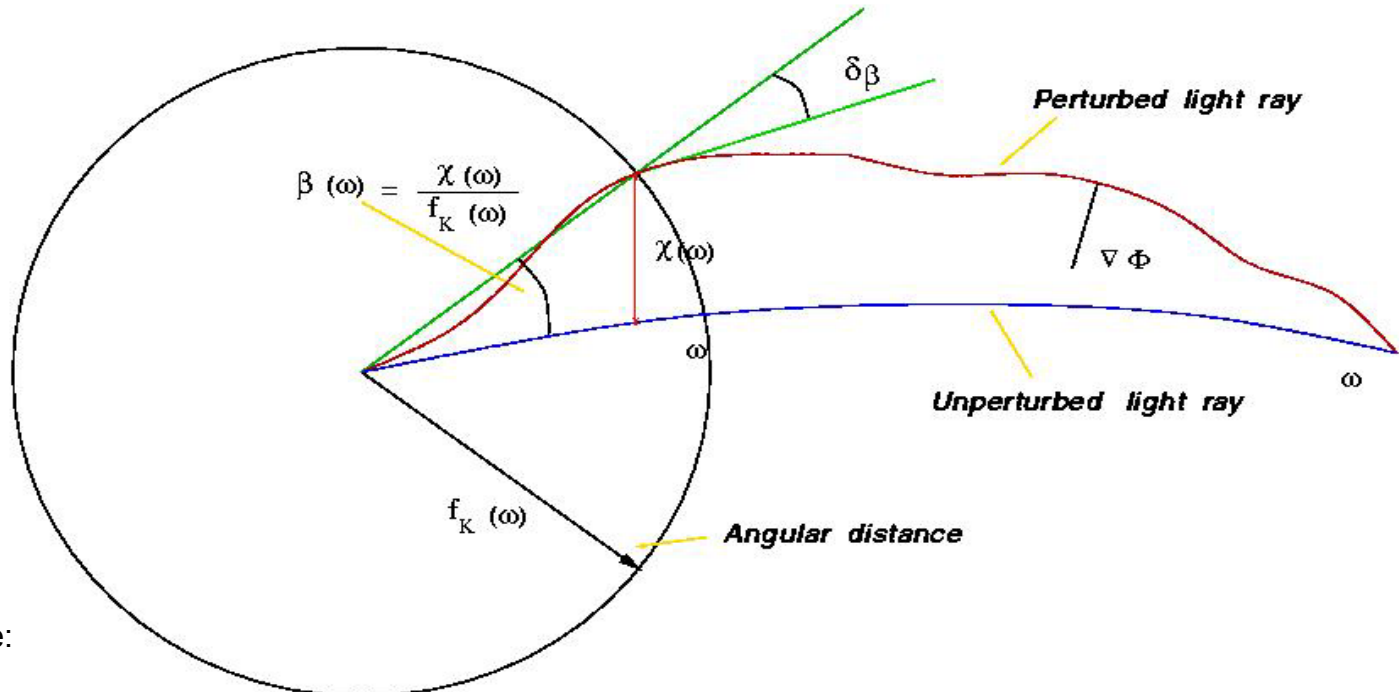


- How can we measure the signal?
- Is the signal-to-noise high enough?
- What can we derive on cosmology from it?

~ Gpc

# Weak gravitational lensing and cosmology: Light propagation in inhomogeneous universes

$$ds^2 = c^2 dt^2 - a^2(t) [dw^2 + f_K^2(w) d\omega^2]$$



Deflection angle:

$$\alpha = -\frac{2}{c^2} \int_S^O \nabla_{\perp} \Phi \cdot dl .$$

# Weak Lensing and Cosmology

- Express the light propagation in a homogeneous and isotropic universe
- Include the effects of (small) perturbations
- Compute of the deflection angle,  $\kappa, \gamma$  as a function of  $\delta = \frac{\delta\rho}{\rho}, \Omega, \lambda$
- Then, infer  $P_\kappa(k)$  and  $P_\delta(k)$
- Analyse the sensitivity to cosmological quantities and propose an observational strategy

# Light deflection in Inhomogeneous Universes

---

We show that

$$\frac{d\vec{x}}{d\omega} = \vec{\alpha} = -\frac{2}{c^2} \int \vec{\nabla}_\perp \Phi dl \quad (157)$$

Consider 2 close photon paths. We are interested in the differential light deflection. It is equivalent to the previous equation:

$$\boxed{\frac{d^2\vec{x}}{d\omega^2} = -\frac{2}{c^2} \vec{\nabla}_\perp \Phi(\vec{x}; \omega')} \quad (158)$$

The solutions of this differential equation are given by the Green's function.

# Light deflection in Inhomogeneous Universes

---

Solution using Green functions

$$\begin{cases} G(\omega - \omega') = f_K(\omega - \omega'), & \text{if } \omega > \omega' \\ 0 & \text{if } \omega < \omega' \end{cases} \quad (160)$$

$$\vec{x}(\omega) = \vec{x}(0) + f_K(\omega) \frac{d\vec{x}}{d\omega}(0) - \frac{2}{c^2} \int_0^\omega f_K(\omega - \omega') \vec{\nabla}_\perp \Phi(\vec{x}; \omega') d\omega' \quad (161)$$

As for a single deflection, we still have the boundary conditions:

$$\vec{x}(0) = 0 ; \frac{d\vec{x}}{d\omega}(0) \vec{\theta} , \quad (162)$$

then:

$$\vec{x}(\omega) = \vec{\theta} f_K(\omega) - \frac{2}{c^2} \int_0^\omega f_K(\omega - \omega') \vec{\nabla}_\perp \Phi(\vec{x}; \omega') d\omega' \quad (163)$$

Where the integral is evaluated *along the unperturbed light-path*

The deflection angle is the difference between the perturbed and unperturbed path :

$$\vec{\alpha} = \frac{\vec{\theta} f_K(\omega) - \vec{x}}{f_K(\omega)} \quad (164)$$

Using  $\vec{x}(\omega) = \vec{\beta} f_K(\omega)$  , we can write the delection angle:

$$\vec{\alpha}(\vec{\theta}; \omega) = \vec{\theta} - \vec{\beta} = \frac{2}{c^2} \int_0^\omega \frac{f_K(\omega - \omega')}{f_K(\omega)} \vec{\nabla}_\perp \Phi(f_K(\omega') \vec{\theta}; \omega) d\omega' \quad (165)$$

This is the deflection angle accumulated along a line path, propagating into direction  $\vec{\theta}$  out to coordinate distance  $\omega$ .

For a flat universe:

$$\vec{\alpha}(\vec{\theta}; \omega) = \vec{\theta} - \vec{\beta} = \frac{2}{c^2} \int_0^\omega \left(1 - \frac{\omega'}{\omega}\right) \vec{\nabla}_\perp \Phi(\omega' \vec{\theta}; \omega) d\omega'$$

(166)

But we are interested in  $\kappa$  and  $\gamma$  ...

$$\vec{\alpha}(\vec{\theta}; \omega) = \vec{\theta} - \vec{\beta} = \frac{2}{c^2} \int_0^\omega \left(1 - \frac{\omega'}{\omega}\right) \vec{\nabla}_\perp \Phi(\omega' \vec{\theta}; \omega) d\omega' \quad (166)$$

we have shown that, from the lens equation:

$$\begin{cases} \vec{\theta} - \vec{\beta} = -\frac{D_{LS}}{D_{OS}} \vec{\alpha} = \vec{\nabla}_{\vec{\theta}} \varphi(\vec{\theta}) \\ \implies \vec{\nabla}_{\vec{\theta}}^2 \varphi(\vec{\theta}) = -\frac{D_{LS}}{D_{OS}} \vec{\nabla}_{\vec{\theta}} \cdot \vec{\alpha} \\ \implies 2\kappa = \frac{1}{2} \vec{\nabla}_{\vec{\theta}} \cdot \vec{\alpha}(\vec{\theta}) = \frac{1}{2} \frac{\partial \alpha_i(\vec{\theta})}{\partial \theta_i} \end{cases} \quad (167)$$

Define the *cumulative effective convergence* along a line of sight is:

$$\begin{aligned} \kappa_{eff} &= \frac{1}{2} \vec{\nabla}_{\vec{\theta}} \cdot \vec{\alpha}(\vec{\theta}; \omega) \\ &= \frac{1}{2} \int_0^\omega \frac{f_K(\omega - \omega') f_K(\omega')}{f_K(\omega)} \frac{\partial^2}{\partial \theta_i \partial \theta_j} \left[ \Phi(f_K(\omega') \vec{\theta}; \omega') \right] d\omega' \end{aligned} \quad (168)$$

# Convergence and Mass Density Contrast

---

The Poisson equation is:

$$\nabla_r^2 \Phi = 4\pi G \bar{\rho} (1 + \delta) \quad (169)$$

Decoupling the background from the perturbation, one can then write

$$\nabla_r^2 \Phi' = 4\pi G \bar{\rho} \delta \quad (170)$$

Using comoving coordinates, we have  $\nabla_x = a \nabla_r$ , so:

$$\nabla_x^2 \Phi = 4\pi G a^2 \bar{\rho} \delta \quad (171)$$

In the matter-dominated universe we have  $\bar{\rho} = a^{-3} \rho_0$ .

$$\implies \vec{\nabla}_x^2 = 4\pi G a^2 \frac{3\Omega_0 H_0^2}{8\pi G a^3} = \frac{3H_0^2}{2a} \Omega_0 \delta \quad (172)$$

$\kappa_{eff}$  can therefore be expressed as function of the mass density contrast and cosmological parameters:

$$\kappa_{eff}(\vec{\theta}; \omega) = \frac{3\Omega_0 H_0^2}{2c^2} \int_0^\omega \frac{f_K(\omega - \omega') f_K(\omega')}{f_K(\omega)} \frac{\delta[f_K(\omega') \vec{\theta}; \omega']}{a(\omega')} d\omega'$$

One can notice the distance ratio factor in the integration, that is similar to the distance ration  $D_{ls}D_{ol}/D_{os}$  found for a single lens case.

## Generalisation for a redshift distribution of sources.

Sources are no longer at distance  $\omega$ , need to define a *mean effective convergence*

$$\langle \kappa_{eff}(\vec{\theta}) \rangle = \int p_\omega(\omega) \kappa(\vec{\theta}; \omega) d\omega \quad (174)$$

$$\left\{ \begin{array}{l} \langle \kappa_{eff}(\vec{\theta}) \rangle = \int_0^{\omega_H} G(\omega) \kappa_{eff}(\theta; \omega) d\omega \\ \text{where } G(\omega) d\omega = P(z) dz \end{array} \right. \quad (175)$$

where  $\omega_H$  is the comoving horizon distance.

# Generalisation for a redshift distribution of sources

We then have:

$$\begin{cases} \langle \kappa_{eff}(\vec{\theta}) \rangle = \int_0^{\omega_H} \bar{W}(\omega) f_K(\omega) \frac{\delta[f_K(\omega')\vec{\theta};\omega']}{a(\omega')} d\omega' \\ \bar{W}(\omega) = \int_{\omega}^{\omega_H} G(\omega') \frac{f_K(\omega'-\omega)}{f_K(\omega')} d\omega' \end{cases} \quad (176)$$

So essentially, the sources are weighted by the ratio  $D_{ls}/D_{os}$  for a density fluctuation located at distance  $\omega$ .

## **2-Point Convergence Correlation Function and Limber Equation**

---

We have:

$$\langle \kappa_{eff}(\vec{\theta}) \rangle = \frac{3H_0^2\Omega_0}{2c^2} \int_0^{\omega_H} \bar{W}(\omega) f_K(\omega) \frac{\delta[f_K(\omega) \vec{\theta}; \omega]}{a(\omega)} d\omega \quad (189)$$

Putting

$$Z(\omega) = \frac{3H_0^2\Omega_0}{2c^2} \bar{W}(\omega) \frac{f_K(\omega)}{a(\omega)} \quad (190)$$

$$\rightarrow \kappa_{eff}(\vec{\theta}) = \int Z(\omega) \delta[f_K(\omega) \theta; \omega] d\omega \quad (191)$$

By definition, the 2-point convergence correlation function is:

$$\xi_{\kappa}(\vec{\theta}) = \langle \kappa^*(\vec{\phi}) \kappa(\vec{\phi} + \vec{\theta}) \rangle \quad (192)$$

$$\xi_{\kappa}(\vec{\theta}) = \int Z(\omega) d\omega \int \int Z'(\omega') d\omega' \langle \delta^*(f_K(\omega) \vec{\phi}; \omega) \delta(f_K(\omega') (\vec{\phi} + \vec{\theta}); \omega') \rangle \quad (193)$$

$$\xi_{\kappa}(\vec{\theta}) = \int Z(\omega) d\omega \int \int Z'(\omega') d\omega' \int \frac{d^3 k}{(2\pi)^3} \int \frac{d^3 k'}{(2\pi)^3} \langle \hat{\delta}(\vec{k}; \omega) \cdot \hat{\delta}^*(\vec{k}'; \omega') \rangle e^{-if_K(\omega)\vec{k}_\perp \cdot \vec{\theta}} e^{if_K(\omega')\vec{k}'_\perp \cdot \vec{\theta}'} \times e^{-ik_3 \omega} e^{ik'_3 \omega'} \quad (194)$$

where  $\vec{k}_\perp$  is the 2-dimension wavenumber vector perpendicular to the line of sight.

# Assumptions

- Assume there is no power in mass density fluctuations on scales larger than a typical coherent scale  $L_{coh}$ . This is valid because the power spectrum  $P_\delta$  decreases as  $k \rightarrow 0$ . This results from:

$$\begin{cases} P_\delta \propto k & \text{if } k \ll k_0 \\ k^{-3} & \text{if } k \gg k_0 \end{cases} \quad (195)$$

# Assumptions

- Assume there is no power in mass density fluctuations on scales larger than a typical coherent scale  $L_{coh}$ . This is valid because the power spectrum  $P_\delta$  decreases as  $k \rightarrow 0$ . This results from:

$$\begin{cases} P_\delta \propto k & \text{if } k \ll k_0 \\ k^{-3} & \text{if } k \gg k_0 \end{cases} \quad (195)$$

- On the other hand, though  $\delta$  changes with time, we assume it is almost constant over a typical timescale  $L_{coh}/c$ .

# Assumptions

- Assume there is no power in mass density fluctuations on scales larger than a typical coherent scale  $L_{coh}$ . This is valid because the power spectrum  $P_\delta$  decreases as  $k \rightarrow 0$ . This results from:

$$\begin{cases} P_\delta \propto k & \text{if } k \ll k_0 \\ k^{-3} & \text{if } k \gg k_0 \end{cases} \quad (195)$$

- On the other hand, though  $\delta$  changes with time, we assume it is almost constant over a typical timescale  $L_{coh}/c$ .
- Finally, we assume  $Z$  is almost constant over a physical scale  $\Delta\omega \leq L_{coh}$ .  $\implies$  the correlation function  $C_{\delta\delta} \neq 0$  only on a physical scale  $|\omega - \omega'| \leq L_{coh}$ .

$$\implies f_K(\omega) \simeq f_K(\omega') \text{ and } Z(\omega) \simeq Z(\omega')$$

Therefore the correlation function writes:

$$\xi_{\kappa}(\vec{\theta}) = \int Z(\omega) \int Z'(\omega) \int \frac{d^3 k}{(2\pi)^3} P_{\delta}(|\vec{k}|; \omega) e^{if_k(\omega)\vec{k}_\perp \cdot (\vec{\theta} - \vec{\theta}')} \times e^{-ik_3 \omega} \int e^{ik'_3 \omega'} d\omega'$$

Knowing that

$$\int e^{ik'_3 \omega'} d\omega' = 2\pi \delta_D(k_3)$$

For an isotropic universe, the correlation function writes:

$$\Rightarrow \boxed{\xi_{\kappa}(\vec{\theta}) = \int Z(\omega) \int Z'(\omega) \frac{k dk}{2\pi} P_{\delta}(k; \omega) J_0[f_k(\omega) \theta k]}$$

# The Convergence Power Spectrum

Can be derived from the inverse transform of the correlation function:

$$P_\kappa(l) = \int d^2\vec{\theta} \xi(\vec{\theta}) e^{i\vec{l}\cdot\vec{\theta}} \quad (204)$$

Using the expression of  $Z$ , and  $Z = Z'$  we have

$$P_\kappa(l) = \frac{9H_0^4\Omega_0^2}{4c^4} \int \frac{\bar{W}(\omega)^2}{a(\omega)} P_\delta\left(\frac{l}{f_K(\omega)}; \omega\right) \quad (208)$$

- This is valid if the largest scales structures in  $\delta$  are much smaller than the effective range  $\Delta\omega$  in the projection.

- This is valid if the largest scales structures in  $\delta$  are much smaller than the effective range  $\Delta\omega$  in the projection.
- The expression above expresses the fact that the power of the convergence at scale  $1/l$  is obtained from the 3-dimensional power spectrum on the mass density fluctuation at scale  $f_K(\omega)(1/l)$ , integrated over  $w$ . This is what we could expect.

- This is valid if the largest scales structures in  $\delta$  are much smaller than the effective range  $\Delta\omega$  in the projection.
- The expression above expresses the fact that the power of the convergence at scale  $1/l$  is obtained from the 3-dimensional power spectrum on the mass density fluctuation at scale  $f_K(\omega)(1/l)$ , integrated over  $w$ . This is what we could expect.
- If one can observe the 2-D  $P_\kappa$  one can get constraints on the 3-D  $P_\delta$

# Relation Between the Convergence and the Shear Power Spectrum

We have

$$\begin{cases} \kappa = \frac{1}{2} \left( \frac{\partial^2}{\partial x^2} + \frac{\partial^2}{\partial yx^2} \right) \Psi \\ \gamma = \frac{1}{2} \left( \frac{\partial}{\partial x} + i \frac{\partial}{\partial y} \right)^2 \Psi \end{cases} \quad (209)$$

In Fourier space:

$$\begin{cases} \hat{\kappa} = \frac{1}{2} (l_x^2 + l_y^2) \hat{\Psi} \\ \hat{\gamma} = \frac{1}{2} (l_x^2 - l_y^2 + 2il_x l_y) \hat{\Psi} \end{cases} \quad (210)$$

Therefore

$$\begin{cases} \langle \hat{\kappa}(\vec{l}) \hat{\kappa}^*(\vec{l}) \rangle = \frac{1}{4} \langle (l_x^2 + l_y^2)^2 \rangle = |\vec{l}|^4 \\ \langle \hat{\gamma}(\vec{l}) \hat{\gamma}^*(\vec{l}) \rangle = \frac{1}{4} \langle (l_x^2 - l_y^2)^2 + 4l_x^2 l_y^2 \rangle = |\vec{l}|^4 \end{cases} \quad (211)$$

We then have two very important properties:

$$\begin{cases} \langle \hat{\kappa}(\vec{l}) \hat{\kappa}^*(\vec{l}) \rangle = \langle \hat{\gamma}(\vec{l}) \hat{\gamma}^*(\vec{l}) \rangle = (2\pi)^2 \delta_D(\vec{l} - \vec{l}') P_\kappa(l) \\ P_\kappa(l) = P_\gamma(l) \end{cases} \quad (212)$$

# Shear Correlation Functions

Consider the tangential and cross components of the shear with respect to a direction  $\phi$  is

$$\gamma_t = -\Re [\gamma e^{-2i\alpha}] ; \quad \gamma_x = -Im [\gamma e^{-2i\alpha}] \quad (213)$$

and define the correlation function of the tangential shear as

$$\langle \gamma_t \gamma'_t \rangle = \xi_{tt}(\phi) = \frac{1}{(2\pi)^2} \int dl P_{\gamma_t}(l) e^{-i \vec{l} \cdot \vec{\phi}} \quad (214)$$

In Fourier space we have

$$\hat{\gamma}_t = -\frac{1}{2} (k_1^2 + k_2^2) \hat{\psi} = \frac{k^2}{2} (\cos^2(\alpha) - \sin^2(\alpha)) \hat{\psi} \quad (215)$$

where  $\psi$  is the effective lensing potential.

The power spectrum is therefore

$$P_\gamma = \frac{k^4}{4} (\cos^2(\alpha) - \sin^2(\alpha))^2 P_\psi \quad (216)$$

Since we know that

$$P_\kappa = \frac{1}{4} (k_1^2 + k_2^2)^2 P_\psi \quad (217)$$

one can derive easily that

$$\langle \gamma_t \gamma'_t \rangle = \frac{1}{2} \int \frac{l dl}{2\pi} P_\kappa(l) [J_0(l\phi) + J_4(l\phi)] \quad (218)$$

Likewise, for the cross component:

$$\langle \gamma_x \gamma'_x \rangle = \xi_{xx}(\phi) = \frac{1}{(2\pi)^2} \int dl P_{\gamma_x}(l) e^{-i \vec{l} \cdot \vec{\phi}} \quad (219)$$

where

$$P_{\gamma_x} = k_1^2 k_2^2 P_\psi = 4 \cos^2(\phi) \sin^2(\phi) P_\kappa \quad (220)$$

one can derive

$$\langle \gamma_x \gamma'_x \rangle = \frac{1}{2} \int \frac{l dl}{2\pi} P_\kappa(l) [J_0(l\phi) - J_4(l\phi)] \quad (221)$$

Finally, one can also compute the mixed correlation function

$$P_{\gamma_t \gamma_x} = \frac{4}{k^4} (k_1^2 - k_2^2) k_1 k_2 P_\kappa \quad (222)$$

$$P_{\gamma_t \gamma_x} = 2 (\cos^2(\alpha) - \sin^2(\alpha)) \cos(\alpha) \sin(\alpha) P_\kappa \quad (223)$$

Because of the cross sincos terms , vanishes. Therefore

$$\xi_{tx}(\phi) = 0 \quad (224)$$

Using this property, it is useful to define two new correlation functions:

$$\xi_{\pm} = \langle \gamma_t \gamma'_t \rangle \pm \langle \gamma_x \gamma'_x \rangle \text{ and } \xi_x = \langle \gamma_t \gamma'_x \rangle \quad (225)$$

so that

$$\xi_+(\varphi) = \frac{1}{2} \int \frac{l dl}{2\pi} P_\kappa(l) J_0(l\phi) \quad (226)$$

$$\xi_-(\varphi) = \frac{1}{2} \int \frac{l dl}{2\pi} P_\kappa(l) J_4(l\phi) \quad (227)$$

$$\xi_x(\varphi) = 0 \quad (228)$$

The last correlation function being zero, it can be used to control systematic errors on cosmic shear measurements.

# The E- and B-modes of the Shear Field

---

Both the shear and the convergence are combination of the second derivatives of the projected scalar potential  $\Rightarrow$  they are related:

$$\vec{\nabla} \kappa = \begin{pmatrix} \partial_1 \gamma_1 + \partial_2 \gamma_2 \\ \partial_2 \gamma_1 - \partial_1 \gamma_2 \end{pmatrix} = \vec{u} \quad (229)$$

that defines  $\vec{u}$  as the gradient of the "potential"  $\kappa$ .

Define the E- and B- components of the convergence field as function of the gradient and curl part of  $\vec{u}$ :

$$\vec{\nabla}^2 \kappa^E = \vec{\nabla} \cdot \vec{u} ; \quad \vec{\nabla}^2 \kappa^B = \vec{\nabla} \times \vec{u} \quad (230)$$

And define also the E- and B-mode potentials, from the Poisson equation:

$$\vec{\nabla}^2 \psi^{E,B} = 2\kappa^{E,B} \quad (231)$$

And write the relation using complex quantities:

$$\psi = \psi^E + i\psi^B ; \quad \kappa = \kappa^E + i\kappa^B \quad (232)$$

In that case we still write de Poisson equation as  $\vec{\nabla}^2 \psi = 2\kappa$ , and the complexe shear ,  $\gamma = (1/2)(\partial_1\partial_1 - \partial_2\partial_2) \psi + i\partial_1\partial_2 \psi$  writes:

(233)

$$\gamma = \gamma_1 + i\gamma_2 = \quad (233)$$

$$\frac{1}{2}(\partial_1\partial_1\psi^E - \partial_2\partial_2\psi^E) - \partial_1\partial_2\psi^B + i \left[ \partial_1\partial_2\psi^E + \frac{1}{2}(\partial_1\partial_1\psi^B - \partial_2\partial_2\psi^B) \right] \quad (234)$$

These relations are consistent with the definitions of the lensing convergence and shear in absence of B modes.

This generalisation to any field turns out to be very useful to make clear assessments on the lensing nature of the distortion field and on systematics in the real data.

One can also define the E-, B- and cross power spectra as follows:

$$EE = \langle \hat{\kappa}^E(\vec{l}) \hat{\kappa}^E(\vec{l}') \rangle = (2\pi)^2 \delta_D(\vec{l} - \vec{l}') P_\kappa^E(l) \quad (235)$$

$$BB = \langle \hat{\kappa}^B(\vec{l}) \hat{\kappa}^B(\vec{l}') \rangle = (2\pi)^2 \delta_D(\vec{l} - \vec{l}') P_{\kappa}^B(l) \quad (236)$$

$$EB = \langle \hat{\kappa}^E(\vec{l}) \hat{\kappa}^B(\vec{l}') \rangle = (2\pi)^2 \delta_D(\vec{l} - \vec{l}') P_{\kappa}^{EB}(l) \quad (237)$$

and the correlations of  $\gamma$  in Fourier space:

$$\langle \hat{\gamma}(\vec{l}) \hat{\gamma}^*(\vec{l}') \rangle = (2\pi)^2 \delta_D(\vec{l} - \vec{l}') [P_{\kappa}^E(l) + P_{\kappa}^B(l)] \quad (238)$$

and

$$\langle \hat{\gamma}(\vec{l}) \hat{\gamma}(\vec{l}') \rangle = (2\pi)^2 \delta_D(\vec{l} - \vec{l}') [P_{\kappa}^E(l) - P_{\kappa}^B(l) + 2iP_{\kappa}^{EB}(l)] \quad (239)$$

For parity-symmetric shear fields,  $P^{EB}$  vanishes.

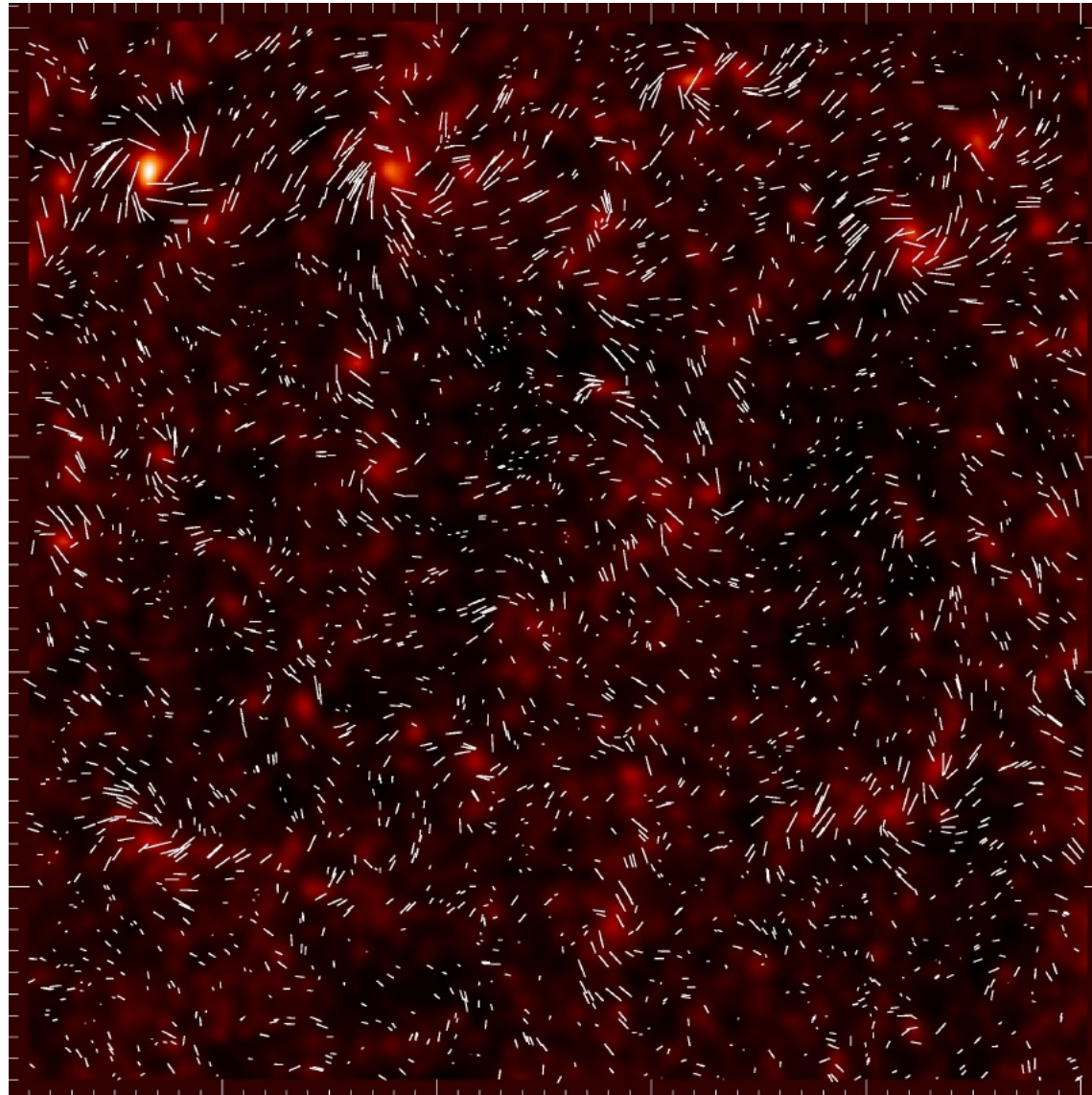
# Testing systematics and reliability of cosmic shear signal:

Gravitational lensing does not produce B-modes (Curl=0)

E projection

Pure gravity signal

45 degrees rotated  
galaxies, E  $\rightarrow$  B



## **Relations Between $P^{E,B}$ and $\xi_+$**

---

It is easy to show that

$$\xi_+(\theta) = \frac{1}{2} \int_0^\infty dl l J_0(l\theta) \left[ P(l)^E + P(l)^B \right] \quad (240)$$

$$\xi_-(\theta) = \frac{1}{2} \int_0^\infty dl l J_4(l\theta) \left[ P(l)^E - P(l)^B \right] \quad (241)$$

and

$$P(l)^E = \pi \int_0^\infty d\theta \theta [\xi_+(\theta) J_0(l\theta) + \xi_-(\theta) J_4(l\theta)] \quad (242)$$

$$P(l)^B = \pi \int_0^\infty d\theta \theta [\xi_+(\theta) J_0(l\theta) - \xi_-(\theta) J_4(l\theta)] \quad (243)$$

# The Top Hat Shear Variance

Consider the mean shear inside a circular aperture of radius  $\theta$ :

$$\bar{\gamma}_i(\theta) = \int_0^\theta \frac{d^2 \vec{\phi}^2}{\pi \theta^2} \gamma(\vec{\phi}) \quad (244)$$

The shear variance inside the aperture is therefore:

$$\langle |\gamma|^2 \rangle = \int_0^\theta \frac{d^2 \vec{\phi}^2}{\pi \theta^2} \int_0^\theta \frac{d^2 \vec{\phi}'^2}{\pi \theta^2} \langle \gamma(\vec{\phi}) \gamma^*(\vec{\phi}') \rangle \quad (245)$$

$$\langle |\gamma|^2 \rangle = \frac{1}{(2\pi)^2} \int P_\kappa(l) d^2 \vec{l} \int_0^\theta \frac{d^2 \vec{\phi}^2}{\pi \theta^2} \int_0^\theta \frac{d^2 \vec{\phi}'^2}{\pi \theta^2} e^{-il \cdot (\vec{\phi} - \vec{\phi}')} \quad (246)$$

That is:

$$\langle |\gamma|^2 \rangle = 2\pi \int P_\kappa(l) l dl \left[ \frac{1}{\pi l^2 \theta^2} \int_0^{l\theta} J_0(x) x dx \right]^2 \quad (248)$$

Using:

$$x^n J_{n-1} dx = d(x^n J_n(x)) \quad (249)$$

$$\langle |\gamma(\theta)|^2 \rangle = 2\pi \int P_\kappa(l) l dl \left( \frac{J_1(l\theta)}{\pi l \theta} \right)^2 \quad (250)$$

# The Aperture Mass Statistics

As for the top hat shear variance, one can also compute the aperture mass variance.

$M_{ap}$  and  $M_{\perp}$  are simply defined with the tangential and cross component of the shear  $\implies$  relations with  $\xi_{\pm}$  and the E- and B-modes are

- Very simple
- Very useful !

We have

$$M_{ap}(\vec{\theta}_0) = \int Q(|\vec{\theta}|) \gamma_t(\vec{\theta}; \vec{\theta}_0) d^2\vec{\theta} \quad (251)$$

where

$$Q(\theta) = \frac{2}{\theta} \int_0^\theta d\theta' \theta' U(\theta') - U(\theta) \quad (252)$$

and

$$M_\perp(\vec{\theta}_0) = \int Q(|\vec{\theta}|) \gamma_x(\vec{\theta}; \vec{\theta}_0) d^2\vec{\theta} \quad (253)$$

One can show that:

$$\langle M_{ap}^2 \rangle(\theta) = \frac{1}{2\pi} \int dl l P_\kappa^E(l) \hat{U}^2(l\theta) \quad (254)$$

$$\langle M_\perp^2 \rangle(\theta) = \frac{1}{2\pi} \int dl l P_\kappa^B(l) \hat{U}^2(l\theta) \quad (255)$$

where  $\hat{U}$  is the Fourier transform of the filter function  $U$ .

- $M_{ap}$  provides the E-modes and  $M_{\perp}$  provides the B-modes.
- Since the filter function  $\hat{U}$  is very narrow, the aperture mass statistics provide a highly localized measure of the corresponding power spectra.

# Cosmic Shear Statistics and Power Spectrum

(Blandford et al 1991, Miralda-Escudé 1991, Kaiser 1992, 1998, Bernardeau et al 1997, Jain & Seljak 1997, Schneider et al 1998)

Top-hat shear variance at scale  $\theta_c$ :

$$\langle \gamma^2 \rangle = \frac{2}{\pi \theta_c^2} \int_0^\infty \frac{dk}{k} P_\kappa(k) [J_1(k\theta_c)]^2$$

Aperture mass (Map) variance at scale  $\theta_c$ :

$$\langle M_{ap}^2 \rangle = \frac{288}{\pi \theta_c^4} \int_0^\infty \frac{dk}{k^3} P_\kappa(k) [J_4(k\theta_c)]^2$$

Shear correlation function at separation  $\theta$ :

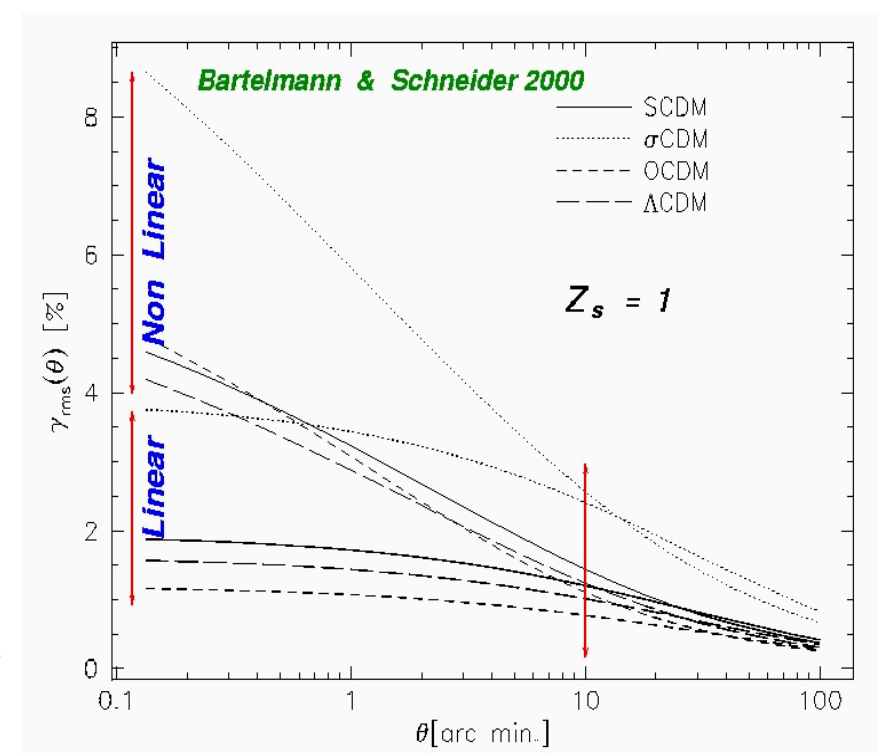
$$\langle \gamma(r)\gamma(r+\theta) \rangle_r = \frac{1}{2\pi} \int_0^\infty dk k P_\kappa(k) J_0(k\theta)$$

Convergence (projected mass) power spectrum:

$$P_\kappa(k) = \frac{9}{4} \Omega_0^2 \int_0^\infty dz \cdot P_{3D}\left(\frac{k}{D_L(z)}; z\right) \cdot F[z, z_{\text{source}}]^2$$

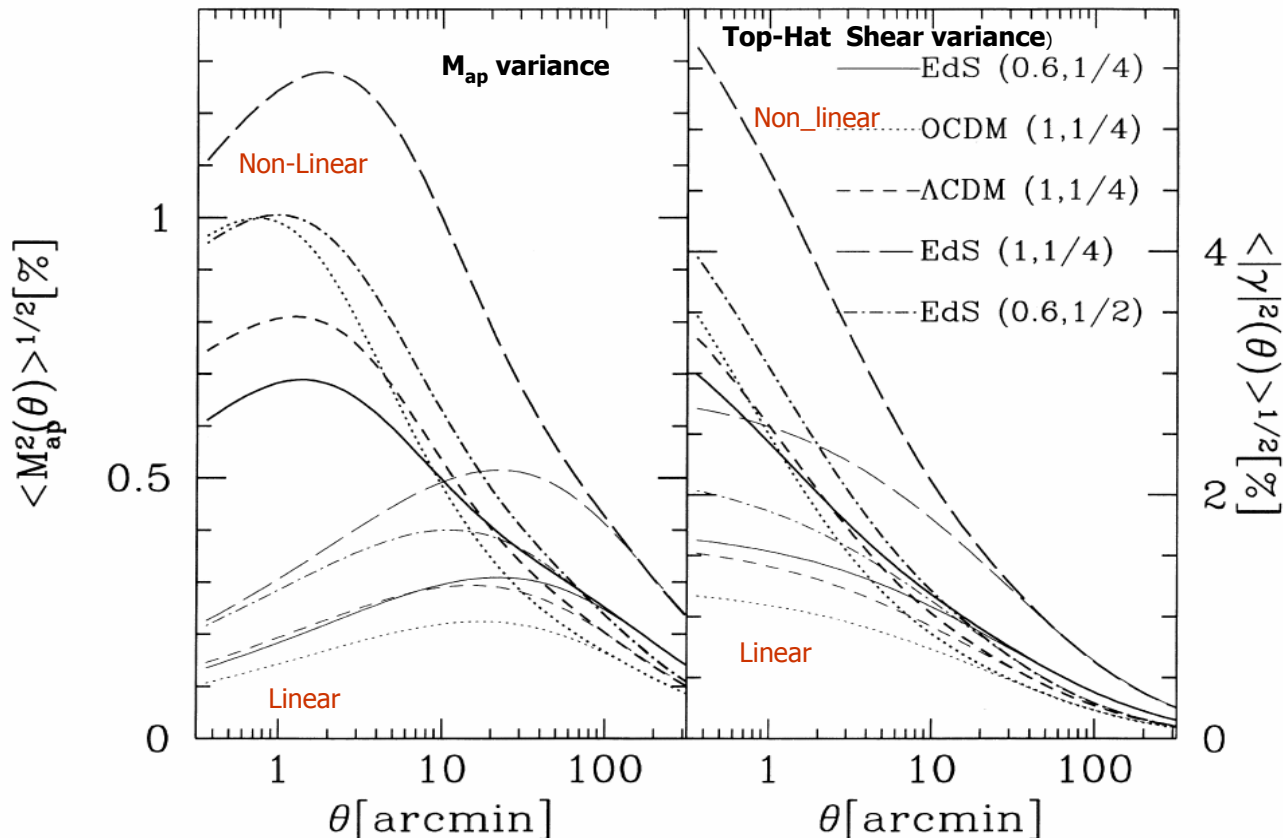
Assuming a single lens-plane and  $P(k) \propto k^n$ :

- $\langle \kappa^2(\theta) \rangle^{1/2} \approx 0.01 \sigma_8 \Omega^{0.8} \left(\frac{\theta}{1 \text{deg.}}\right)^{-\frac{n+2}{2}}$  z<sub>s</sub> 0.75
- $\langle \kappa^2(\theta) \rangle = \langle \gamma^2(\theta) \rangle$



# Shear Statistics : Theoretical Predictions

(Blandford et al 1991, Miralda-Escudé 1991, Kaiser 1992, 1998, Bernardeau et al 1997, Jain & Seljak 1997, Schneider et al 1998)



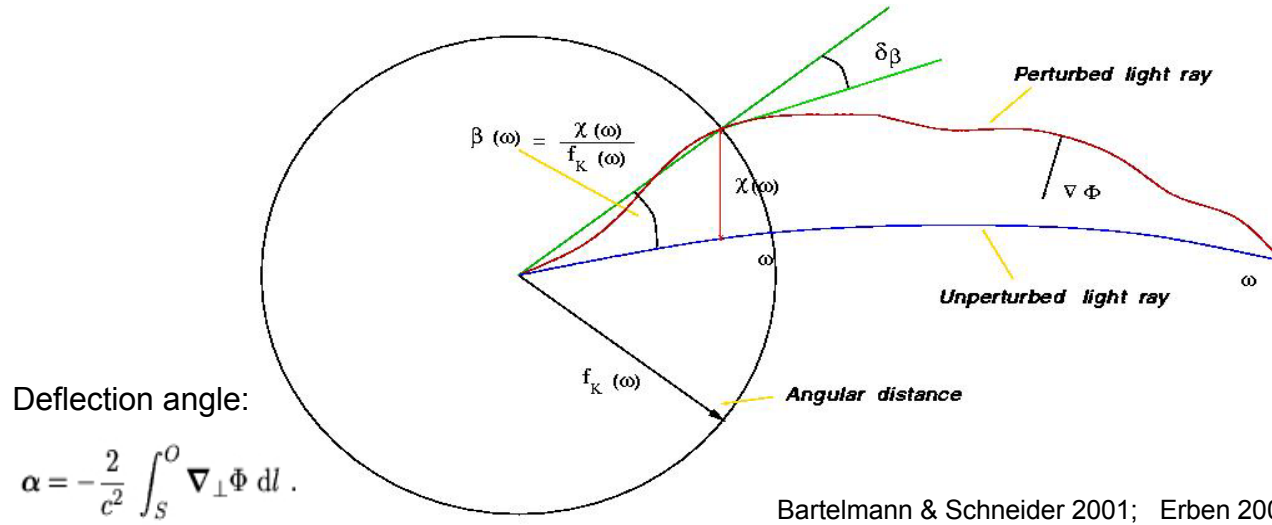
Bartelmann & Schneider 2001 : theoretical predictions from the gravitational instability scenario

**See:** Bacon et al 2000\*, 2001 ; Kaiser et al. 2000\* ; Maoli et al. 2000\* ; Rhodes et al 2001\* ; Refregier et al 2002 ; van Waerbeke et al. 2000\* ; van Waerbeke et al. 2001, 2005 ; Wittman et al. 2000\* ; Hammerle et al. 2001\* ; Hoekstra et al. 2002\* ; Brown et al. 2003 ; Hamana et al. 2003\* ; Jarvis et al. 2003 ; Casertano et al 2003\* ; Rhodes et al 2004 ; Massey et al. 2004 ; Heymans et al 2004\* ; Sembolini et al 2006 ; Hoekstra et al 2005, Hetterscheidt et al 2006, Schrabback et al 2006, Fu et al 2006

# Measuring and interpreting cosmic shear

# Weak gravitational lensing and cosmology:

$$ds^2 = c^2 dt^2 - a^2(t) [dw^2 + f_K^2(w) d\omega^2]$$

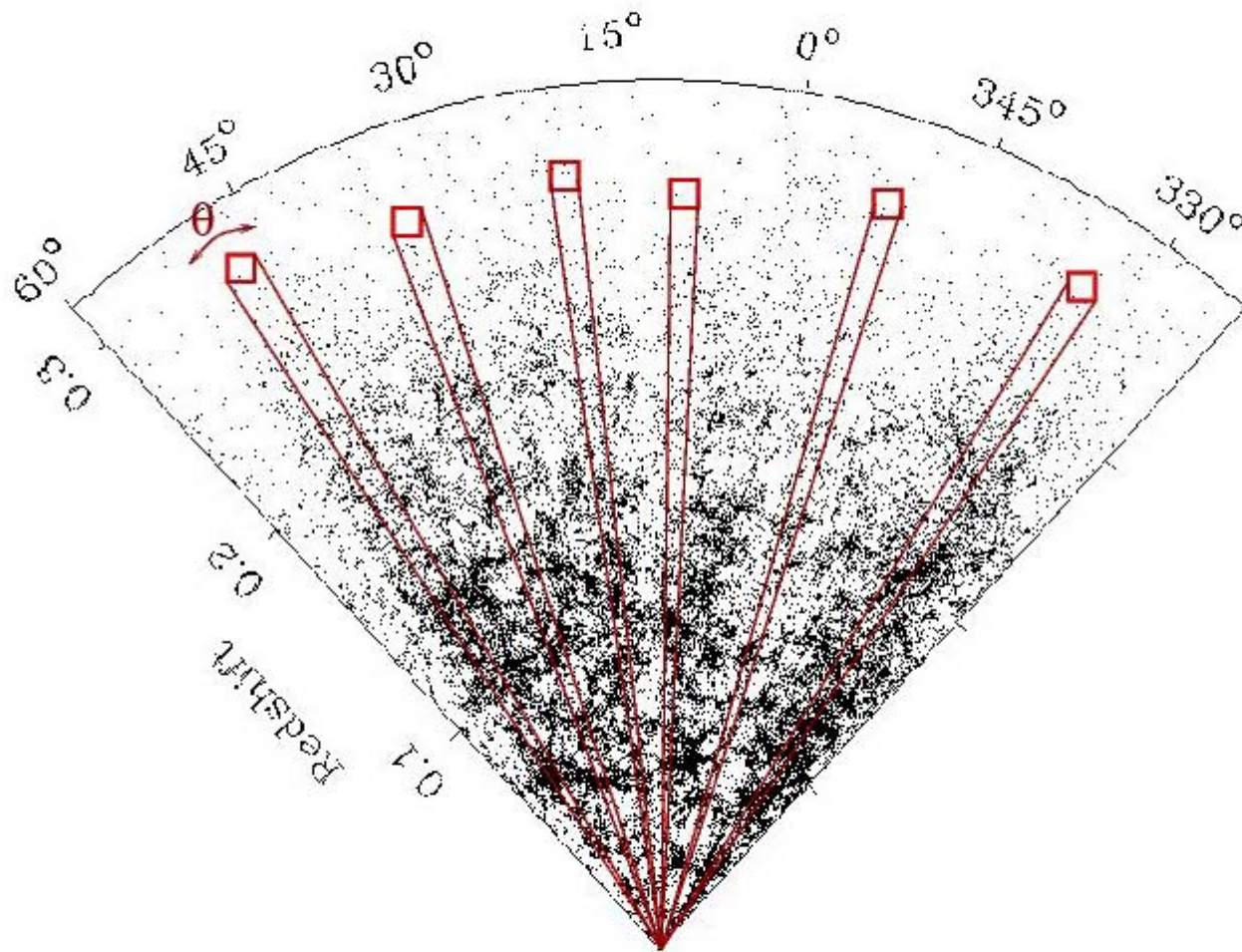


$$\kappa_{eff} = \frac{3H_0^2 \Omega_0}{2c^2} \int_0^\omega \frac{f_K(\omega - \omega') f_K(\omega')}{f_K(\omega)} \frac{\delta[f_K(\omega') \theta; \omega']}{a(\omega')} d\omega'$$

Distances

Power spectrum,  
growth rate of structure

Both depend on the dark matter and dark energy content in the Universe



**MEASURING THE SHEAR ON A GIVEN SCALE  $\Theta$   
ON MANY UNCORRELATED FIELDS**

# Properties of cosmic shear signal

Simple case, assuming a single lens plane and  $P(k) \sim \sigma_8 k^n$

$$\langle \kappa^2(\theta) \rangle^{1/2} \approx C \sigma_8 \Omega_m^{0.8} \left( \frac{\theta}{1\text{deg.}} \right)^{-\frac{n+2}{2}} z_s^{0.75}$$

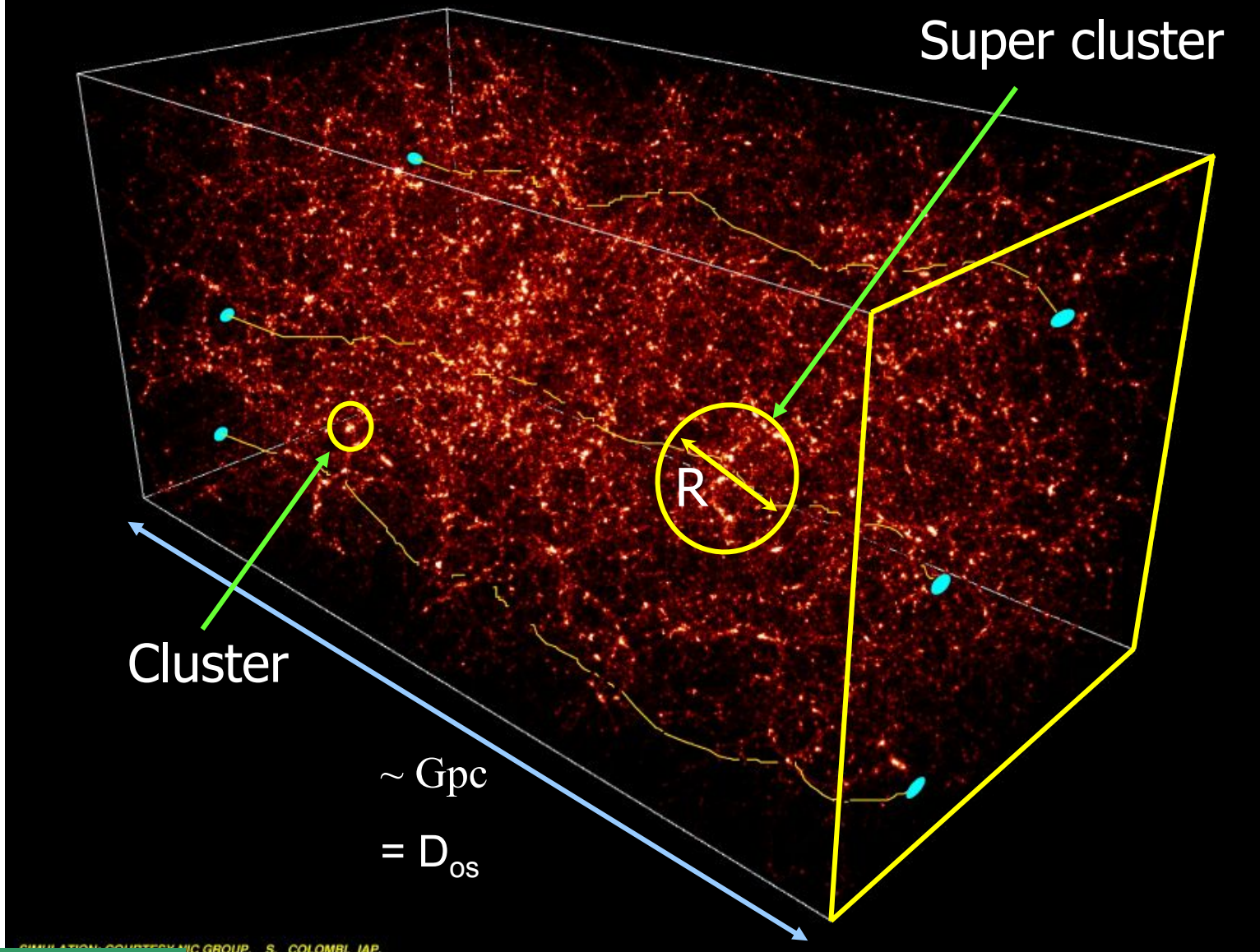
# Properties of cosmic shear signal

Simple case, assuming a single lens plane and  $P(k) \sim \sigma_8 k^n$

$$\langle \kappa^2(\theta) \rangle^{1/2} \approx C \sigma_8 \Omega_m^{0.8} \left( \frac{\theta}{1\text{deg.}} \right)^{-\frac{n+2}{2}} z_s^{0.75}$$

? ....Amplitude of the lensing signal ?

# Mean number of structures crossed by light beams?



# Amplitude of cosmic shear signal

Amplitude for a single perturbation of size R.....

$$\kappa \approx \frac{3}{2} \left( \frac{H_o}{c} \right)^2 \Omega_o \frac{D_{ol} D_{ls}}{D_{os}} \times R \frac{\delta\rho}{\rho}$$

- Net magnification= random cumulative in all directions,
  - After crossing N perturbations with typical size  $R$  .....
- $$N \approx \frac{D_{os}}{R},$$

$$\kappa \approx \frac{3}{2} \left( \frac{H_o}{c} \right)^2 \Omega_o \frac{D_{ol} D_{ls}}{D_{os}} \times R \frac{\delta\rho}{\rho} \times \left( \frac{D_{os}}{R} \right)^{1/2}$$

$$\begin{aligned} <\kappa^2>^{1/2} &\approx \frac{3}{2} \Omega_0 f_{fracHub} \sqrt{\frac{R}{D_{Hubble}}} <\left(\frac{\delta\rho}{\rho}\right)^2>^{1/2} \\ \sim 0.1 &\quad \times \quad \sim 0.1 \quad \text{for supercluster} \quad \times \quad \sim 1 : 1 \% \end{aligned}$$

The diagram illustrates the components of the amplitude equation. It shows three terms circled in different colors (red, yellow, and blue) with arrows pointing from each term to its corresponding value below. The red circle contains the term  $\frac{3}{2} \Omega_0 f_{fracHub}$ . The yellow circle contains the term  $\sqrt{\frac{R}{D_{Hubble}}}$ . The blue circle contains the term  $<\left(\frac{\delta\rho}{\rho}\right)^2>^{1/2}$ .

# Properties of cosmic shear signal

Simple case, assuming a single lens plane and  $P(k) \sim \sigma_8 k^n$

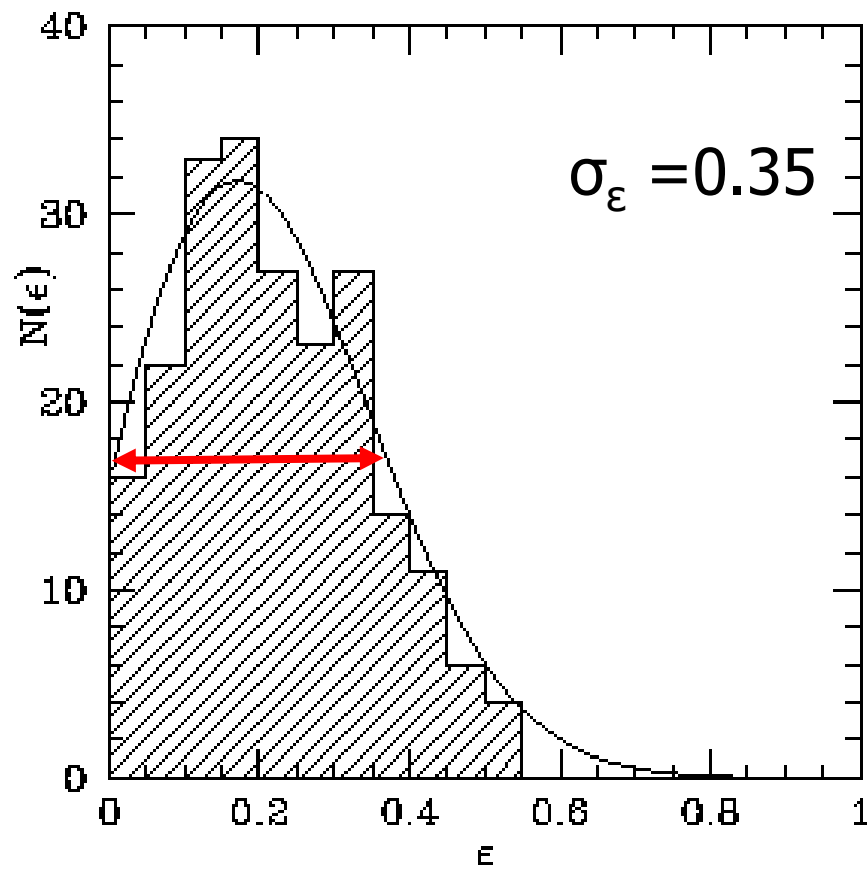
$$\langle \kappa^2(\theta) \rangle^{1/2} \approx 0.01 \sigma_8 \Omega_m^{0.8} \left( \frac{\theta}{1\text{deg.}} \right)^{-\frac{n+2}{2}} z_s^{0.75}$$



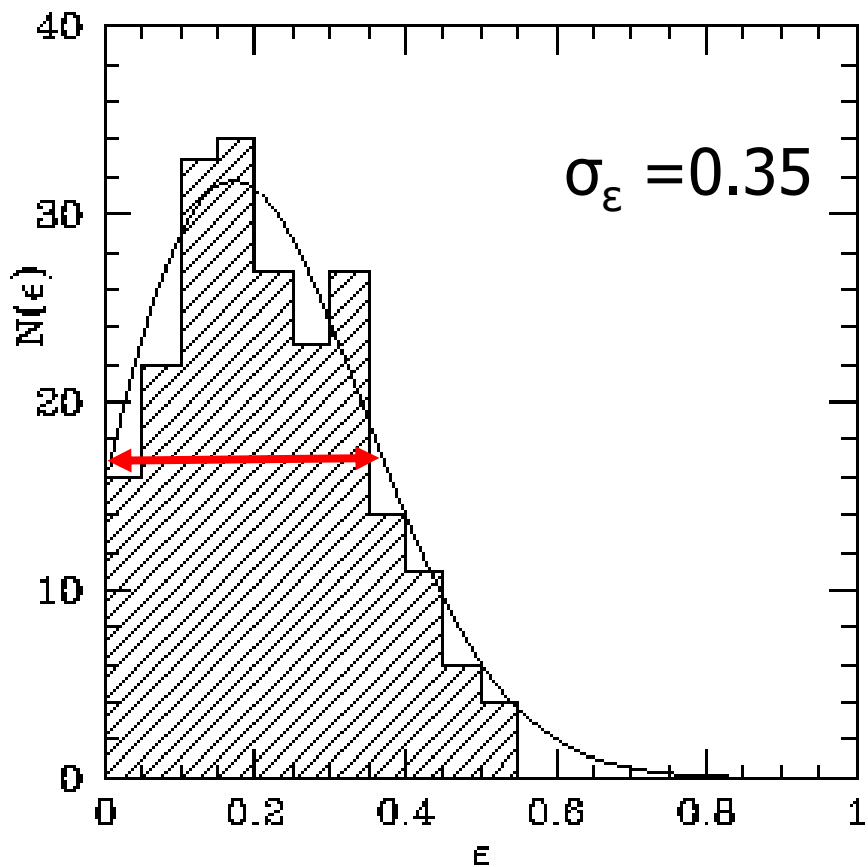
Amplitude of the lensing signal

If shear = ellipticity, then the S/N is basically a comparison with the intrinsic ellipticity distribution of galaxies (projected on the sky)

# Intrinsic projected ellipticity distribution of galaxies



# Beating intrinsic ellipticity distribution



Assume a shear amplitude of 1%

- Minimum number of galaxies
- $n_g = (0.35/0.01)^2$
- About 10000 galaxies just for 3-sigma detection

# Summary

Simple case, assuming a single lens plane and  $P(k) \sim \sigma_8 k^n$

$$\langle \kappa^2(\theta) \rangle = \langle \gamma^2(\theta) \rangle$$

Gravitational convergence      From ellipticities      Gravitational shear = ellipticity induced by gravitational lensing on galaxies

The diagram consists of two boxes. The top box contains the equation  $\langle \kappa^2(\theta) \rangle = \langle \gamma^2(\theta) \rangle$ . The bottom box contains the formula  $\langle \kappa^2(\theta) \rangle^{1/2} \approx 0.01 \sigma_8 \Omega_m^{0.8} \left( \frac{\theta}{1\text{deg.}} \right)^{-\frac{n+2}{2}} z_s^{0.75}$ . A double-headed vertical arrow connects the two boxes. Red arrows point from the text 'Gravitational convergence' to the left side of the top box, and from the text 'Gravitational shear = ellipticity induced by gravitational lensing on galaxies' to the right side of the top box.

$$\langle \kappa^2(\theta) \rangle^{1/2} \approx 0.01 \sigma_8 \Omega_m^{0.8} \left( \frac{\theta}{1\text{deg.}} \right)^{-\frac{n+2}{2}} z_s^{0.75}$$

Width of intrinsic ellipticity distribution of galaxies :  $\sim 30\%$

# Is Cosmic Shear measurable?

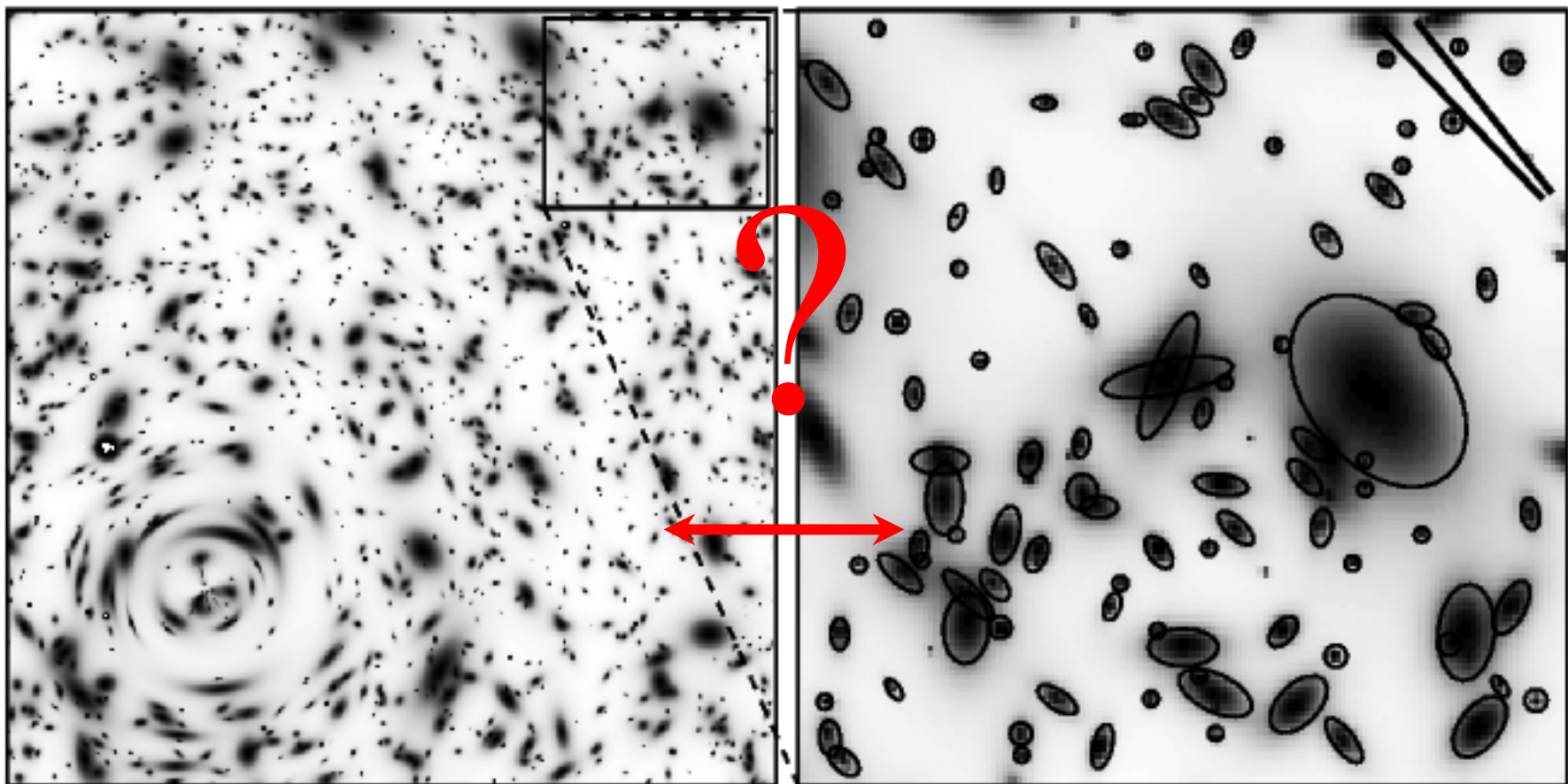
---

$z_s = 1$ , Top Hat Filter ,  $n = 30 \text{ gal.arcmin}^{-2}$

FOV (deg. $\times$ deg.)	S/N Variance $\Omega = 1$	S/N Variance $\Omega = 0.3$	S/N Skewness $\Omega = 1$	S/N Skewness $\Omega = 0.3$
$1.25 \times 1.25$	7	5	1.7	2
$2.5 \times 2.5$	11	10	2.9	4
$5 \times 5$	20	20	5	8
$10 \times 10$	35	42	8	17

# Measuring the distortion of galaxies induced by gravitational shear

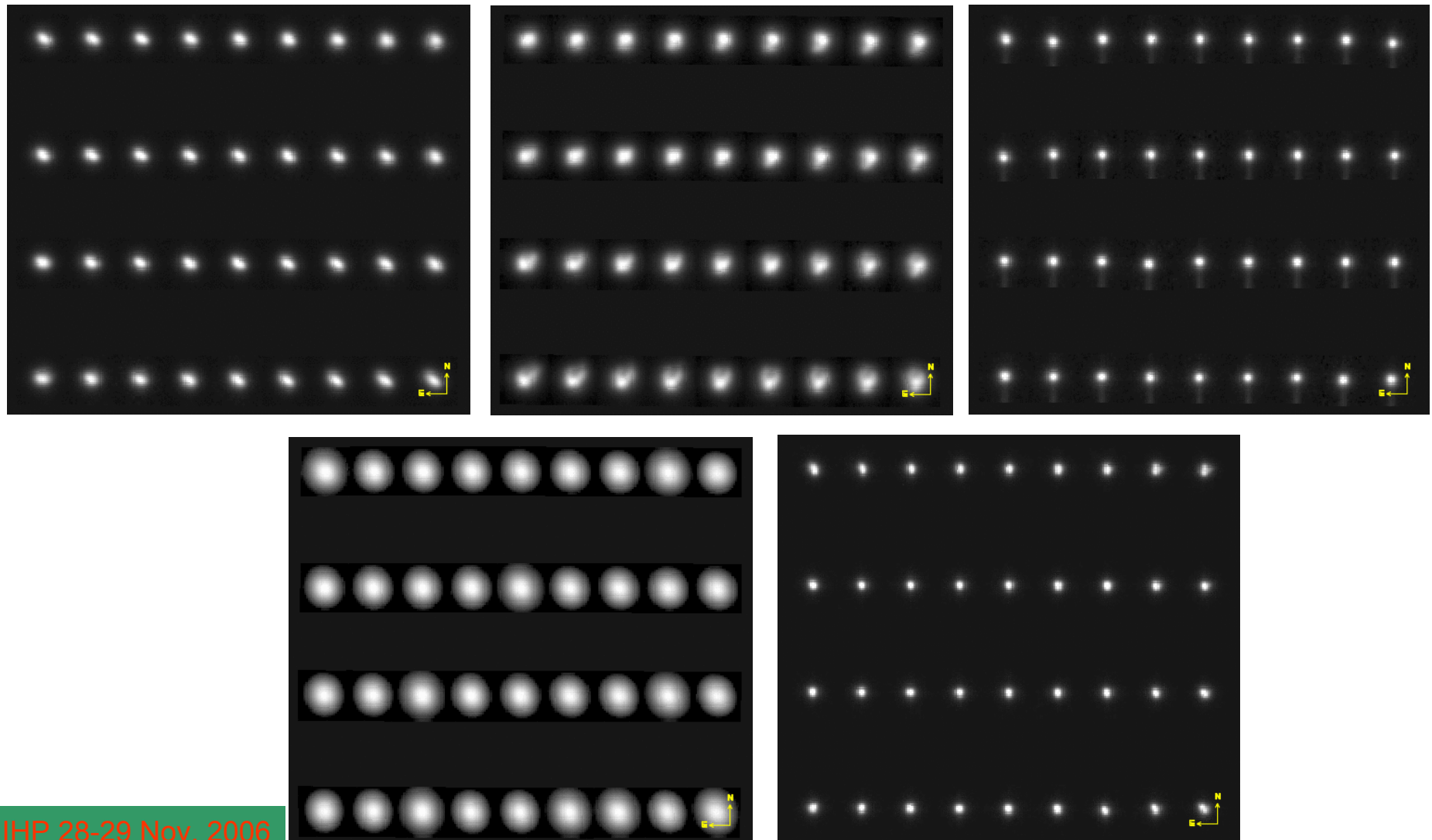
# Measuring weak lensing ⇒ measuring shape of galaxies



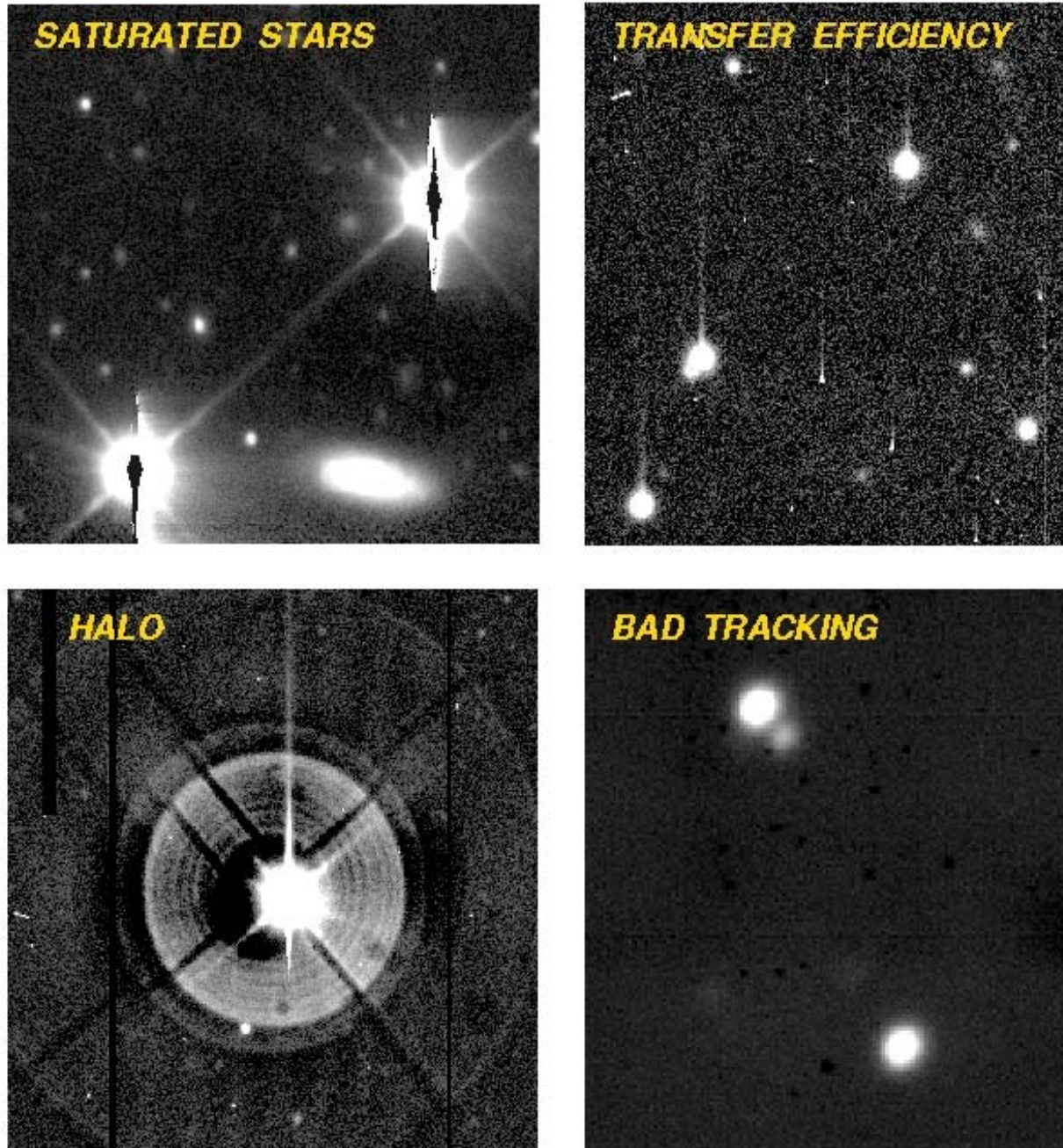
Unfortunately...

Ellipticity is contaminated

# The MegaPrime Point Spread Function (PSF): star analysis over the 36 CCDs of Megacam field



# PSF anisotropy



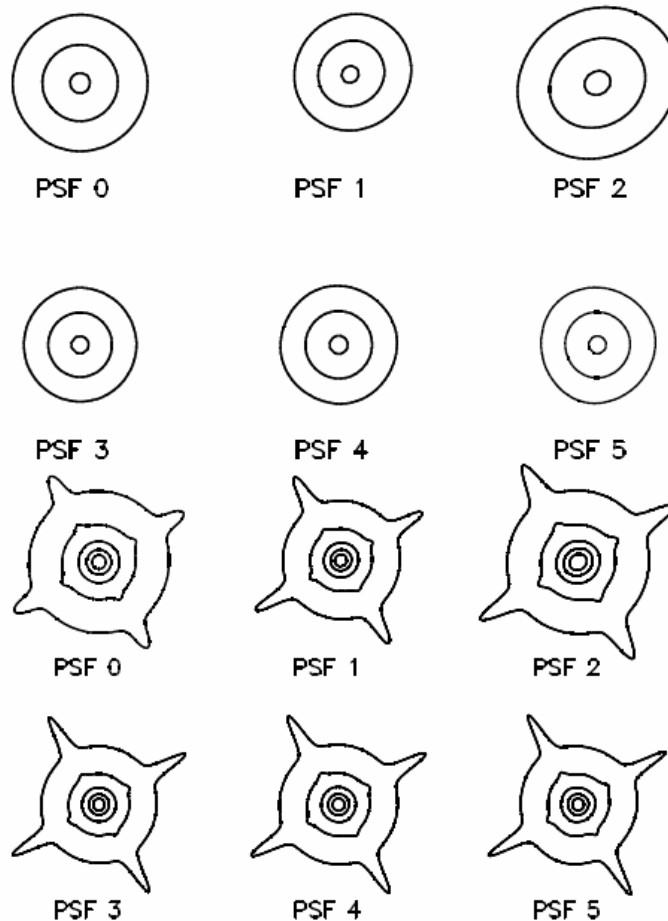
# Non-gravitational PSF

PSF ID	PSF type	Ellipticity
0	no anisotropy	0.00
1	coma	~ 0.04
2	jitter, tracking error	~ 0.08
3	defocus	~ 0.00
4	astigmatism	~ 0.00
5	triangular (trefoil)	0.00

## PSF smearing and anisotropy

### Time varying PSF

- Optical aberrations
- Diffraction limit of the telescope
- Image sampling
- Thermal instability (defocus)
- Detector distortion
- Charge transfer efficiency
- Charge diffusion
- Seeing
- Atmospheric refraction



# Correction needed

But corrections mean

- Noise
- Systematic residuals after correction
- → Quality control and check the correction is robust and reliable

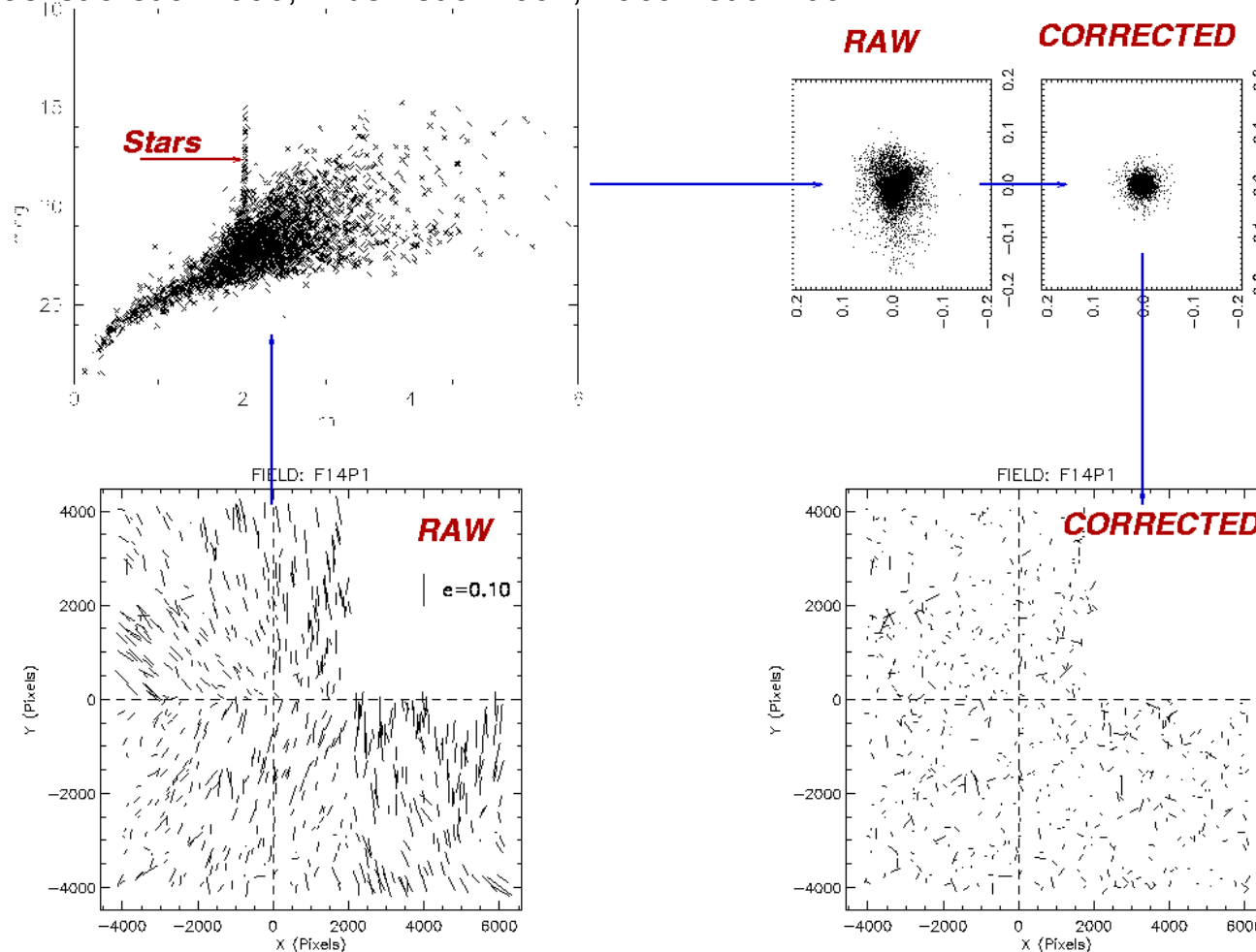
# Correction : principle

- Find objects that
  - are not lensed
  - are distorted by all other effects

→ **stars**
- Find the corrections to apply to each star at each star position
- Interpolate the correction for any field position
- Apply the correction to galaxies

# Using stars for the PSF correction

Hoekstra et al 2000, Erben et al 2001, Bacon et al 2001



Fahlman et al 1994, Bonnet & Mellier 1994, Mould et al 1994, KSB 1995, Kuijken 1999, Refregier et al 2001, Bernstein et al 2001

# Correction : principle

- Since need to extrapolate, the more stars you have, the better the sampling of the field is, the more accurate the extrapolation and the correction are... so...
- Go to crowded star fields!! Choose the galactic bulge!
- Unfortunately, the more stars you have the more likely you will find very bright stars: CCD saturation, ghosts, scattering
- On an the less crowded fields: already one 8<sup>th</sup>-mag. star per deg<sup>2</sup>
- So... better to go to empty fields... at the expense of the star sampling... : noise
- Moreover, the star density is not totally uniform: noise

# The PSF correction

- The key technical and most debated problem of weak lensing over the past 5 years
- Several methods used, more or less successful
- No brute force deconvolution possible (time consuming on Tera-bytes of images, no clear convergence criteria, very sensitive to the noise and PSF variation)

# PSF corrections

## Heuristic methods (early works)

Valdes & Tyson (1987): FOCAS shape analysis (subtraction of second moments)

Bonnet & Mellier (1993): shape filtered in a annulus+cutoffs. Calibrated with simulations.

Mould et al (1994): FOCAS shape analysis (subtraction second moments with regression)

## Statistics on images and first order corrections

KSB (1994): perturbative method. Weighted second moment in circular Gaussian with adapted size. Linear decomposition of the isotropic and anisotropic PSF terms+filter+weightings

Kaiser (2000): PSF model and PSF circulation process

Kuijken (1999): multiple Gaussian decomposition

## PSF model fitting + deconvolution

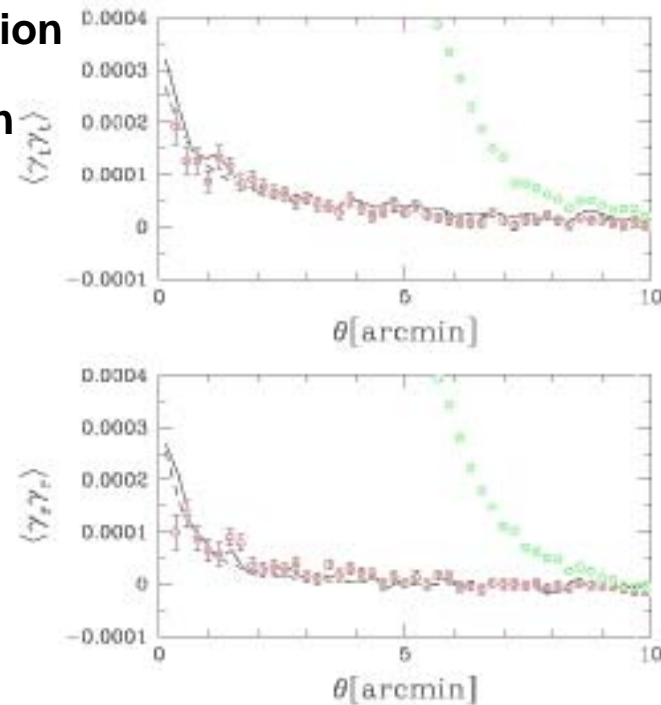
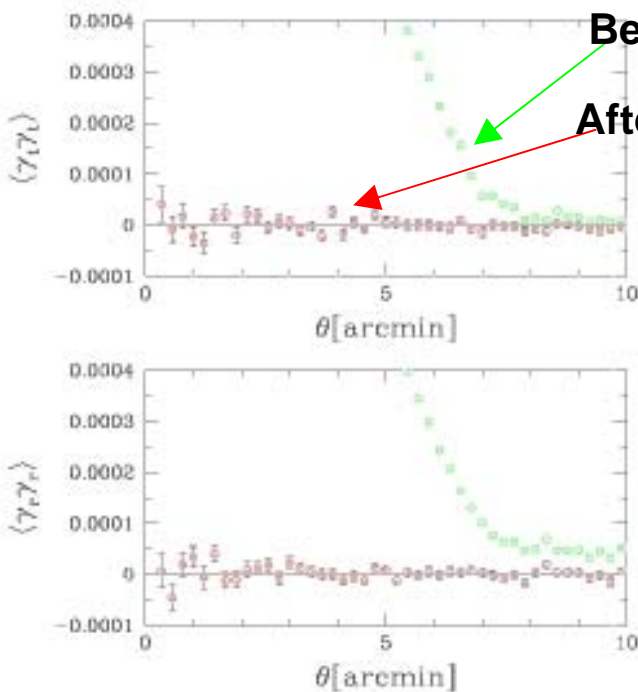
Réfrégier & Bacon (2002): shapelet decomposition and PSF model fitting deconvolution

Bernstein & Jarvis (2002): Laguerre expansion + adaptive elliptical weight

Bridle (2002): Gaussian decompostion

Kuijken (2005): shapelet decompostion

# Example : Simulated cosmic shear survey analysed with KSB



# PSF correction

Best techniques can measure weak lensing with enough accuracy (i.e. accuracy requested for today scientific goals)

But controls of systematics and the quality of PSF correction must be demonstrated for each survey

Minimum that MUST be done:

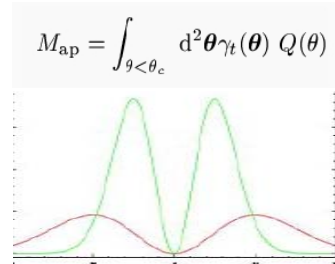
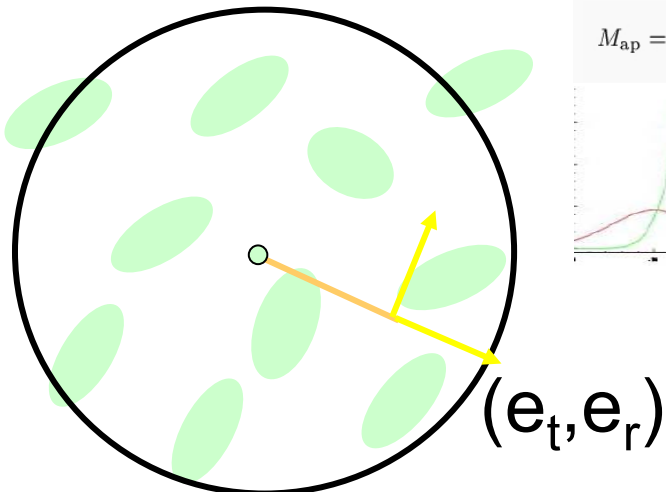
B-modes : curl terms

uncorrected stars/corrected galaxy cross correlations :  
check the extrapolation between stars (1 star per arc-min<sup>2</sup>  
only, but 20 galaxies per arc-min<sup>2</sup>)

# Weak lensing : results

# Analysing the galaxy ellipticity: 2-points statistics

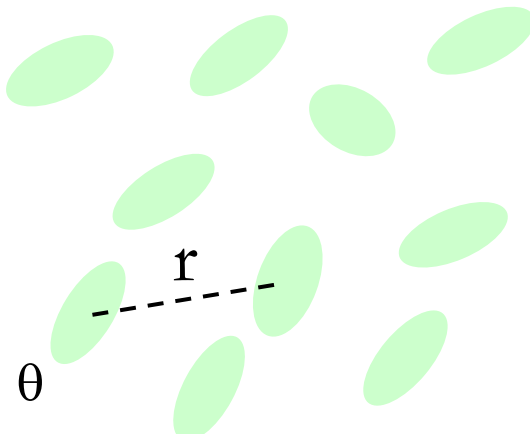
## Map variance



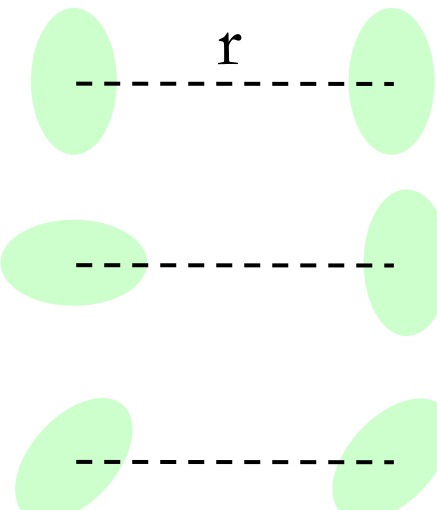
## Shear variance:



$$\langle e^2 \rangle \sim \gamma^2$$



## Shear correlation functions:

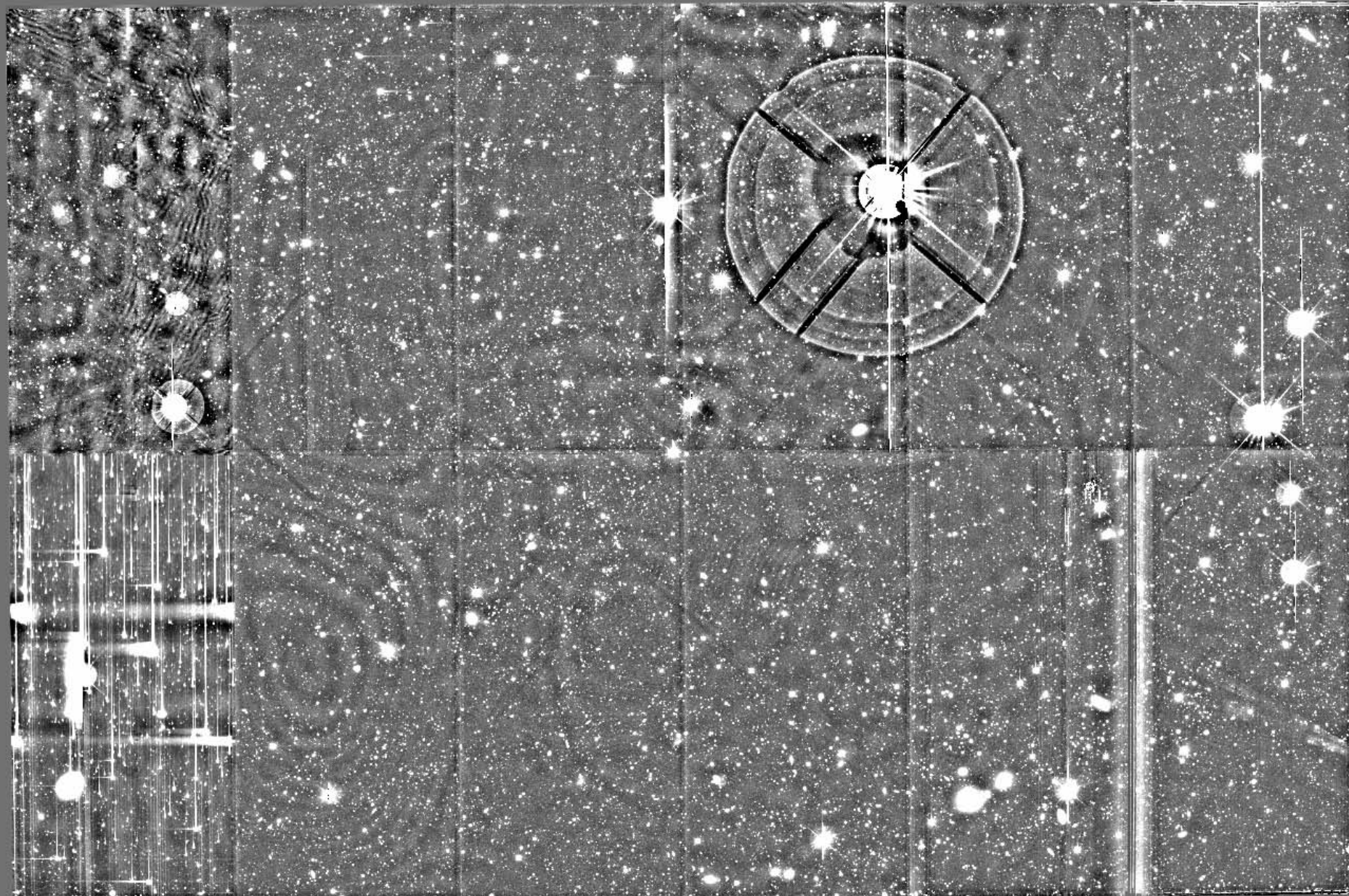


$$\langle \gamma_t \gamma_t \rangle > 0$$

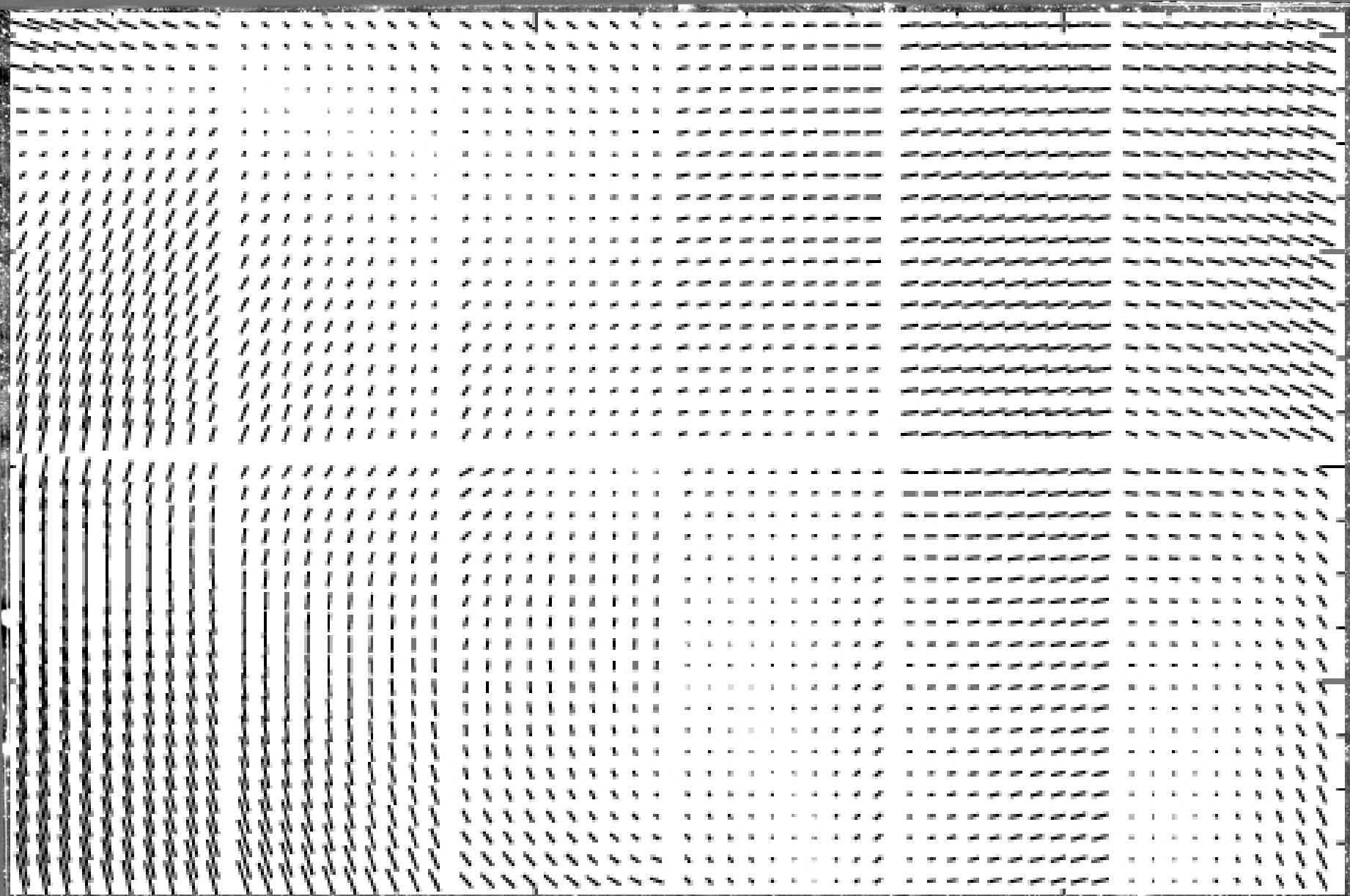
$$\langle \gamma_t \gamma_t \rangle < 0$$

$$\langle \gamma_r \gamma_r \rangle > 0$$

# A look at the real data...



# A look at the real data...



## Measuring shear signal in practice

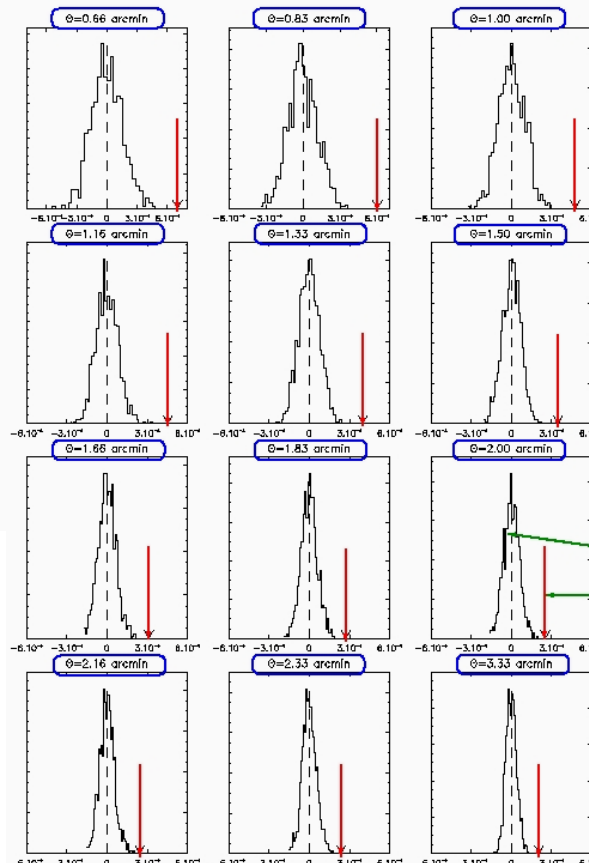
$$E[\gamma^2(\theta_i)] = \frac{\sum_{\alpha=1}^2 \sum_{k \neq l}^{N_i} w_k w_l e_{\alpha}^{\text{gal}}(\theta_k) e_{\alpha}^{\text{gal}}(\theta_l)}{\sum_{k \neq l}^N w_k w_l},$$

$$E[M_{\text{ap}}^2(\theta_i)] = \frac{\sum_{k \neq l}^{N_i} w_k w_l e_t^{\text{gal}}(\theta_k) e_t^{\text{gal}}(\theta_l) Q(\theta_k) Q(\theta_l)}{\sum_{k \neq l}^N w_k w_l},$$

$$E[\gamma\gamma; \theta] = \sum_{\alpha=1}^2 \frac{\sum_{\text{pairs}} w_k w_l e_{\alpha}^{\text{gal}}(\theta_k) e_{\alpha}^{\text{gal}}(\theta_l)}{\sum_{\text{pairs}} w_k w_l}.$$

Detection level: 5.5- $\sigma$

# Measuring cosmic shear



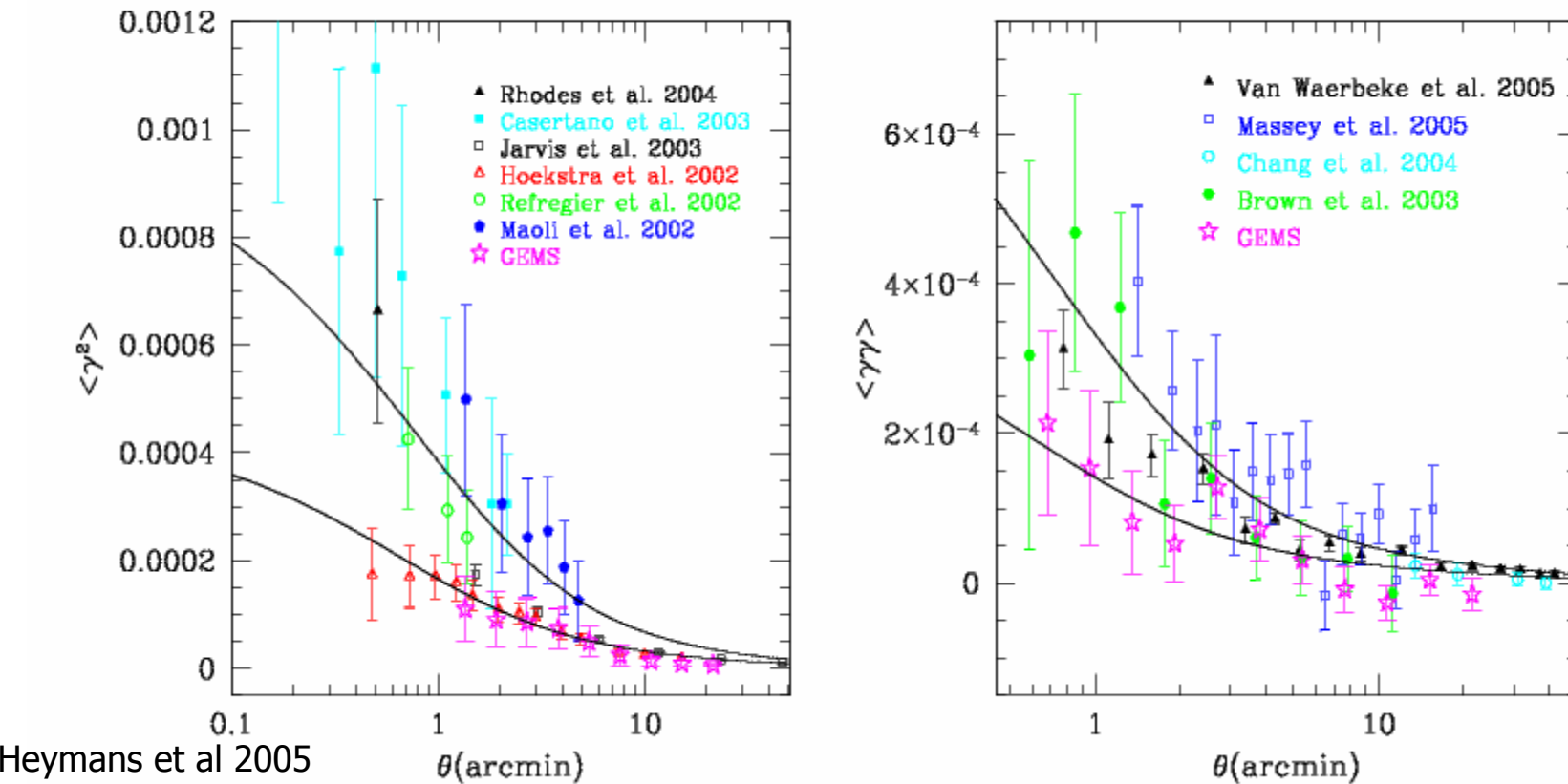
VAN WAERBEKE et al (2000)

*Amplitude of the measured signal as function of the smoothing scale for the CFH12K data.*

*Histograms: randomised catalogs.  
Red arrows: signal measured.*

Van Waerbeke et al 2000

# Top-hat and shear correlation functions from recent space or ground-based weak lensing surveys

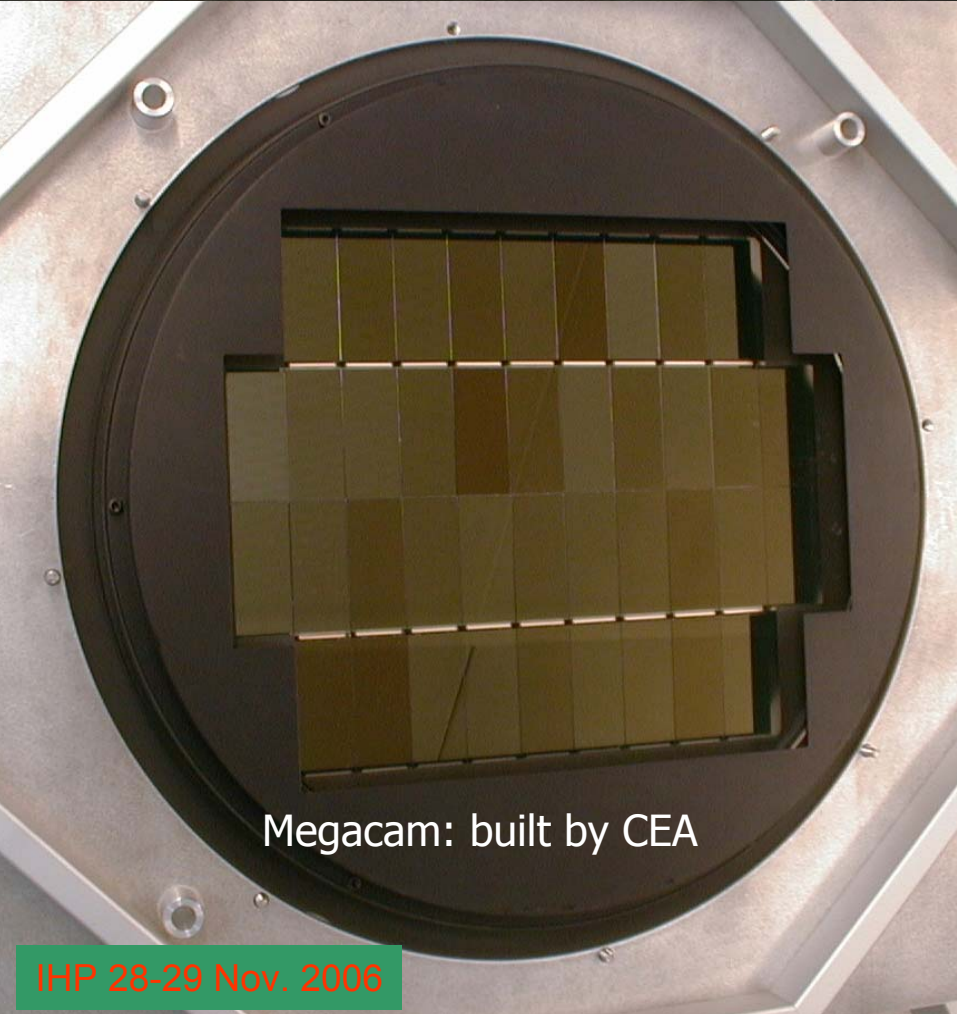


## An example:

### The Canada France Hawaii Telescope Cosmic Shear Legacy Survey (CSLS)

K. Benabed (IAP), F. Bernardeau (CEA/SPhT), A. Benjamin (UBC, Vancouver), J? Coupon (IAP), L. Fu (IAP), S. Gwyn (U. Victoria), C. Heymans (UBC Vancouver), H. Hoekstra (U. Victoria), M. Hudson (U. Waterloo), R. Maoli (IAP), Y. Mellier (IAP), L. Parker (U. Waterloo), U.L. Pen (CITA), C. Schimd (CEA/SPP+IAP), E. Semboloni (IAP), I. Tereno (IAP), L. van Waerbeke (UBC, Vancouver), J.-P. Uzan (IAP)

CFHT telescope: built and operated by CNRS/INSU, CNRC et UH



Megacam: built by CEA



MegaPrime: CNRS/INSU, CNRC, UH

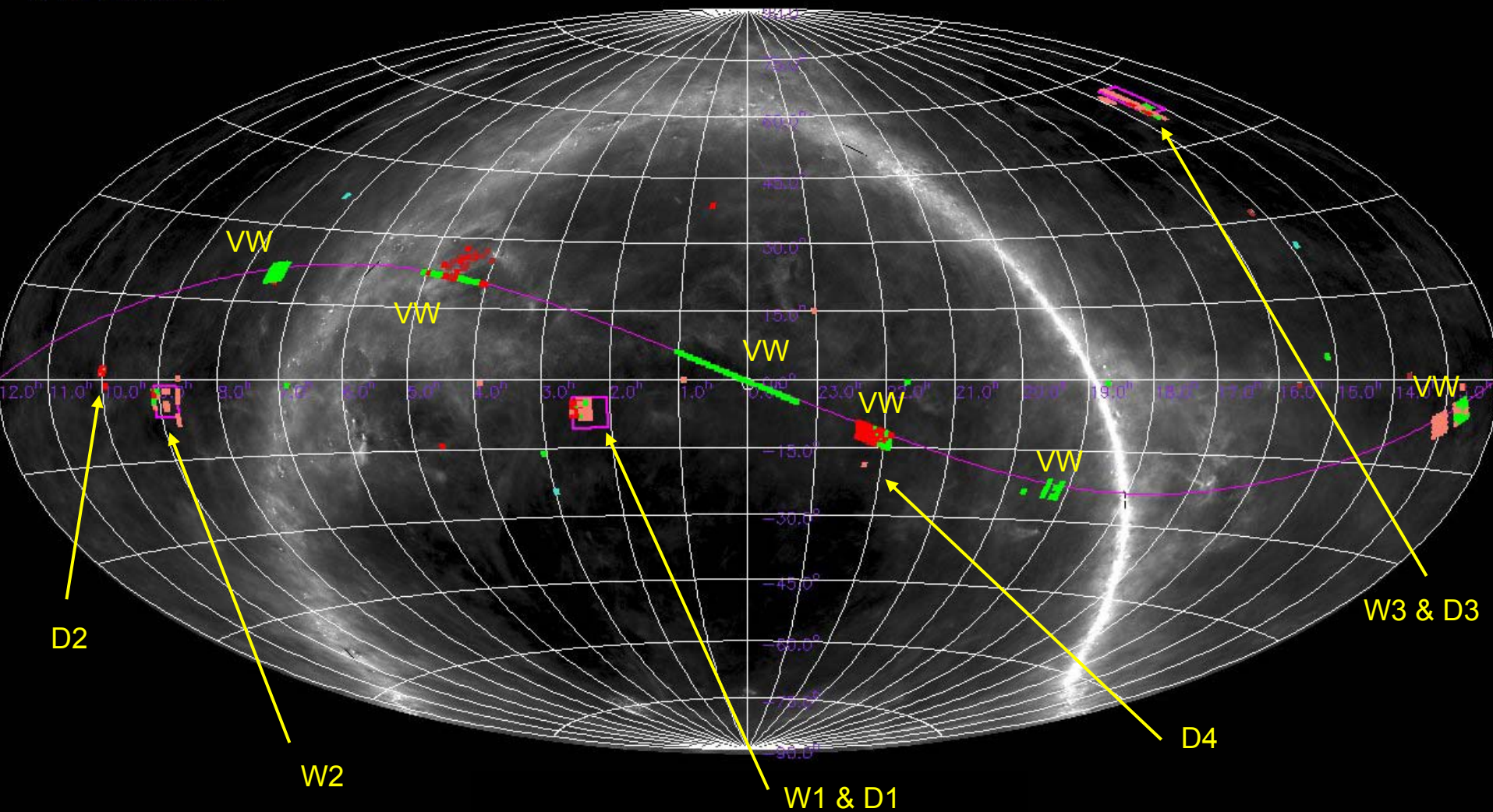
Data processed and released by Terapix.  
Archived at CADC



# Canada-France-Hawaii Telescope Legacy Survey: Canada-France collaboration

Legend  
--- g  
--- i  
--- r  
--- u  
--- z

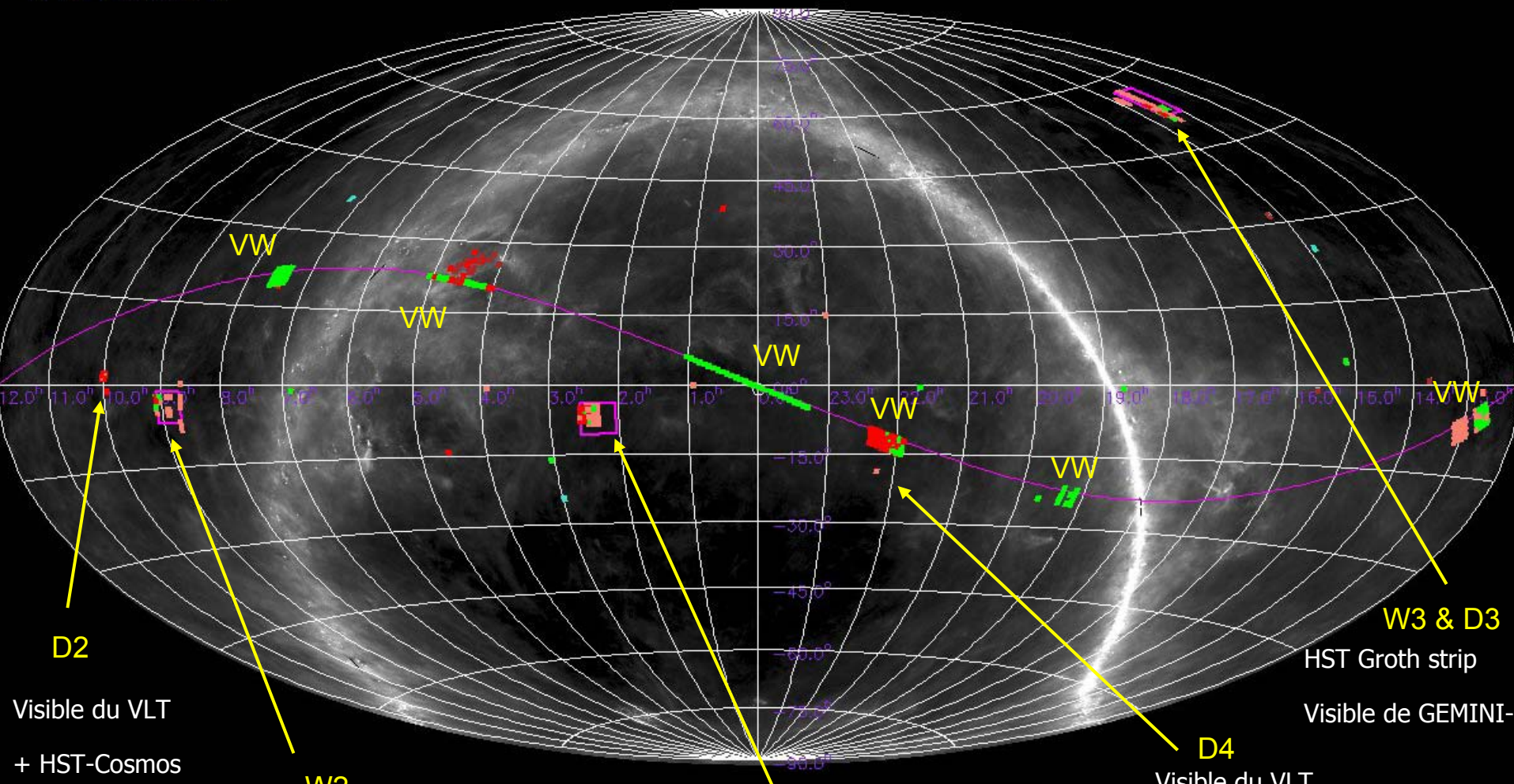
- 3 champs W de  $50 \text{ deg}^2$  (CFHTLS-Wide), 4 champs de  $1 \text{ deg}^2$  (CFHTLS-Deep)
- 500 nuits entre Juin 2003 and Juin 2008 (temps de télescope CNRS/INSU+CNRC)





# Canada-France-Hawaii Telescope Legacy Survey: Canada-France collaboration

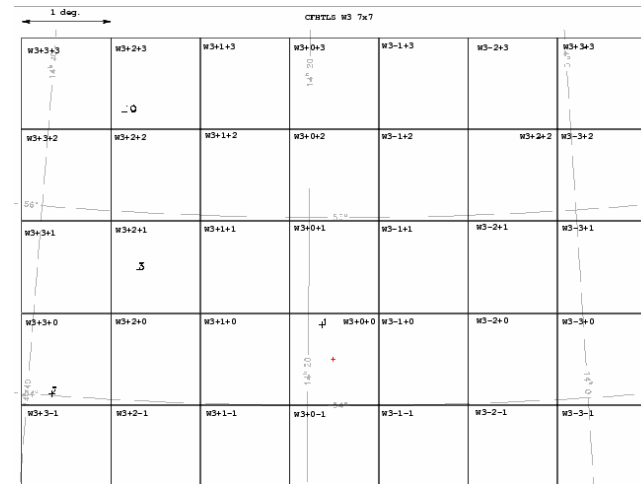
- 3 champs W de  $50 \text{ deg}^2$  (CFHTLS-Wide), 4 champs de  $1 \text{ deg}^2$  (CFHTLS-Deep)
- 500 nuits entre Juin 2003 and Juin 2008 (temps de télescope CNRS/INSU+CNRC)



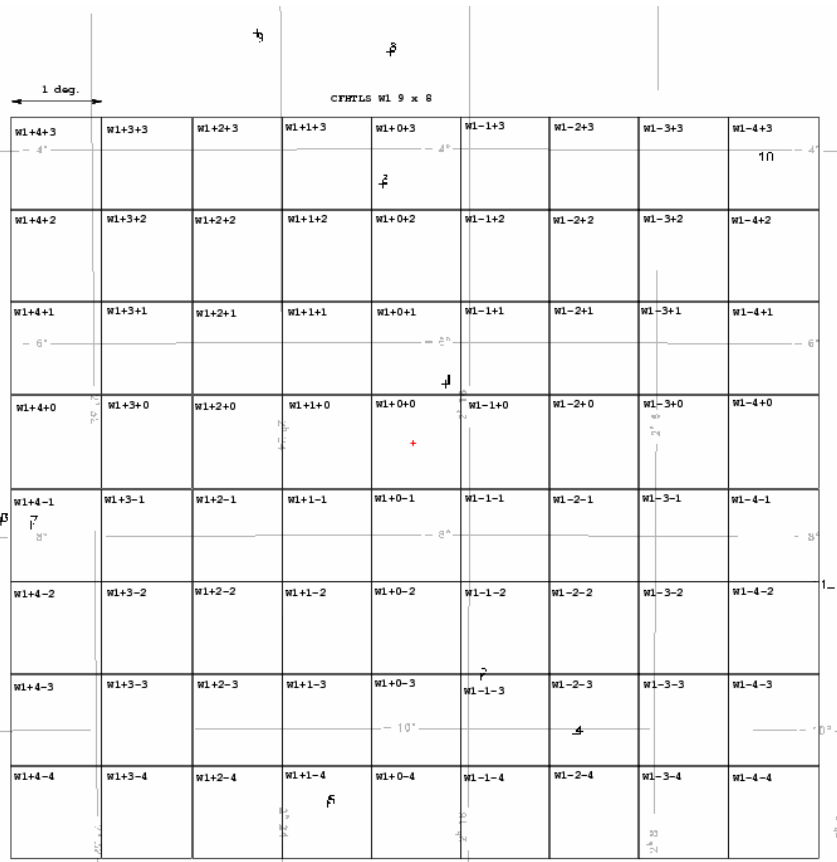
# CFHTLS Wide

$u^*$	$g$	$r$	$i$	$z$
6000s	2500s	2000s	4300s	7200s
26.40	26.60	25.90	25.50	24.80

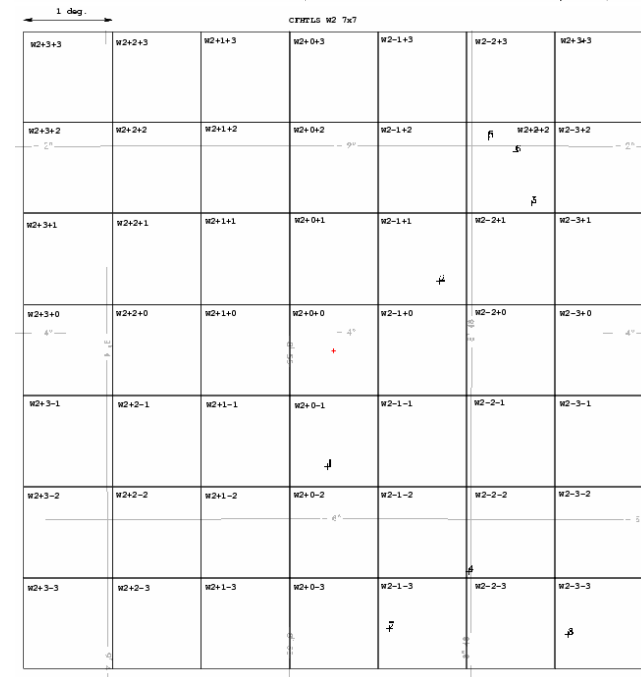
W3: 7x7



W1: 9x8

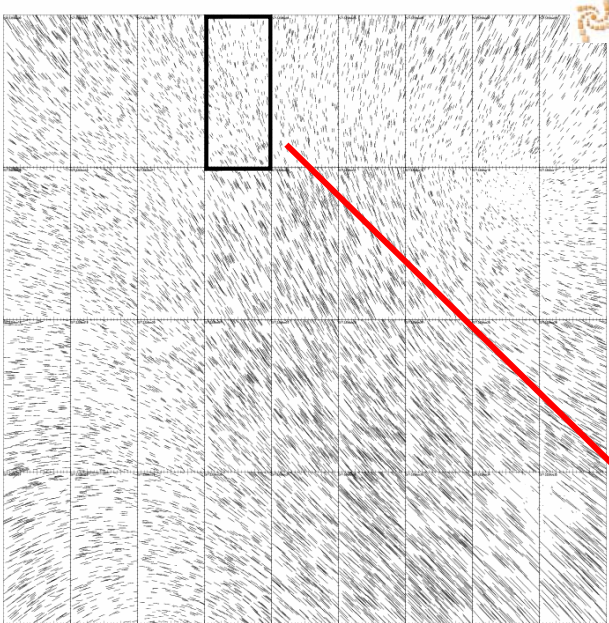


W2: 7x7



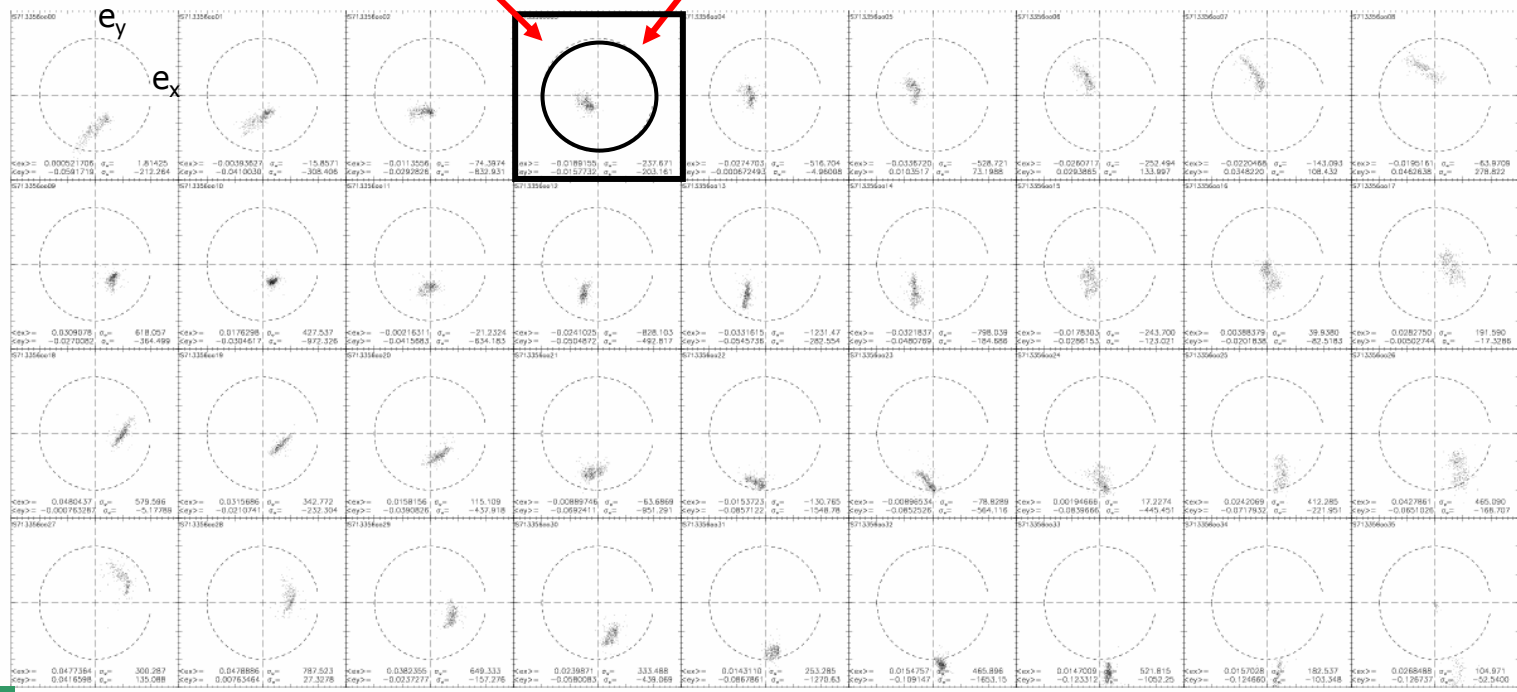
# MegaPrime image quality and weak lensing specifications:

a concern: may produce strong systematics



Megacam field:  
shape of stars

Amplitude of PSF anisotropy must be inside the circle.  
Otherwise star ellipticity is too large to be corrected with  
enough accuracy for cosmic shear.

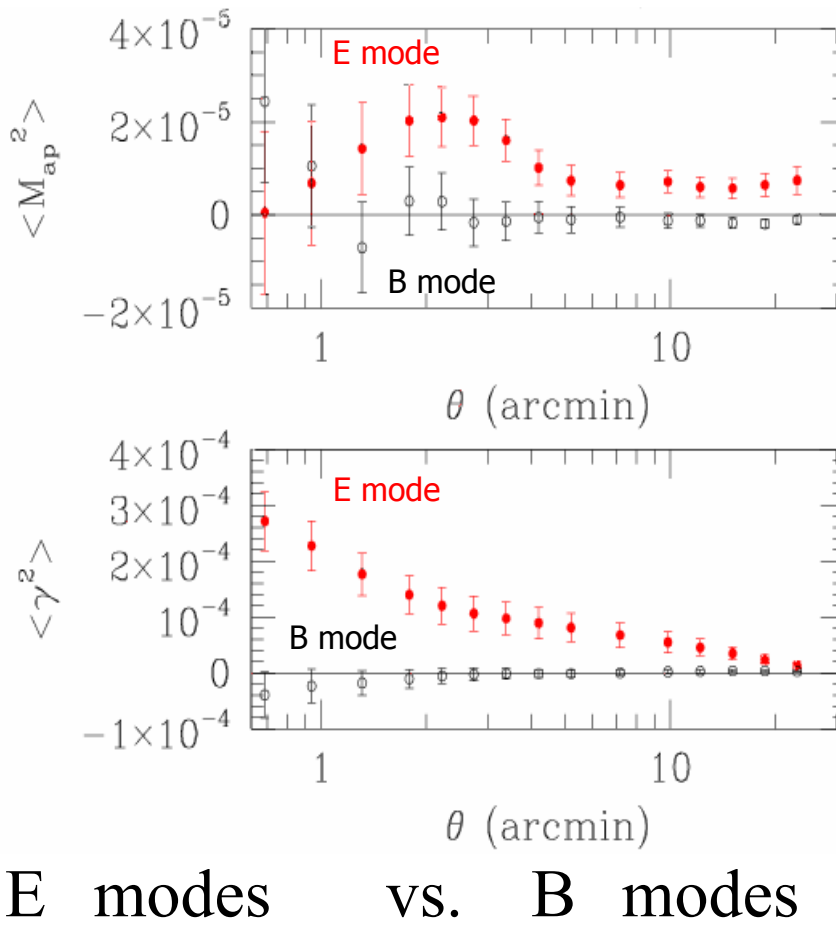


# Reliability of Cosmic shear with CFHTLS data

- 2 independent pipelines:
  - One in Canada (UVic+UBC+Waterloo), one in France (IAP)
  - Each pipeline does astrometric calibration and image stacking differently
  - Two different IMCAT version used
- Both pipelines check B-modes .
- Both used 3 different cosmic shear statistics
- Cross-check: shapes and amplitudes are similar for the 2 pipelines.
- Deep: check achromaticity using  $i$  and  $r$  data independently
- Check with past results (VIRMOS-Descart)

# Cosmic shear in CFHTLS Deep fields

(Terapix release T0001)

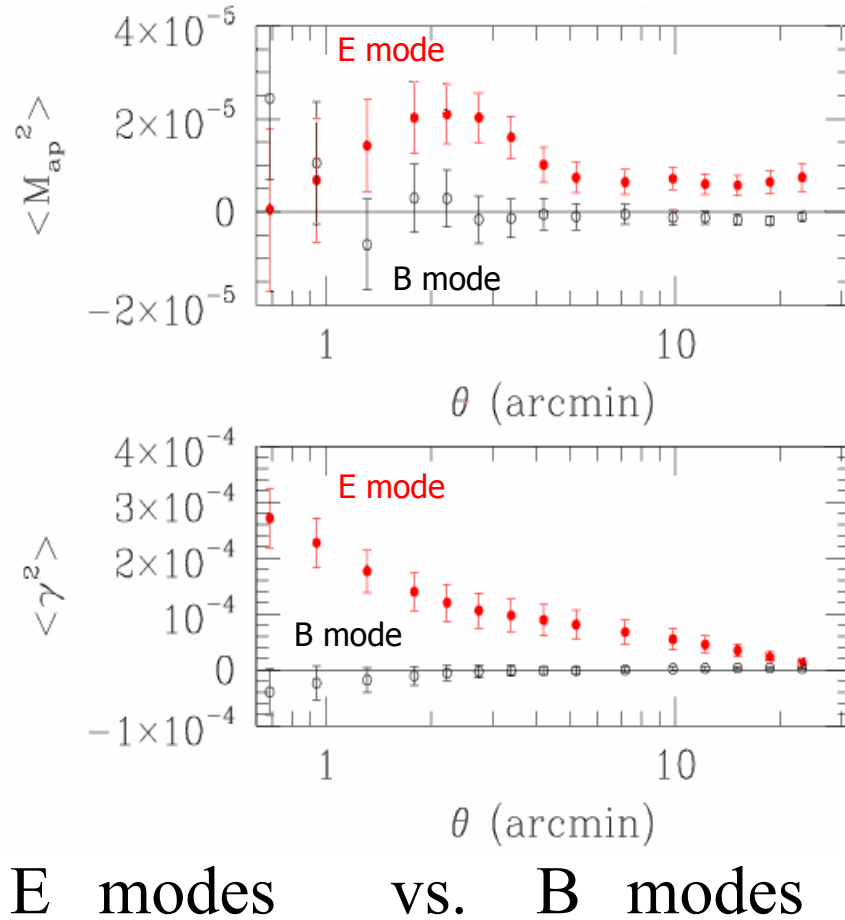


- ✓ Area about 2.1 degrees<sup>2</sup>
- ✓ Magnitudes objects:  $21.5 < R < 25.5$
- ✓ Density of 23 gal /arcmin<sup>2</sup>

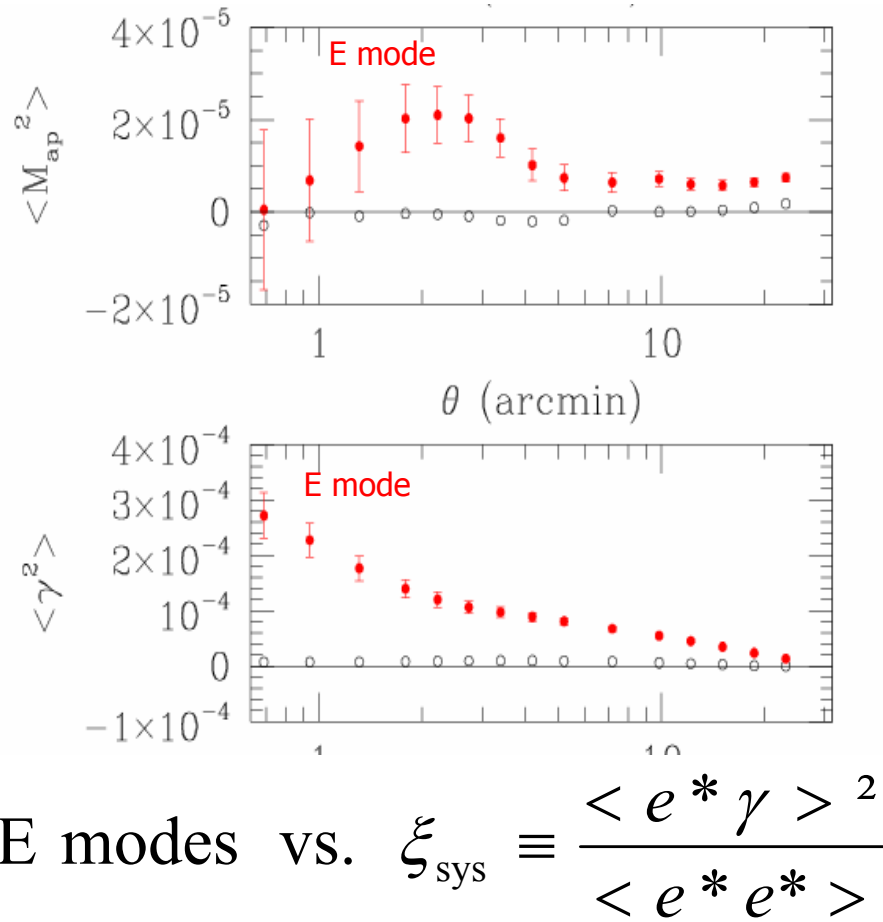
Semboloni et al 2006

# Cosmic shear in CFHTLS Deep fields

(Terapix release T0001)

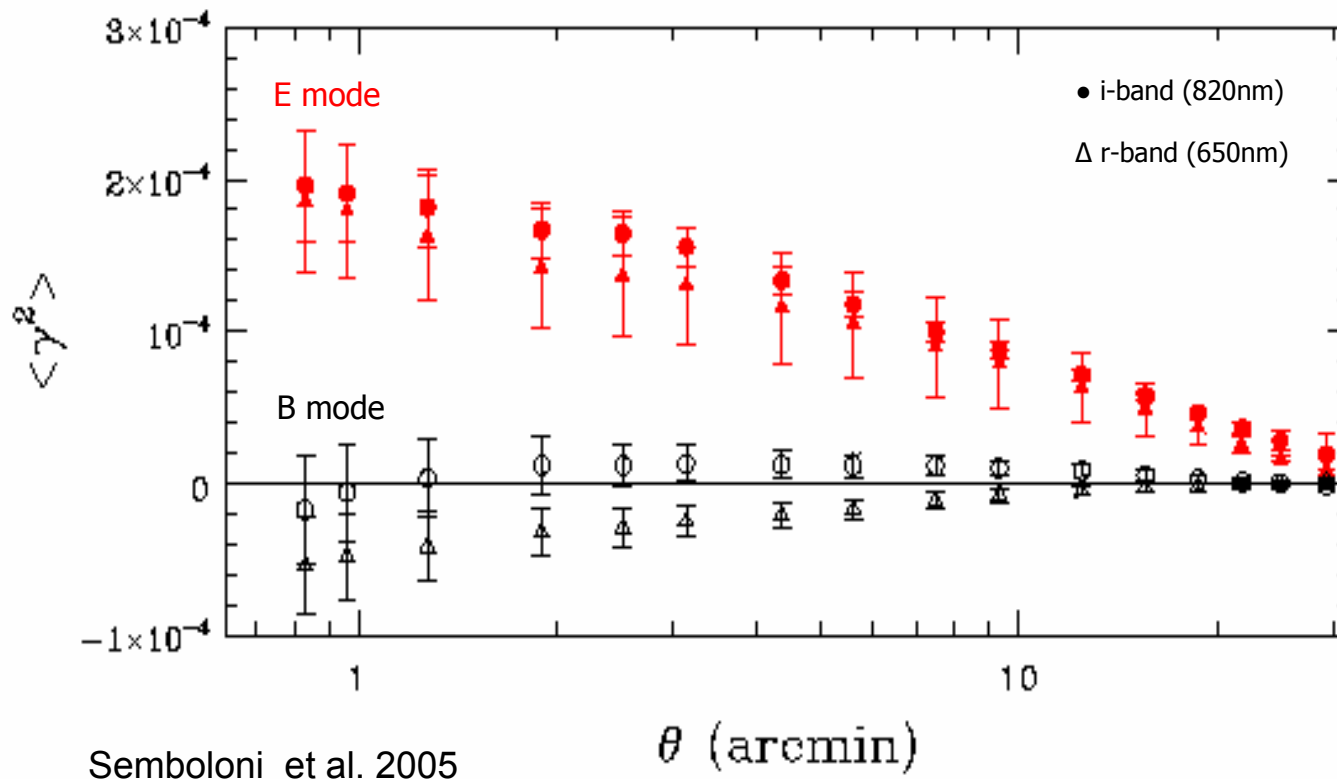


- ✓ Area about 2.1 degrees<sup>2</sup>
- ✓ Magnitudes objects: 21.5 < R < 25.5
- ✓ Density of 23 gal /arcmin<sup>2</sup>



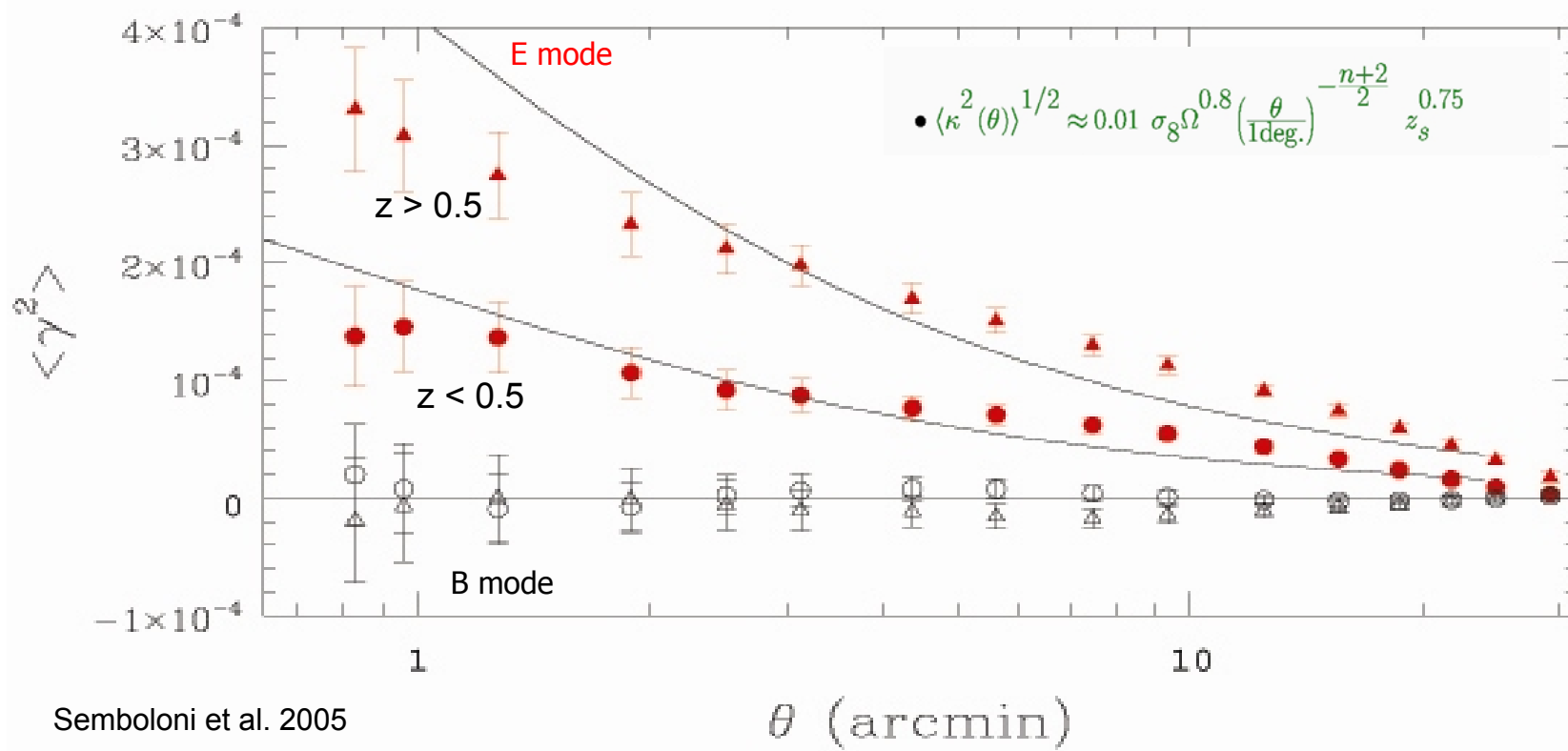
Semboloni et al 2006

# Comparing signal in $r$ and $i$ bands: achromatic effect confirmed

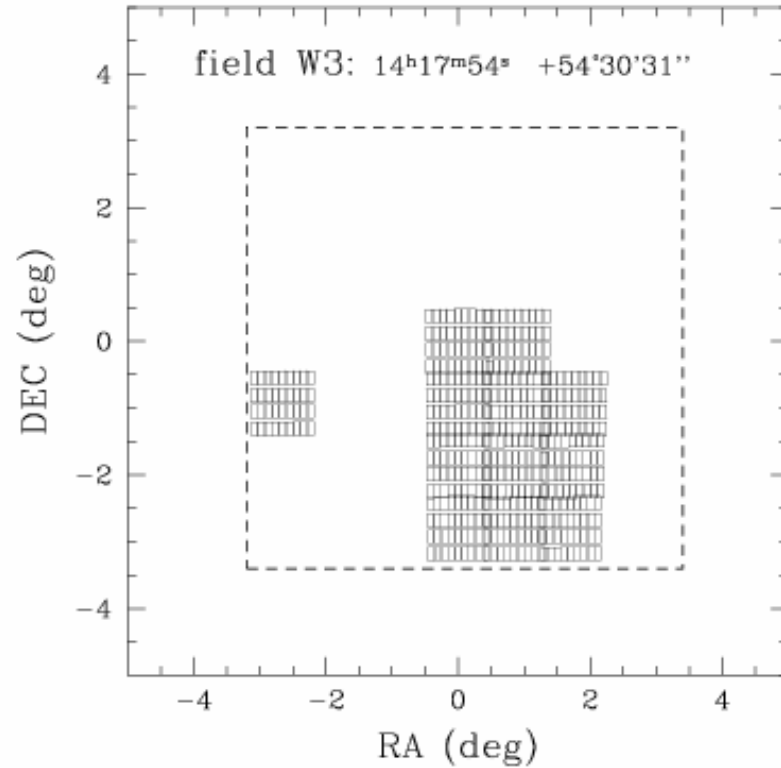
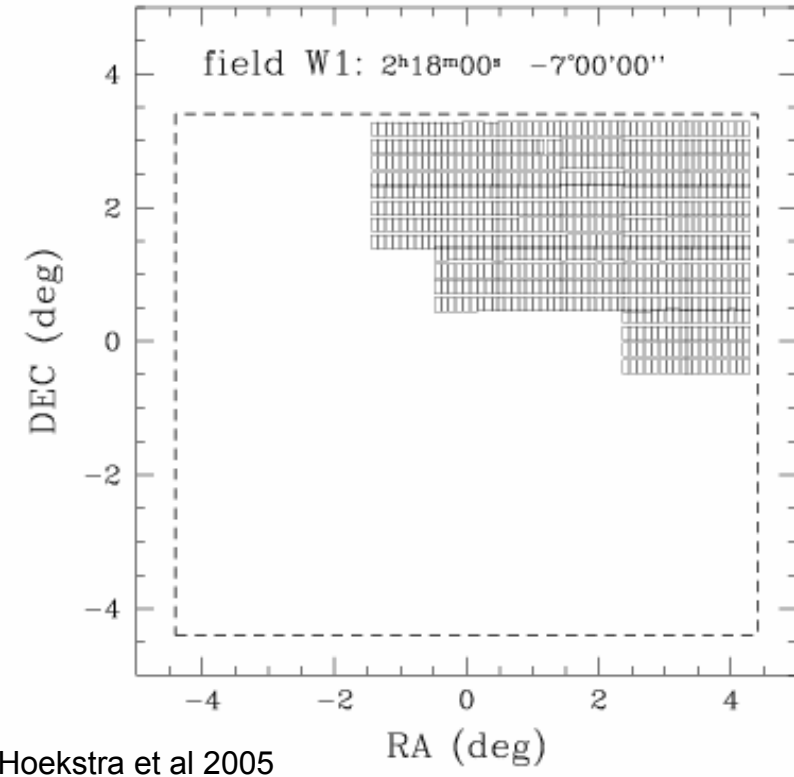


- $i$  and  $r$  band processed independently
- Comparison catalogues contain the same galaxies

# Signal evolution with redshift: cosmological nature of the lensing signal



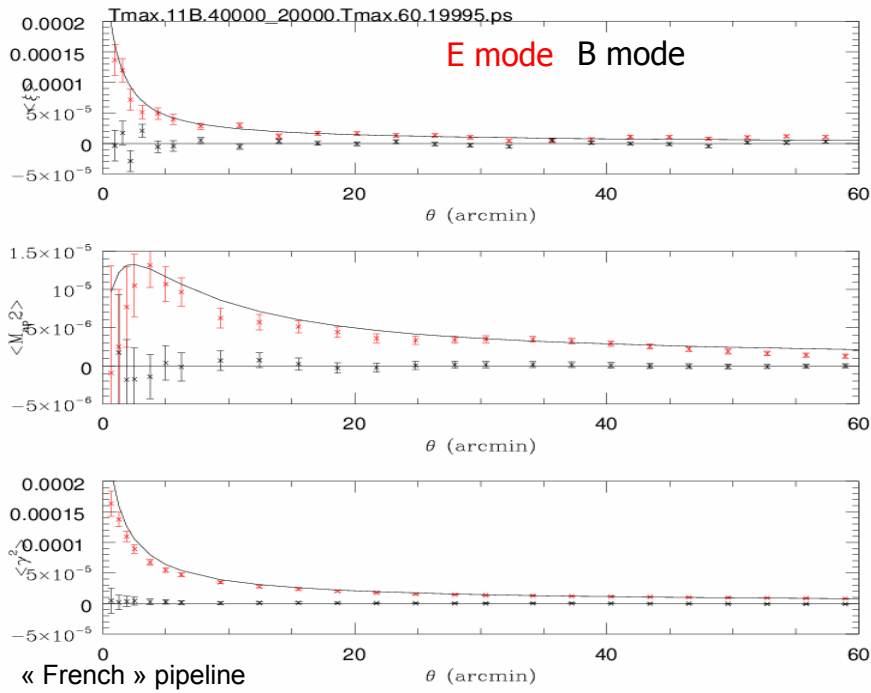
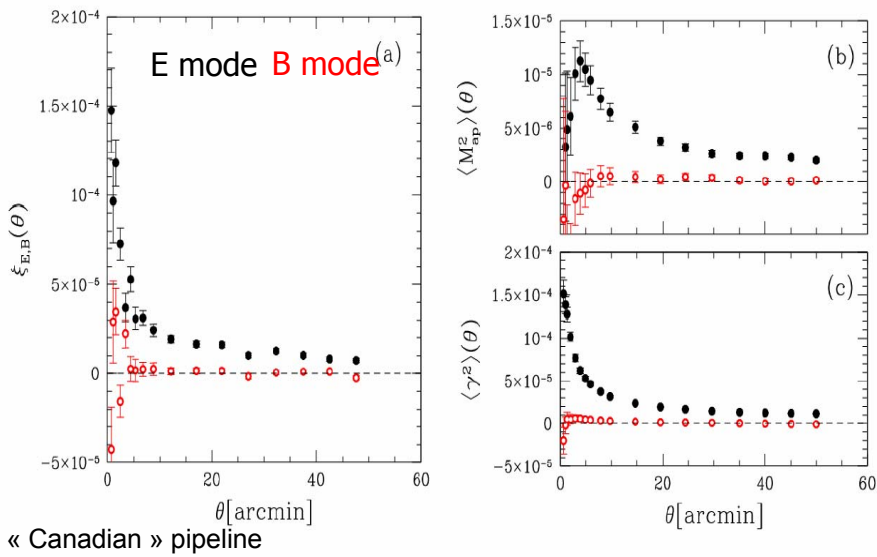
# Cosmic shear with CFHTLS Wide



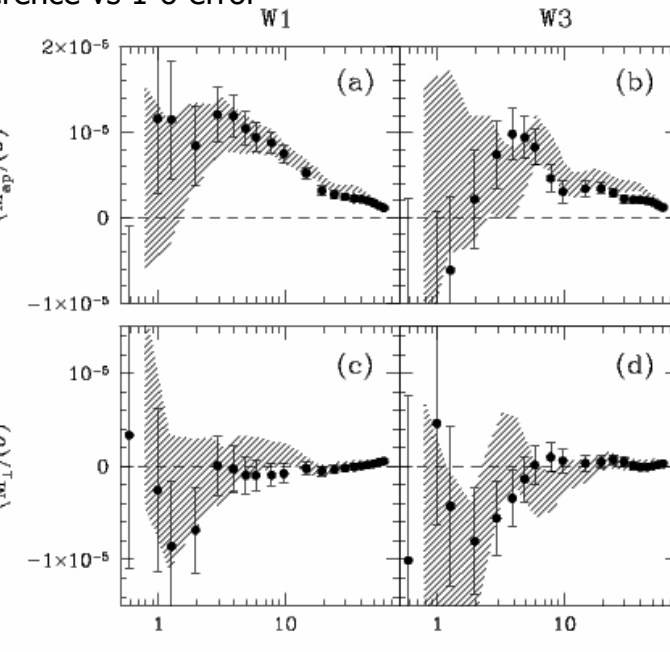
Total:  $\sim 25 \text{ deg}^2$

# Cosmic shear in CFHTLS wide:

2 independent pipelines  
same results



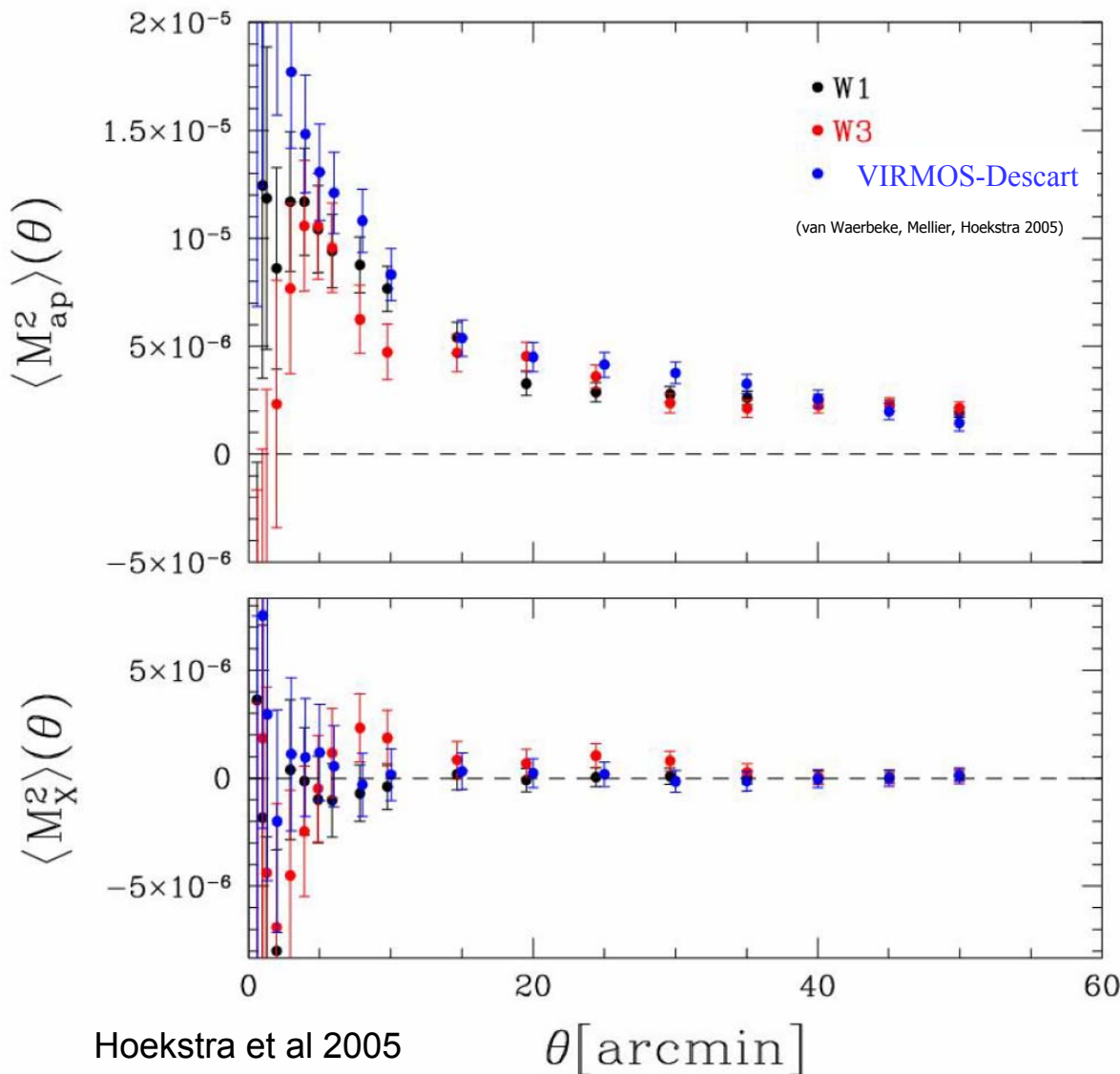
Difference vs 1- $\sigma$  error



Hoekstra et al 2005

Data processed and stacked in 3 different ways, cosmic shear analysed by 2 different pipelines

# Comparison with the VIRIMOS-Descart survey



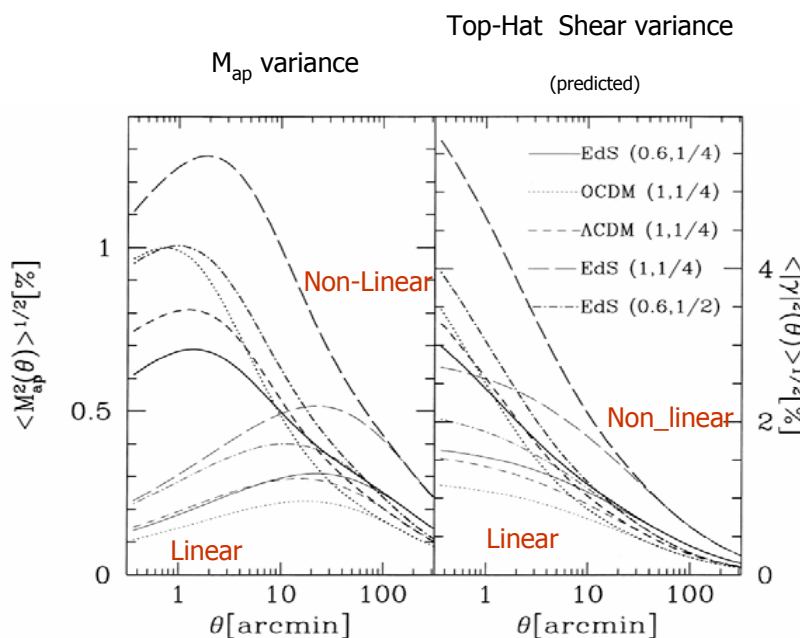
# Summary

- 2 independent pipelines provide the same results ; same results as the previous survey Virmos-Descart: robust and reliable measurements
- No B-modes, no  $\langle e^* \gamma_g \rangle$  cross-correlation: no systematics residuals after PSF correction
- No B-mode at all scales (30'' ; 50'): likely signal from gravity (Curl-free)
- Achromatic: gravitational lensing
- Signal
  - has the amplitude and the shape predicted from theory of structure formation in a CDM-dominated scenario
  - increases with redshift as expected from cosmological structure formation and weak lensing theory

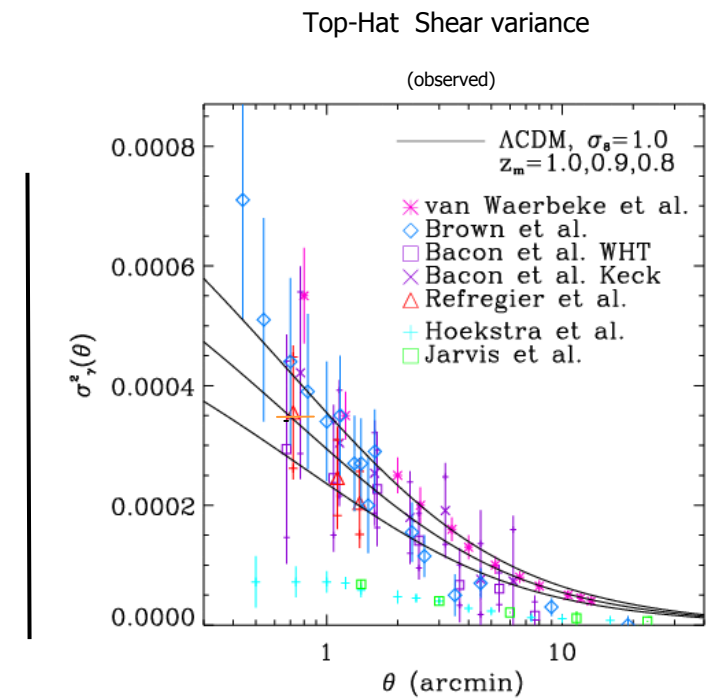
## Cosmological weak lensing

# Weak lensing : cosmological interpretation

# I. The shape and amplitude of the signal is in very good agreement with gravitational instability paradigm in a CDM-dominated universe.



Bartelmann & Schneider 2001 : theoretical predictions from the gravitational instability scenario



Refregier et al 2002

# Redshift distribution

## HDF optical+NIR used

- $\langle \kappa^2(\theta) \rangle^{1/2} \approx 0.01 \sigma_8 \Omega^{0.8} \left( \frac{\theta}{1\text{deg.}} \right)^{-\frac{n+2}{2}}$

$z_s = 0.75$

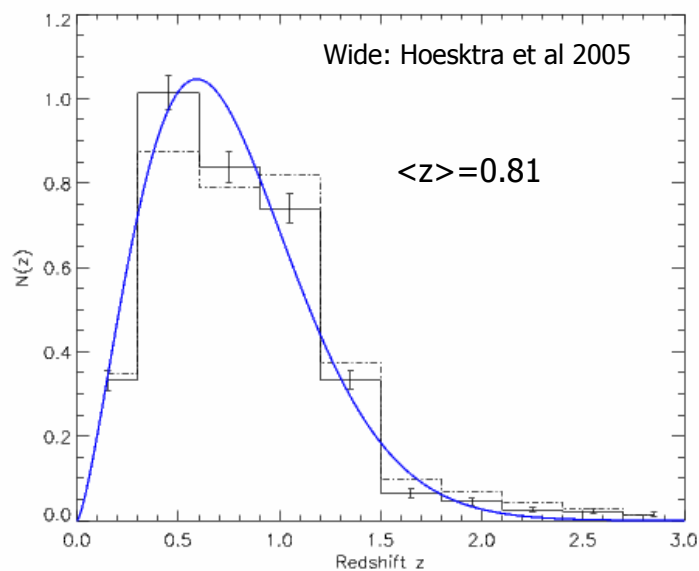


FIG. 10.— Effective redshift distribution of galaxies with  $21.5 < R_{AB} < 24.5$  determined from the Hubble Deep Field North and South. The error bars are the Poisson errors from the finite number of galaxies in each bin. The smooth solid curve represents the best fit model with a mean source redshift of  $\langle z \rangle = 0.81$ . The dashed histogram corresponds to the redshift distribution when the adopted weighting scheme is not taken into account.

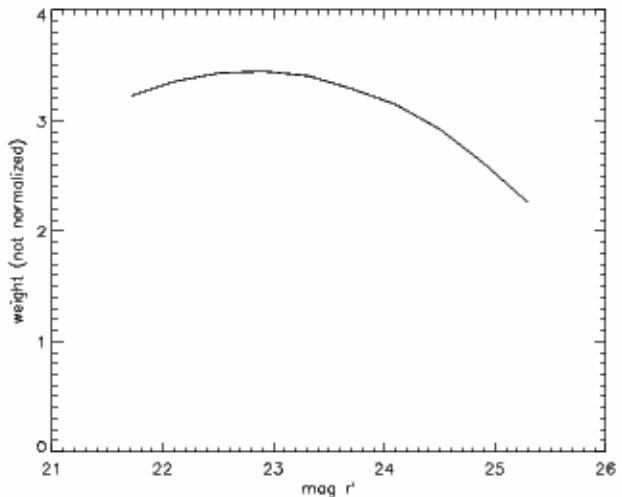


Fig. 12. Plot of mean weight per galaxy as function of magnitude  $21.5 < R_{AB} < 25.5$ .

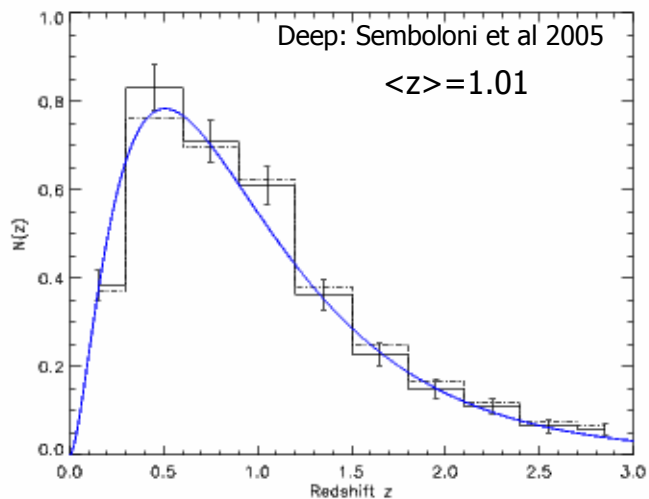
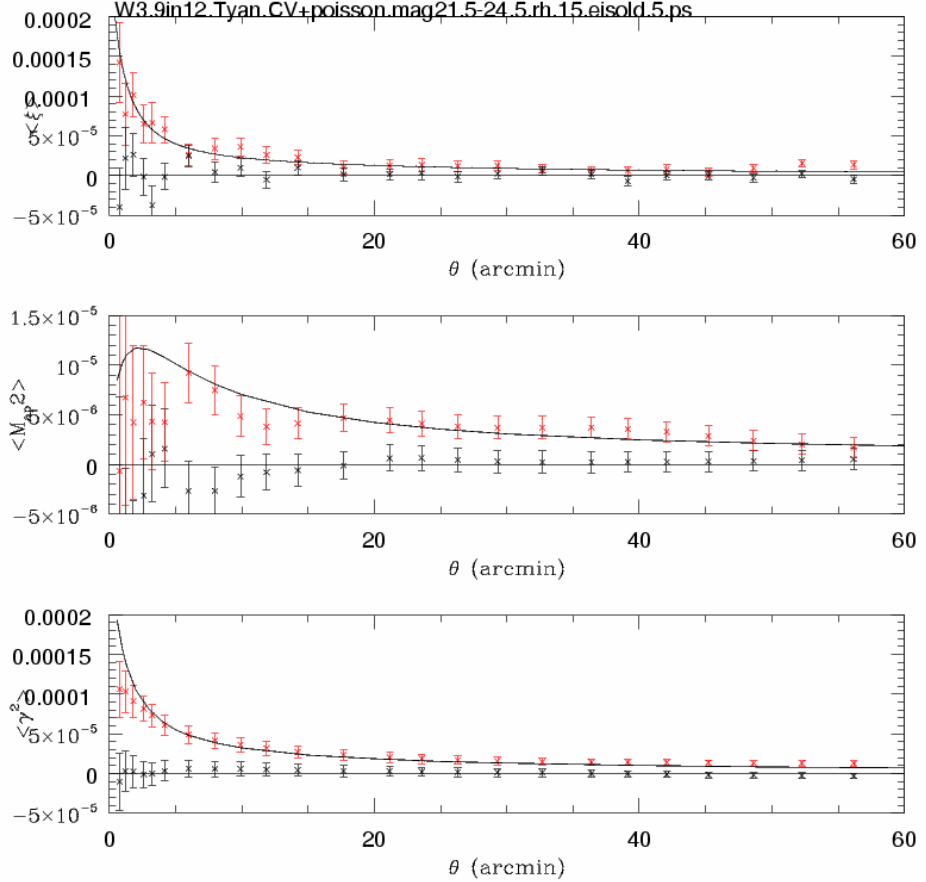
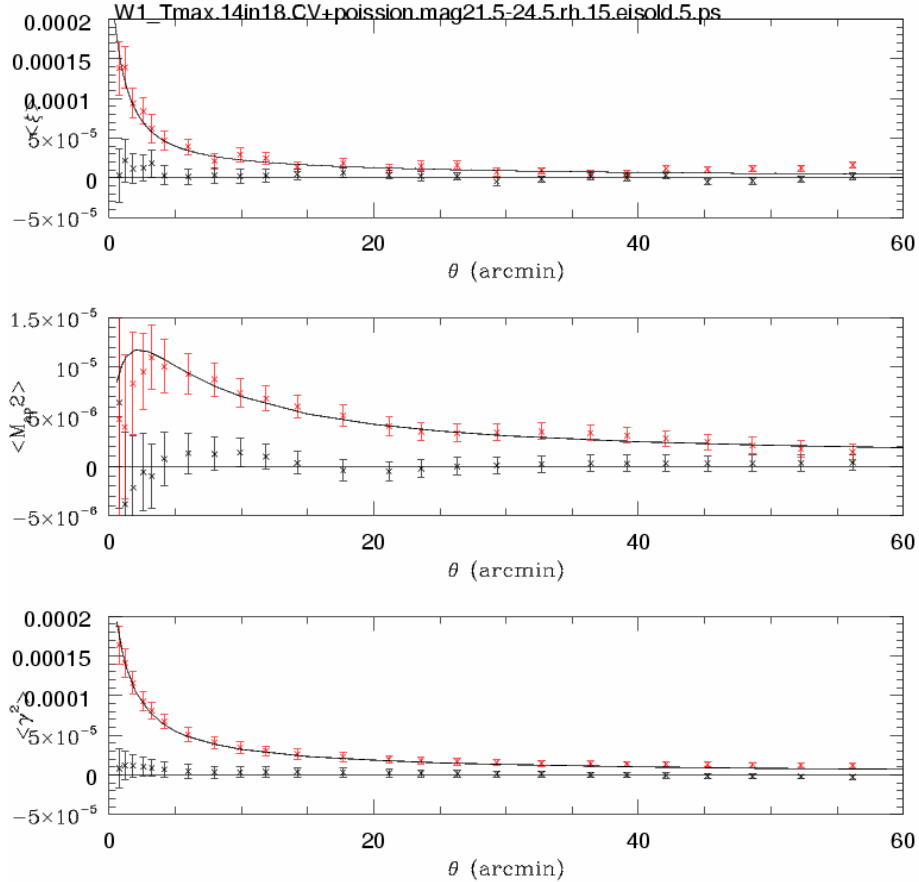


Fig. 13. The histogram shows the photometric redshift distribution of  $21.5 < R_{AB} < 25.5$  galaxies of Hubble Deep Field North and South. The central solid line represents the best fit model, and the two other lines the  $\pm \sigma$  fits.

## II. CSLS in good agreement with the « concordance model »



- Line:  $\sigma_8=0.85$ ;  $\Omega_m=0.27$ ;  $\Lambda=0.73$ ;  $h=0.71$ ;  $\langle z_s \rangle=0.85$ ;  $\sigma_\epsilon=0.36$ ;  $n_{\text{gal}}=15 \text{ gal/arcmin}^2$
- Errors: Poisson+cosmic variance included

Concordance model overplot: no fit

# Constraints on Models

---

Assume we measured the correlation functions  $\xi_{\pm}(\vec{\theta})$ .

Cosmological parameters can then be derived by minimising:

$$\chi^2(p) = \sum_{ij} (\xi_i(p) - \xi_i^{obs}) \text{Cov}_{ij}^{-1} (\xi_j(p) - \xi_j^{obs}) \quad (280)$$

where  $p$  is a set of cosmological parameters and  $\text{Cov}_{ij}^{-1}$  the inverse covariance matrix.

The covariance matrix is derived from the error budget analysis.

$$\text{Cov} = C_0 \sigma_{\varepsilon}^4 + C_1 \sigma_{\varepsilon}^2 \xi \xi + C_2 \xi \xi \quad (281)$$

if intrinsic systematics are discarded.

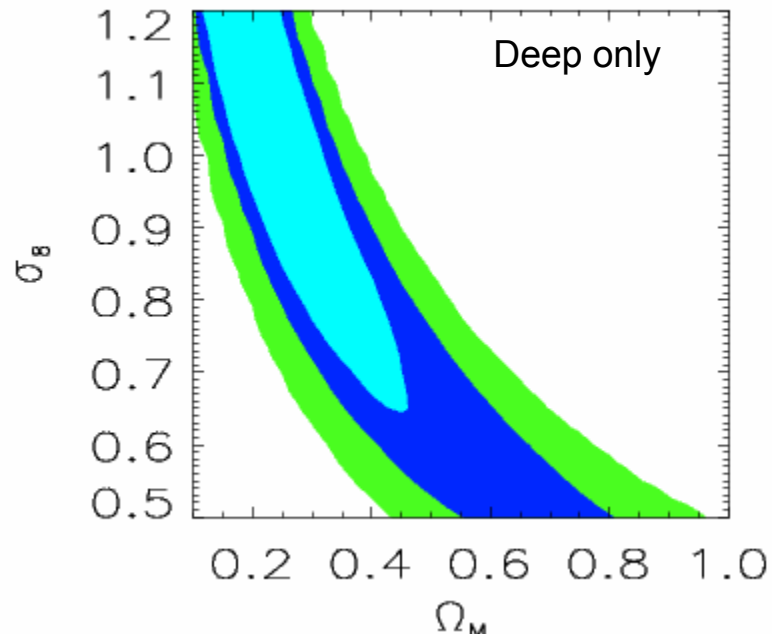
For angular scale reasonably large, the error on the power spectrum is given by

$$\Delta P_k(l) = \sqrt{\frac{2}{(2l+1)f_{sky}}} \left( P_k(l) + \frac{\sigma_{\varepsilon}^2}{2n} \right) \quad (282)$$

# III. Constraints on models

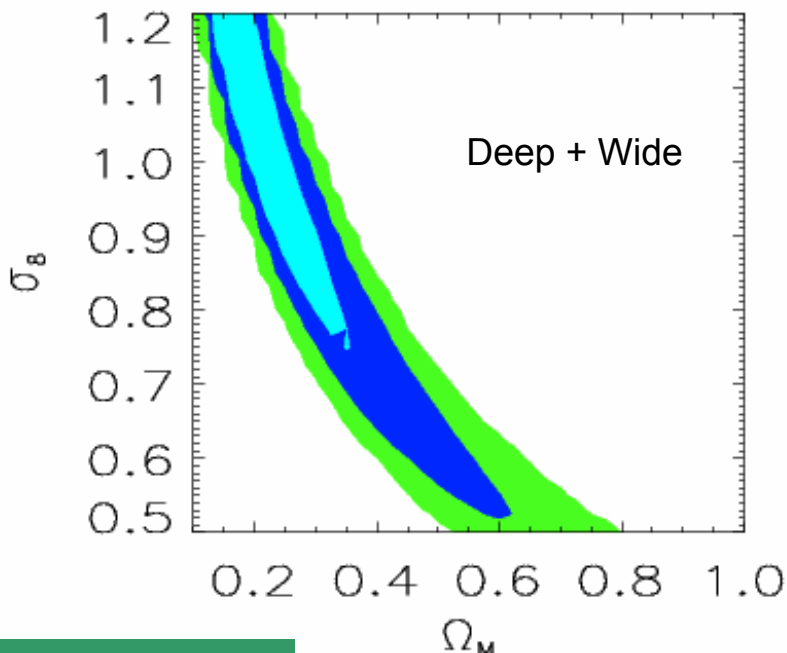
- Analysis of  $\sigma_8$  and  $\Omega_m$ , then DE
- Input data vector:  $d_i = \text{top-hat shear variance at scale } \theta_i$ 
  - $n=16$  number of angular scale bins
  - $\mathbf{C}=16 \times 16$  covariance matrix:  $C_{ij} = \langle (d_i - m_i)^T (d_j - m_j) \rangle$
- $\mathbf{C} = \mathbf{C}_n + \mathbf{C}_s = \text{statistical noise} + \text{cosmic variance matrix}$ 
  - $\mathbf{C}_s$  from Schneider et al 2002 with:
    - the deep:  $2.1 \text{ deg}^2, 23 \text{ gal/arcmin}, \sigma_e = 0.3 \text{ per component}$
    - the wide (W1 and W3 only):  $13.5+8.5 \text{ deg}^2, 12 \text{ gal/arcmin}, \sigma_e = 0.3 \text{ per component}$
  - Cosmic variance assuming Gaussian statistics: wrong on small scales but dominated by statistical noise
  - Matrix components derived from the best fit of WMAP-1:  $\Omega_m = 0.3, \sigma_8 = 0.88, \Omega_\Lambda = 0.7, h = 0.7, \Gamma = 0.21$
- B mode calibrated by marginalising around  $B=0$  within  $1-\sigma$
- Source redshift from HDF,  $n(z)$  analytic form and marginalising over  $2-\sigma$  from best fit
  - +  $0.6 < h < 0.8$  (+  $0.7 < \sigma_8 < 1.0$  for  $w_0$ )
- NL power spectrum : P&D or Halo fit (P&D only for DE)

# Power spectrum; Dark Matter



# CSLS: constraints on $\Omega_m$ - $\sigma_8$

- $\langle \kappa^2(\theta) \rangle^{1/2} \approx 0.01 \sigma_8 \Omega^{0.8} (\frac{\theta}{1\text{deg.}})^{-\frac{n+2}{2}} z_s^{0.75}$
- $\langle \kappa^2(\theta) \rangle = \langle \gamma^2(\theta) \rangle$



Deep+Wide assuming  $\Omega_m=0.3$  :

$$\sigma_8 = 0.89 \pm 0.06 \text{ (P&D)}$$

$$\sigma_8 = 0.86 \pm 0.05 \text{ (Halo fit)}$$

Deep effective area:  $2.1 \text{ deg}^2$   
Wide effective area :  $22 \text{ deg}^2$

# $\sigma_8$ with CSLS

Van Waerbeke et al 2005 (Virgos-Descart):

$$\sigma_8 = 0.83 \pm 0.07$$

Hoekstra et al 2003 (RCS):

$$\sigma_8 = 0.85 \pm 0.07$$

Sembolini et al (2005, CFHLS-Deep) +

Hoekstra et al (2005, CFHTLS-Wide):

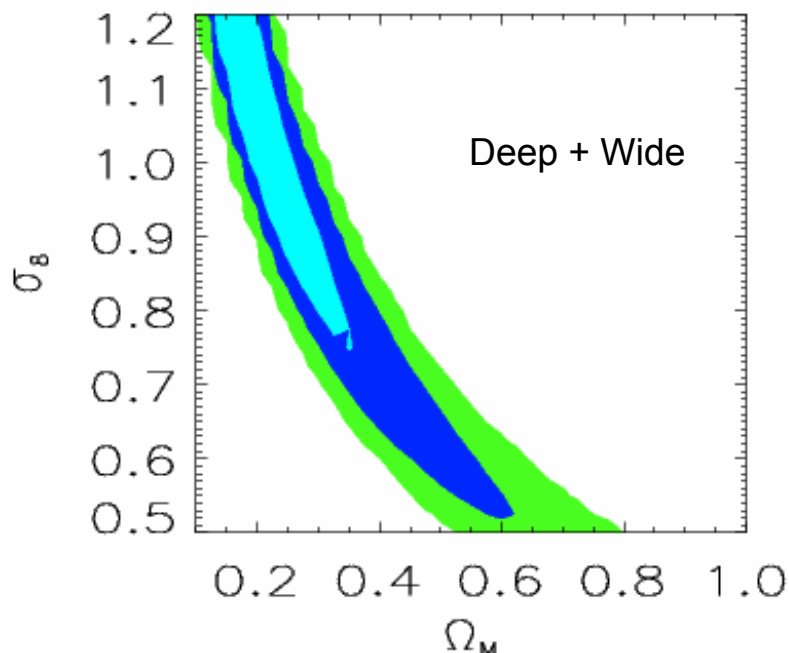
$$\sigma_8 = 0.89 \pm 0.06 \text{ (P&D)}$$

$$\sigma_8 = 0.86 \pm 0.05 \text{ (Halo fit)}$$

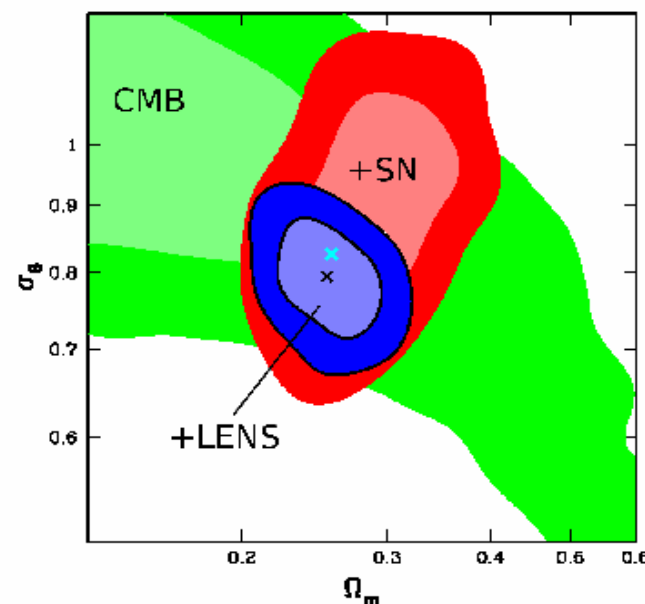
... internal uncertainty agree within 5%

# $\Omega_m$ - $\sigma_8$ :

CFHTLS DEEP+WIDE / shallow CTIO 75 deg<sup>2</sup>



Semboloni et al 2005 & Hoekstra et al 2005

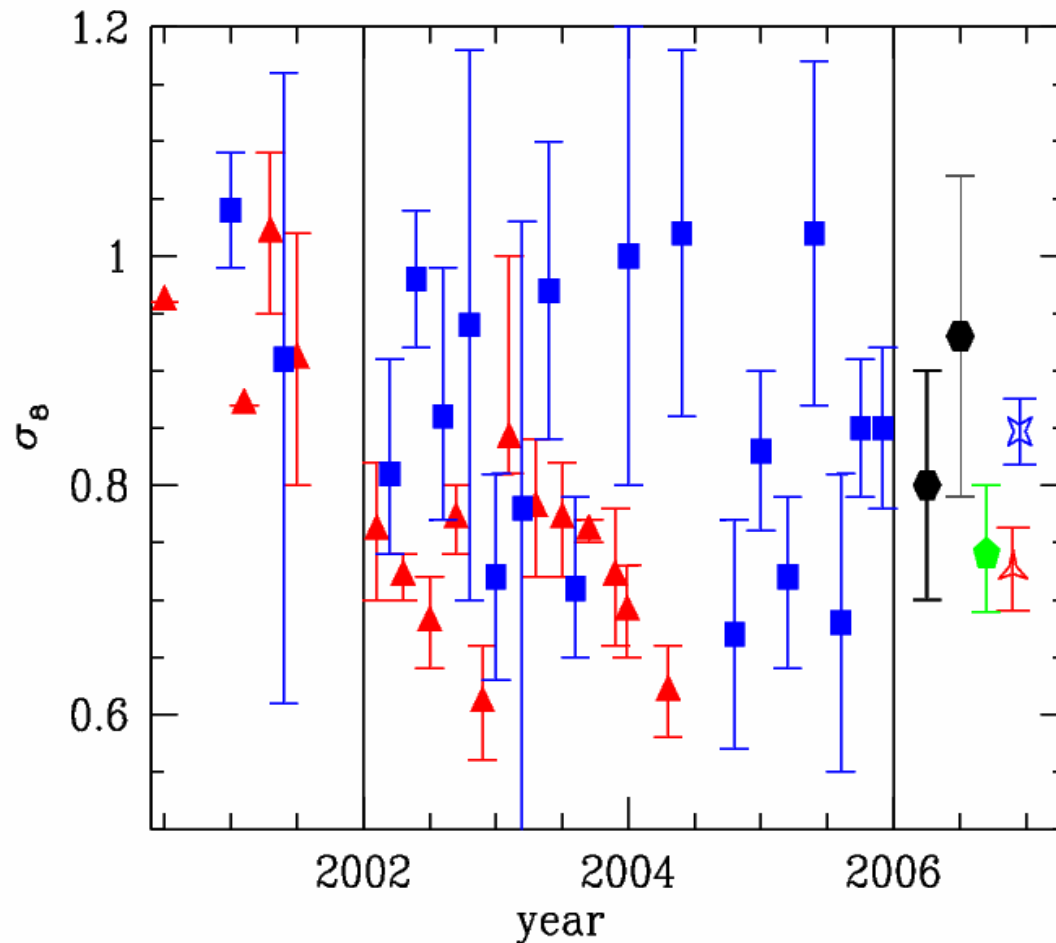


Jarvis, Jain, Bernstein, Dolney 2005

# Cosmological parameters from weak lensing surveys: present status

Survey	Telescope	Sky coverage	n gal/a min <sup>2</sup>	Mag	$\sigma_8$ ( $\Omega_m = 0.3$ )	$w_0$	Ref.
VLT-Descart	VLT	0.65 deg <sup>2</sup>	21	I <sub>AB</sub> = 24.5	1.05 ± 0.05		Maoli et al 2001
Groth Strip	HST/WFPC2	0.05 deg <sup>2</sup>	23	I=26	0.90 <sup>+0.25</sup> <sub>-0.30</sub>		Rhodes et al 2001
MDS	HST/WFPC2	0.36 deg <sup>2</sup>	23	I=27	0.94 ± 0.17		Réfrégier et al 2002
RCS	CFHT CTIO	16.4 deg <sup>2</sup> + 7.6 deg <sup>2</sup>	9	R=24	0.81 <sup>+0.14</sup> <sub>-0.19</sub>		Hoekstra et al 2002a
Virmos-Descart	CFHT	8.5 deg <sup>2</sup>	15	I <sub>AB</sub> =24.5	0.98 ± 0.06	-	van Waerbeke et al 2002
RCS	CFHT CTIO	45.4 deg <sup>2</sup> + 7.6 deg <sup>2</sup>	9	R=24	0.87 <sup>+0.09</sup> <sub>-0.12</sub>		Hoekstra et al 2002b
COMBO-17	2.2m	1.25 deg <sup>2</sup>	32	R=24.0	0.72 ± 0.09		Brown et al 2003
Keck + WHT	kECK WHT	0.6 deg <sup>2</sup> 1.0 deg <sup>2</sup>	27.5 15	R=25.8 R=23.5	0.93 ± 0.13		Bacon et al 2003
CTIO	CTIO	75 deg <sup>2</sup>	7.5	R=23	0.71 <sup>+0.06</sup> <sub>-0.08</sub>		Jarvis et al 2003
SUBARU	SUBARU	2.1 deg <sup>2</sup>	32	R=25.2	0.78 <sup>+0.55</sup> <sub>-0.25</sub>		Hamana et al 2003
COMBO-17	2.2m	1.25 deg <sup>2</sup>	R	R=24.0	0.67 ± 0.10		Heymans et al 2004
FIRST	VLA	10000 deg <sup>2</sup>	0.01	1 mJy	1.0 ± 0.2		Chang et al 2004
GEMS	HST/ ACS	0.22 deg <sup>2</sup>	60	I=27.1	0.68 ± 0.13		Heymans et al 2005
WHT + COMBO-17	WHT 2.2m	4.0 deg <sup>2</sup> + 1.25 deg <sup>2</sup>	15 32	R <sub>AB</sub> =25.8 R=24.0	1.02 ± 0.15		Massey et al 2005
Virmos-Descart	CFHT	8.5 deg <sup>2</sup>	12.5	I <sub>AB</sub> =24.5	0.83 ± 0.07		van Waerbeke et al 2005
CTIO	CTIO	75 deg <sup>2</sup>	7.5	R=23	0.71 <sup>+0.06</sup> <sub>-0.08</sub>		Jarvis et al 2006
CFHTLS Deep + Wide	CFHT	2.1 deg <sup>2</sup> + 22 deg <sup>2</sup>	22 13	i <sub>AB</sub> =25.5 i <sub>AB</sub> =24.5	0.89 ± 0.06 0.86 ± 0.05		Semboloni et al 2006 Hoekstra et al 2005
GaBoDS	2.2m	15 deg <sup>2</sup>	12.5	R=24.5	0.80 ± 0.10	-	Hetterscheidt et al 2006
ACS parallel + GEMS+GOODS	HST/STIS HST/ACS	0.018 deg <sup>2</sup> 0.027 deg <sup>2</sup>	63 96	R=27.0 ? V=27.0	0.52 <sup>+0.13</sup> <sub>-0.17</sub>		Schrabback et al 2006

# $\sigma_8$ derived from WL (blue) or clusters of galaxies (red)



# Why so much dispersion?

# Why so much dispersion?

- Cosmic shear problem?
- Lyman –alpha problem?
- Cluster of galaxies problem?
- Redshift survey – LSS problem?
- WMAP3 problem?

# From ellipticity to cosmology : not so obvious

Ellipticity badly measured (PSF  
anisotropy corrections, shape  
measurement)

$$\langle e^2 \rangle_\theta^{1/2} = \langle \gamma^2 \rangle_\theta^{1/2} \sim 0.01 \sigma_8 \Omega_m^{0.8} z_s^{0.75} \theta^{-(n+2)/2}$$

Shear is contaminated by non-  
lensing signal (intrinsic alignment of  
galaxies)

Several issues may produce systematic errors

Redshift of sources badly  
estimated (photo-z, too deep for  
spectroscopy)

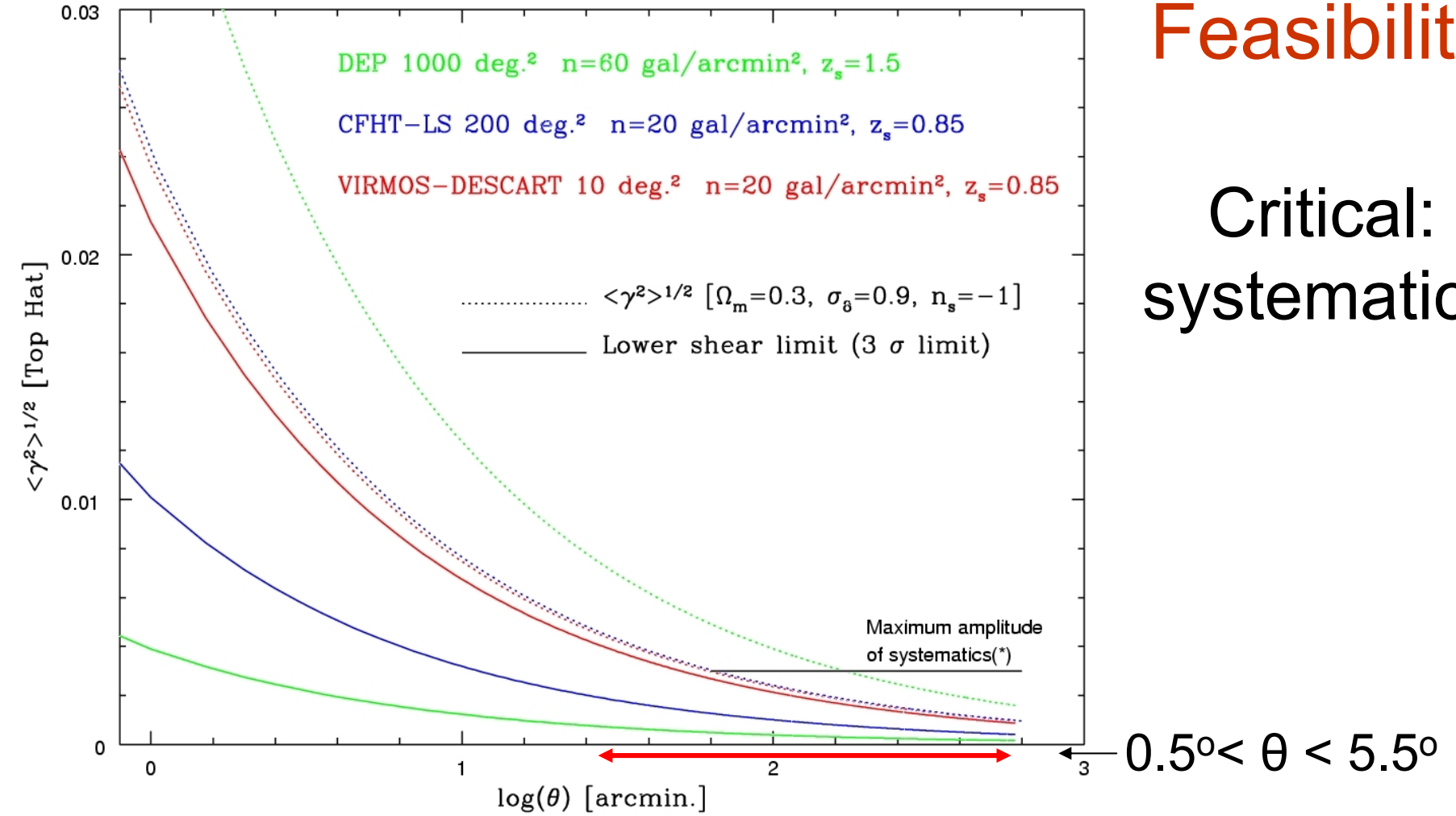
$\theta < 15'$  : Non-linear evolution of dark matter  
power spectrum unknown , extrapolation on  
small scales uncertain

# Errors and systematics uncertainties

- Poisson noise (galaxy number density)
- Cosmic variance (see Schneider et al 2002)
- PSF correction
- Biased galaxy sample
- Intrinsic systematics (astrophysics)

# Feasibility

## Critical: systematics



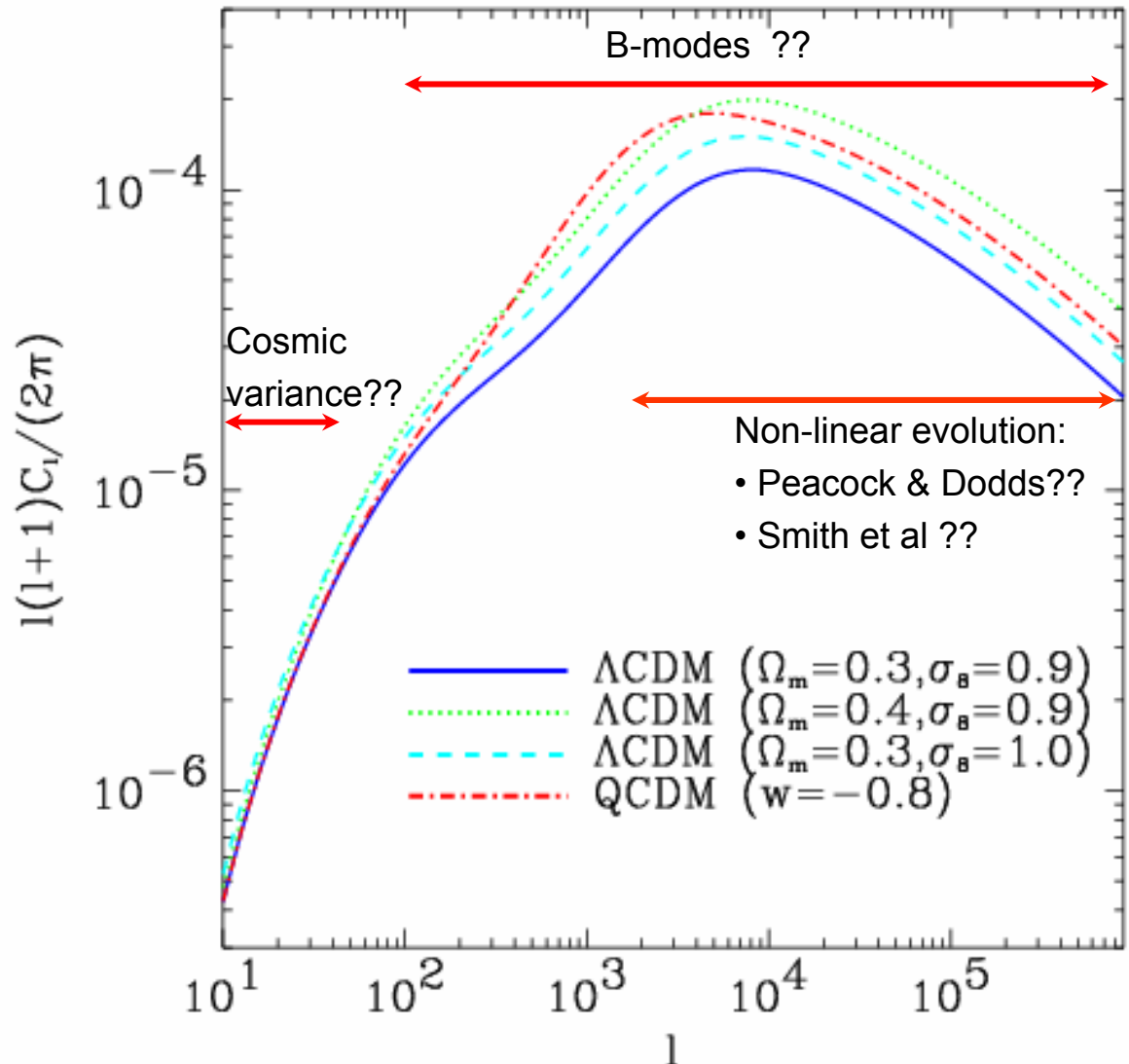
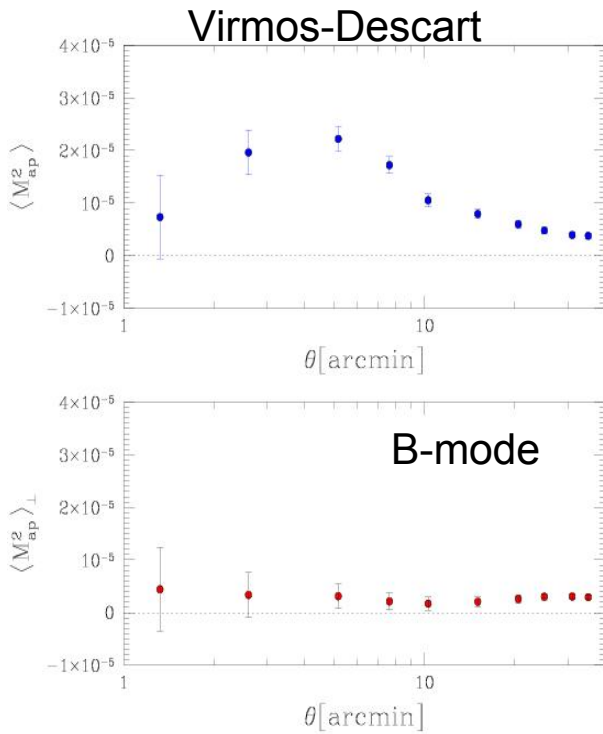
(\*) Assuming the shear measured on the largest VIRMOS-DESCART scale is an upper limit of systematics

$$\langle \gamma(\theta)^2 \rangle_{limit}^{1/2} = 1.2\% \left[ \frac{A_T}{1 \text{ deg}^2} \right]^{-\frac{1}{4}} \times \left[ \frac{\sigma_{\epsilon_{gal}}}{0.4} \right] \times \left[ \frac{n}{20 \text{ gal/arcmin}^2} \right]^{-\frac{1}{2}} \times \left[ \frac{\theta}{10'} \right]^{-\frac{1}{2}}$$

$$\langle \gamma(\theta)^2 \rangle^{1/2} \approx 1\% \sigma_8 \Omega_m^{0.75} z_s^{0.8} \left( \frac{\theta}{10'} \right)^{-\left( \frac{n+2}{2} \right)}$$

# Weak lensing and the dark universe

systematics and errors could kill the cosmic shear signal ?



# Errors and systematics uncertainties

- PSF corrections
- Redshift distribution
- Clustering
- Contamination by overlapping galaxies
- Intrinsic alignment
- Intrinsic foreground/backgound correlations
- Sampling variance
- Non-linear variance
- Non-linear dark matter power spectrum
- + cosmic variance (survey size, survey topology, depth)

# Systematics: intrinsic correlations

Assume we measure an ellipticity

$$\varepsilon = \varepsilon^S + \gamma$$

and we cross-correlate signal from 2 objects, with  $z_1 < z_2$

Then

$$\langle \varepsilon_1 \varepsilon_2^* \rangle = \langle \varepsilon_1^S \varepsilon_2^{S*} \rangle + \langle \varepsilon_1^S \gamma_2^* \rangle + \langle \gamma_1 \varepsilon_2^{S*} \rangle + \langle \gamma_1 \gamma_2^* \rangle$$

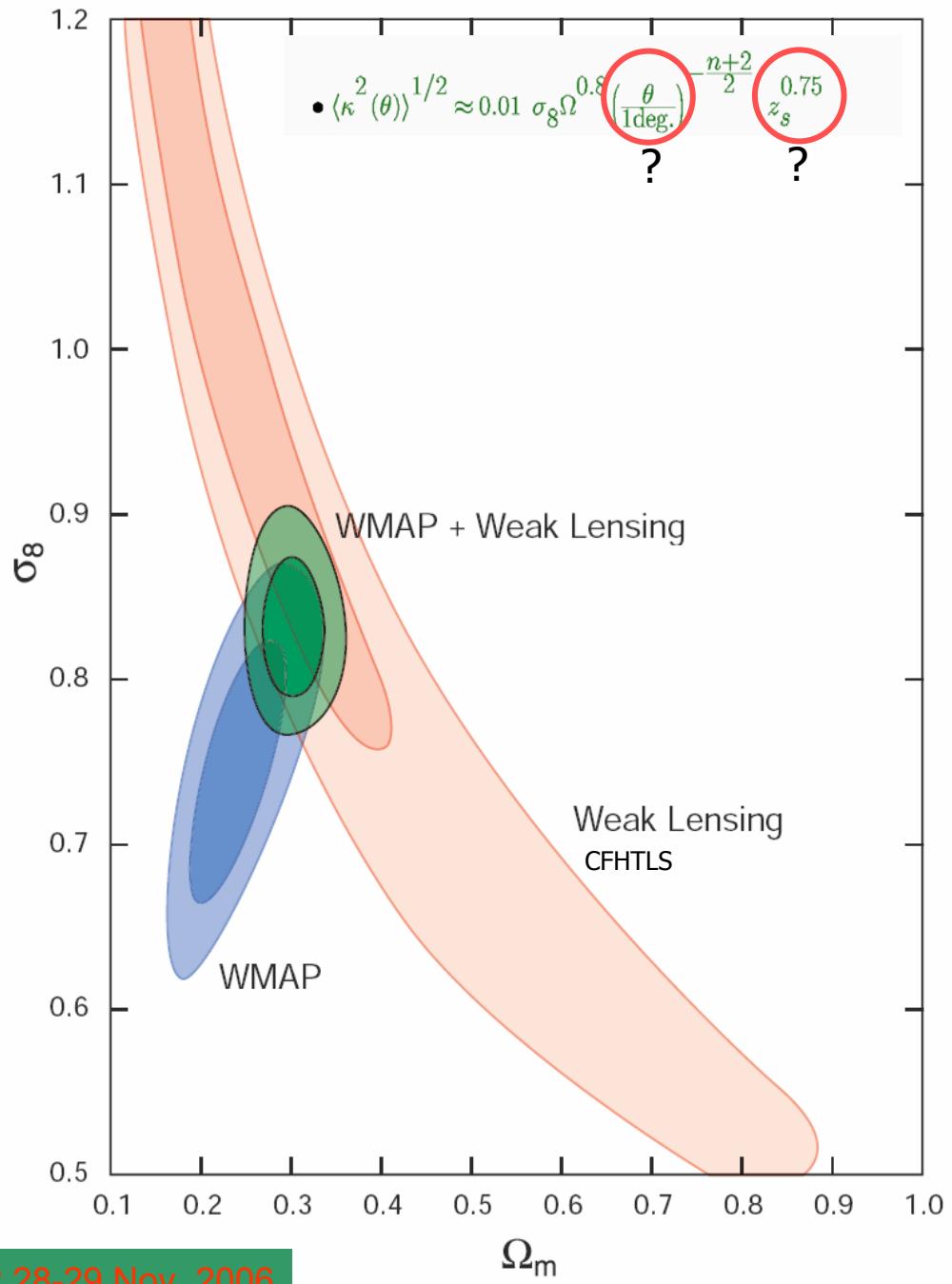
Intrinsic ellipticity correlation (=0 if  $z_1 \ll z_2$ )

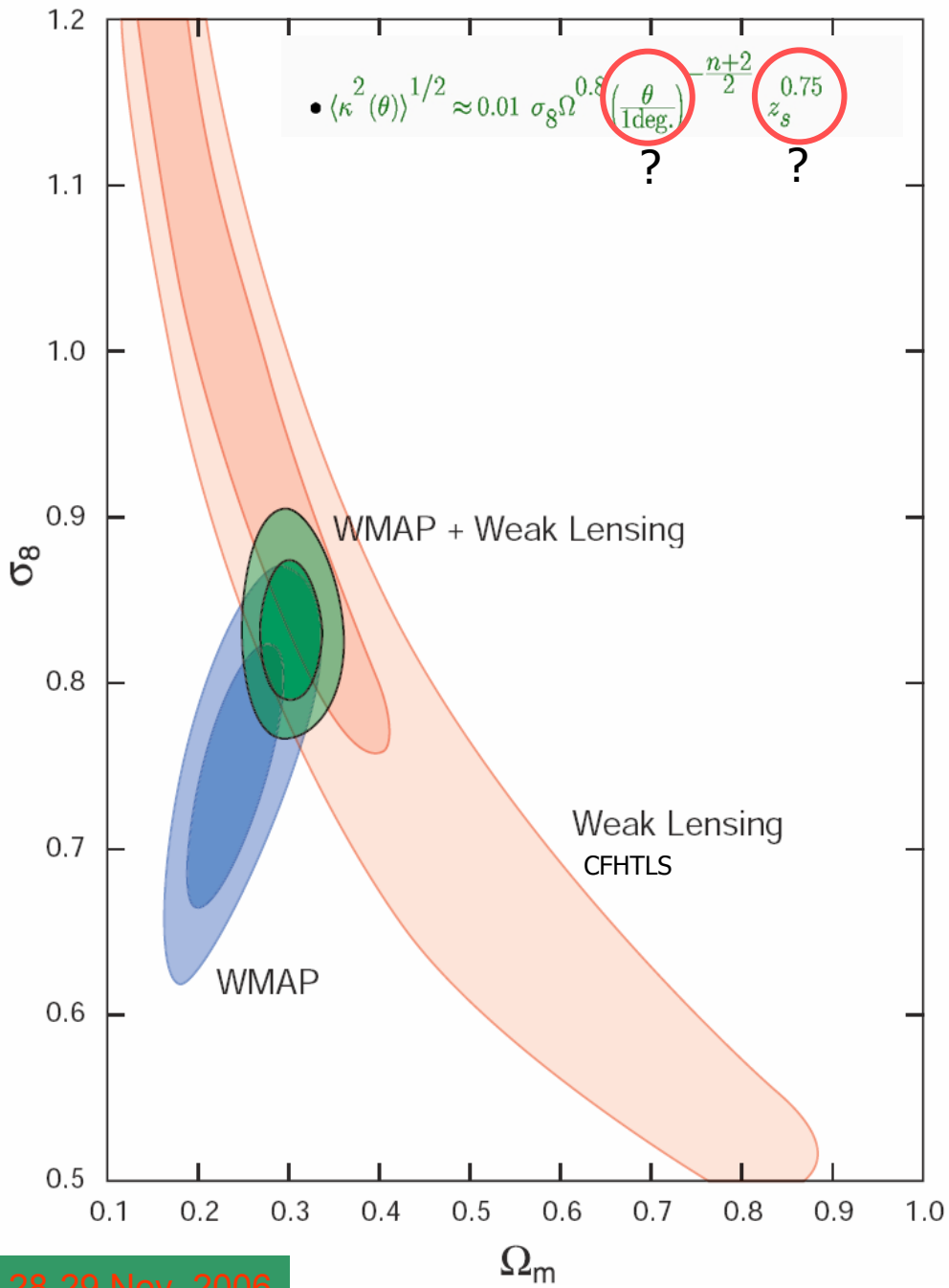
(Correlation may exist if tidal effect on galaxy 1 produced by a massive lensing halo is also responsible for the shear of galaxy 2 (need redshift to control it))

=0 !

Cosmic shear signal

# WMAP3 and CFHTLS cosmic shear

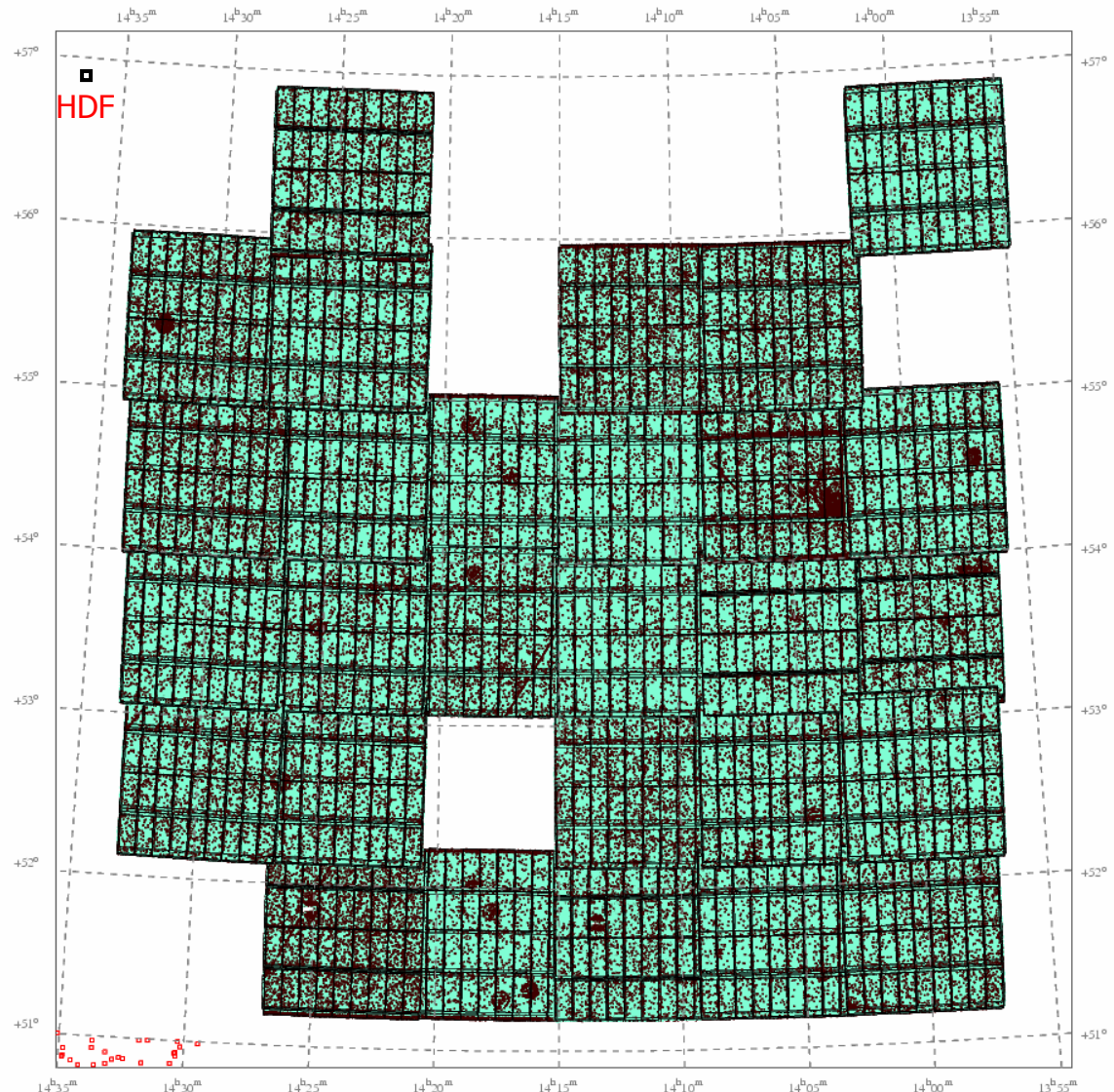




# WMAP3 and CFHTLS cosmic shear

- If cosmic shear problems:
    - Underestimated errors?
    - Systematic effects overlooked?
    - ...  $n(z)$  ? Non linear evolution of structures at small scales. Large scales needed.
  - Or... WMAP3 analysis also wrong?
    - Similar tension exists with Ly-alpha
- Lewis et al 0603753 , Seljak et al 2006

Group CFHTLS: W3 field



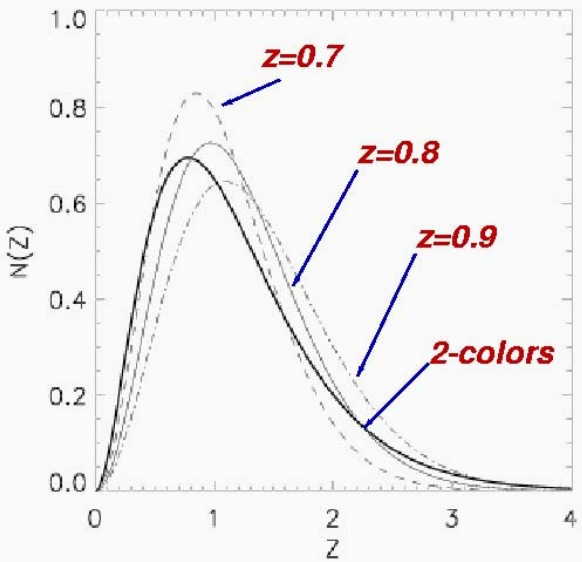
But WL also  
has  
uncertainties

I. sampling  $n(z)$

HST/HDF FOV as  
compared to CFHTLS

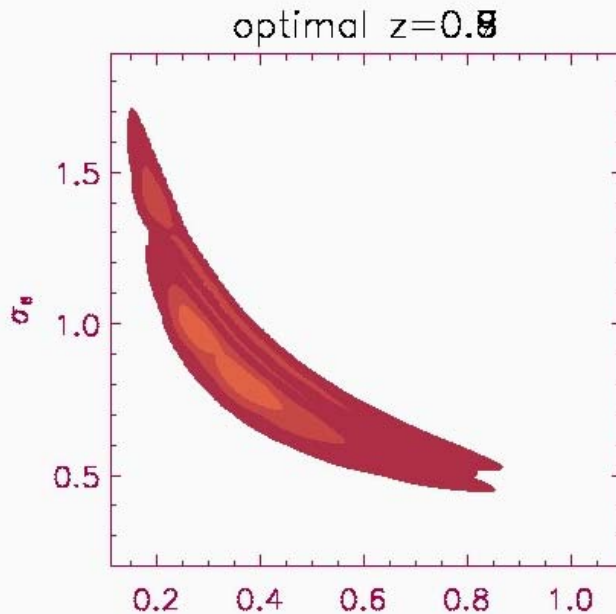
# Sensitivity to redshift of sources

*Redshift distribution of sheared sources*



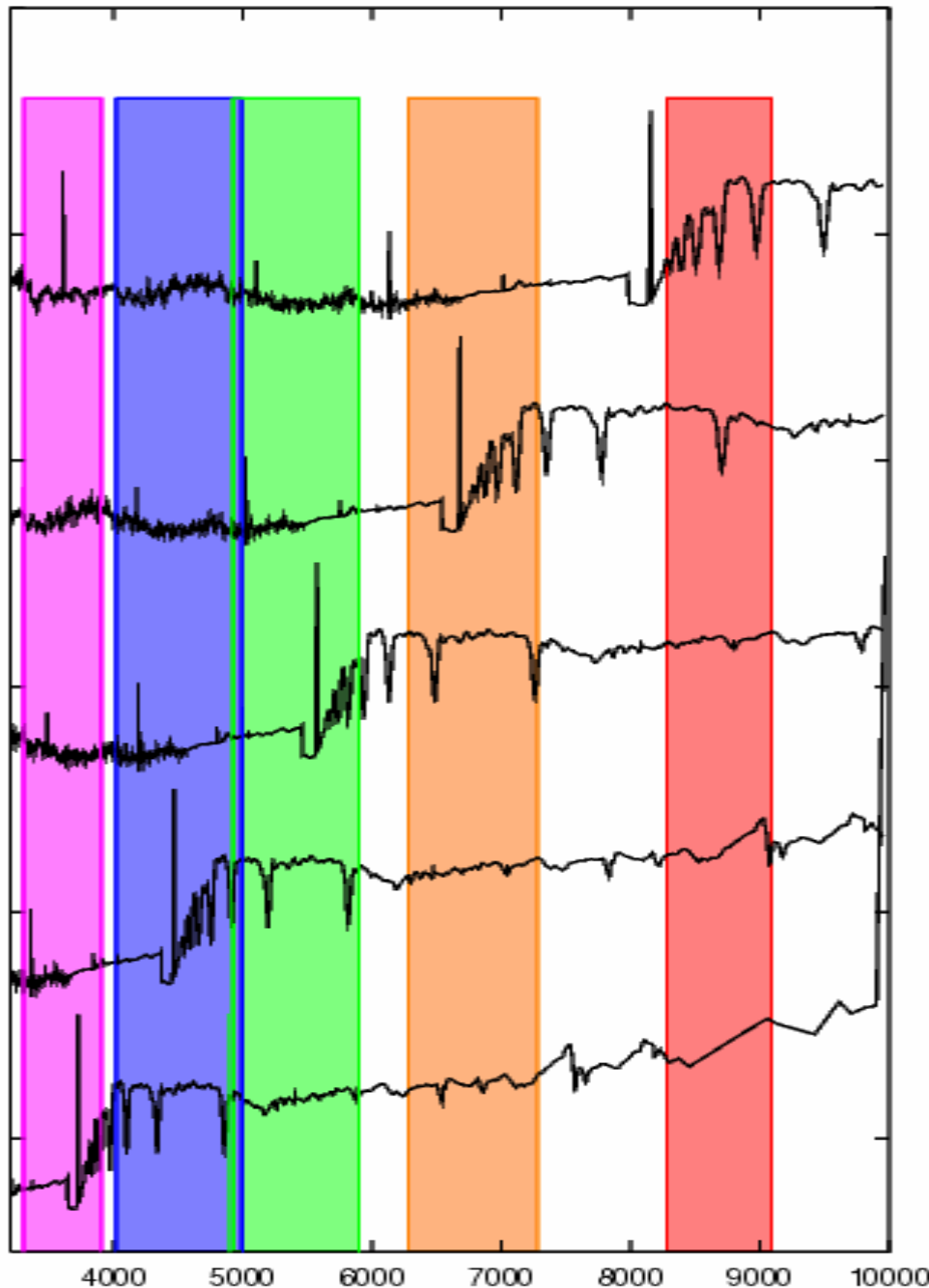
*van Waerbeke et al 2001*

*VIRMOS-DESCART CFH survey*



**6.5 deg<sup>2</sup>** - **450, 000 galaxies** -  **$I=24$**

**$z_s = 0.7+08+09$**  - ***Open CDM*** -  **$\Lambda=0$** ,  **$\Gamma=0.21$**



# Photometric redshift

Bernardeau & Mellier 2003

# The uncertain $n(z)$

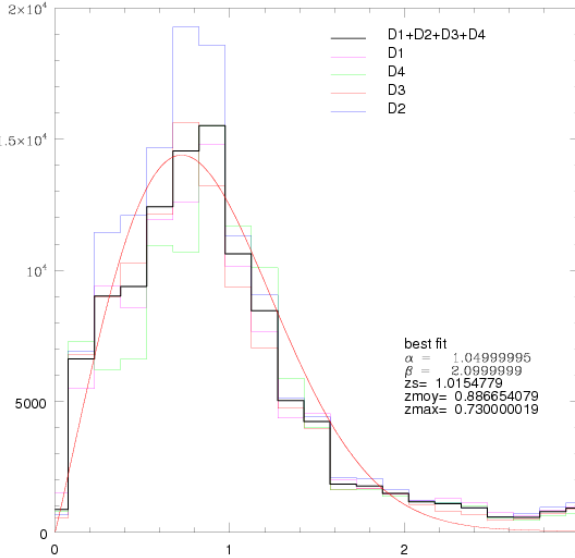
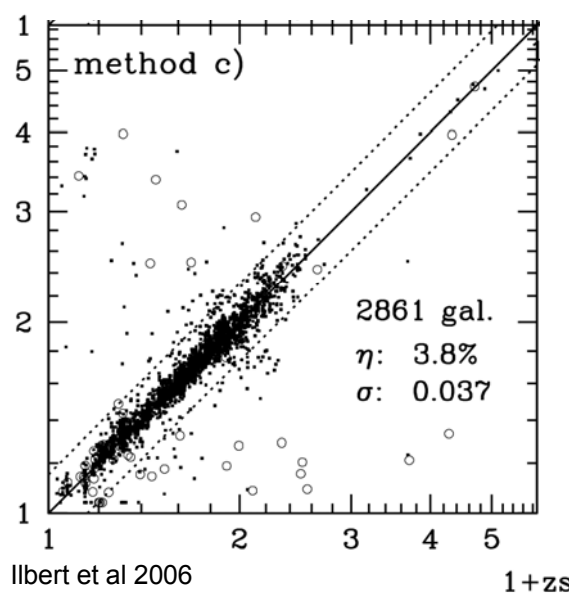


Photo-z in CFHTLS deep  
550000 galaxies with photo-z

HDF size too small as compared to CFHTLS: sampling variance increases error by 10% (van Waerbeke et al 2006)

We use CFHTLS Deep photometry + ESO / VLT / VVDS spectroscopic survey of CFHTLS D1 field

Photo-z from CFHTLS-Deep + VVDS: Seem to peak at higher  $z$  than our HDF  $z$ -calibration? Need to be confirmed. If so, it will decrease  $\sigma_8$

# The uncertain $n(z)$

HDF size too small as compared to CFHTLS: sampling variance increases error by 10%  
(van Waerbeke et al 2006)

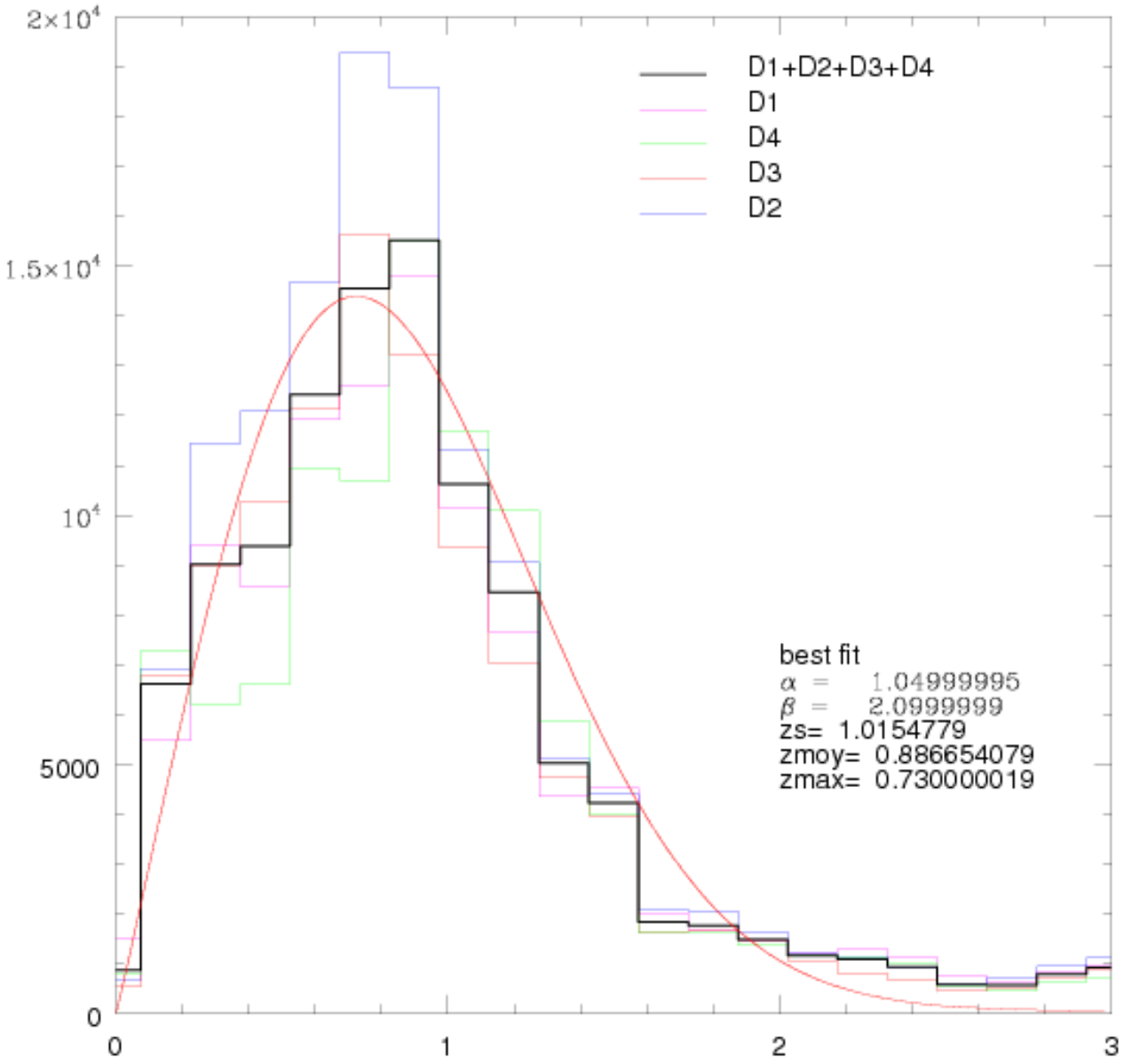


Photo-z from CFHTLS-Deep + VVDS: Seem to peak at higher  $z$  than our HDF  $z$ -calibration?  
Would decrease  $\sigma_8$

# Is the correction method good enough ?

## The Shear TEsting Program (STEP)

All teams measuring weak lensing involved

All techniques blindly tested using public simulations

Then evaluation criteria

$$\gamma - \gamma^{\text{true}} = q(\text{true})^2 + m(\text{true}) + C$$

q = linearity of the correction

m = calibration bias

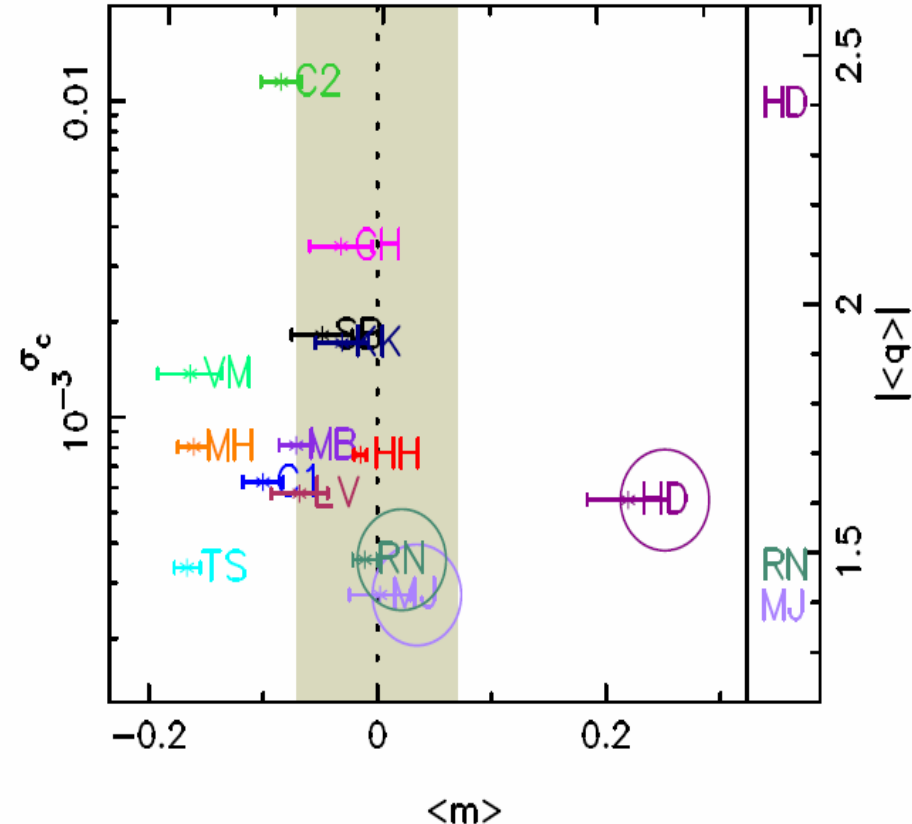
c = PSF systematics and shot noise

Best method reach 1% accuracy

Largest error: calibration bias m

# PSF : correction techniques tested with STEP1

Bridle & Hudelot	SB	Im2shape ( <a href="#">Bridle et al. 2001</a> )
Brown	MB	KSB+ [ <a href="#">Bacon et al. (2000)</a> pipeline]
Clowe	C1 & C2	KSB+
Dahle	HD	K2K ( <a href="#">Kaiser 2000</a> )
Hetterscheidt	MH	KSB+ [ <a href="#">Erben et al. (2001)</a> pipeline]
Heymans	CH	KSB+
Hoekstra	HH	KSB+
Jarvis	MJ	<a href="#">Bernstein &amp; Jarvis (2002)</a> Rounding kernel method
Kuijken	KK	Shapelets to 12 <sup>th</sup> order <a href="#">Kuijken (2006)</a>
Margoniner	VM	<a href="#">Wittman et al. (2001)</a>
Nakajima	RN	<a href="#">Bernstein &amp; Jarvis (2002)</a> Deconvolution fitting method
Schrabback	TS	KSB+ [ <a href="#">Erben et al. (2001)</a> + modifications]
Van Waerbeke	LV	KSB+



## The Shear TEsting Program (STEP)

$$\gamma - \gamma^{\text{true}} = Q(\text{true})^2 + M(\text{true}) + C$$

q = linearity of the correction

m = calibration bias

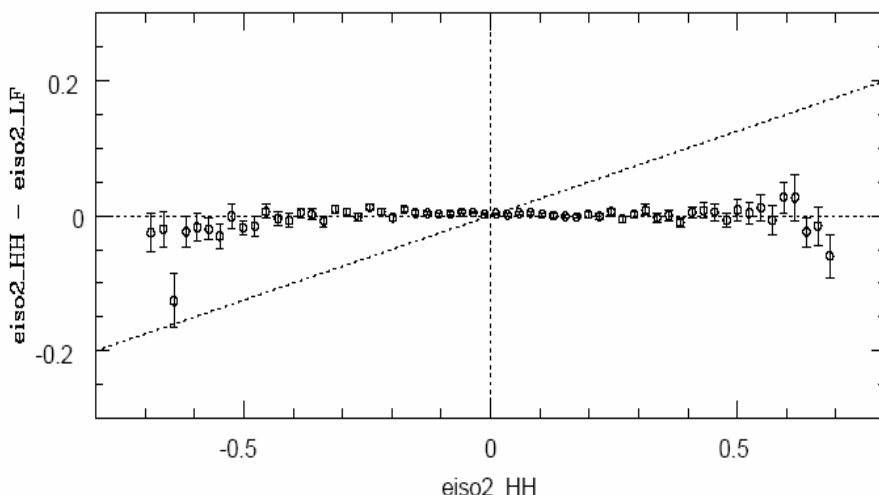
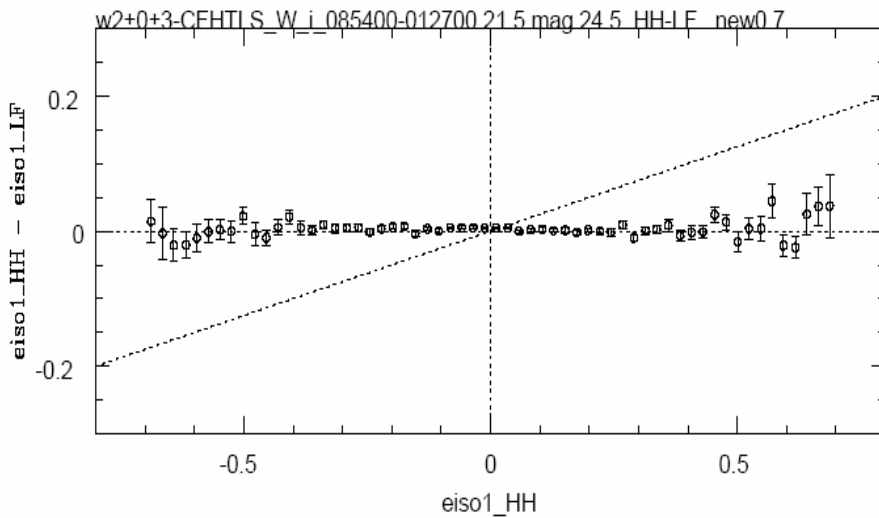
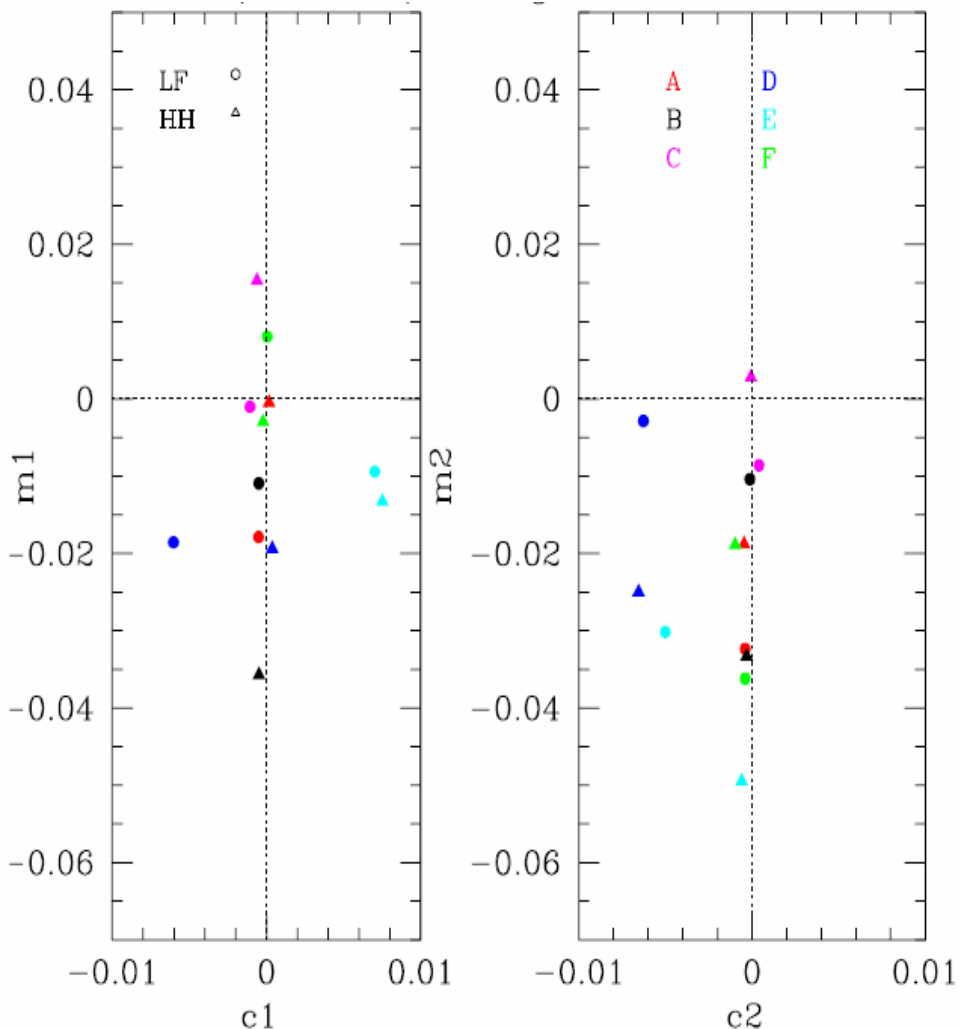
c = PSF systematics and shot noise

**Best method reach 1% accuracy**

Largest error: calibration bias m

# The PSF anisotropy correction revisited

< 2% underestimate



A posteriori: the residual bias had no impact on cosmological parameters

# Cosmic Shear

VIRMOS-Descart +  
CFHTLS-T0001 WIDE+Deep

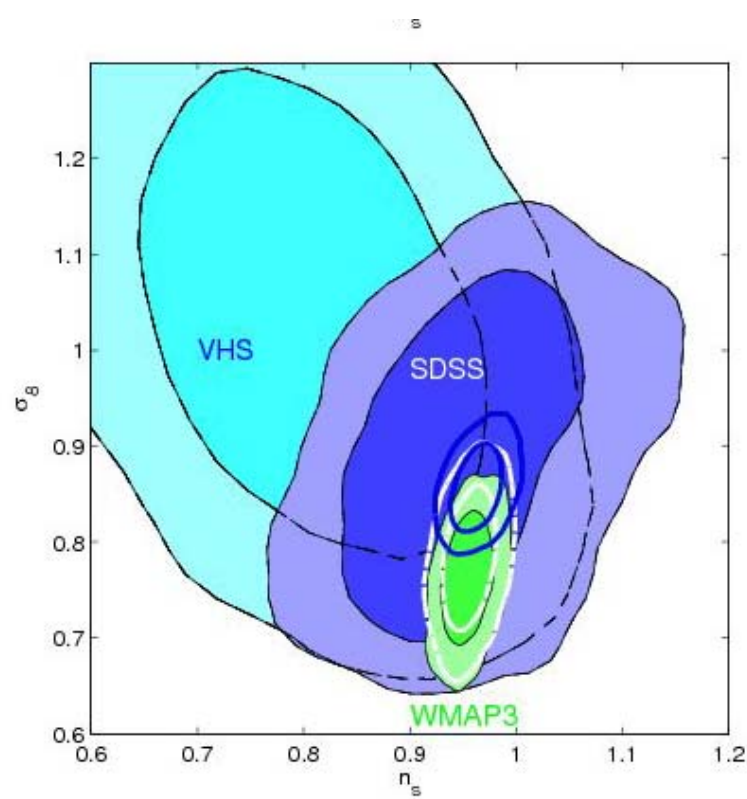
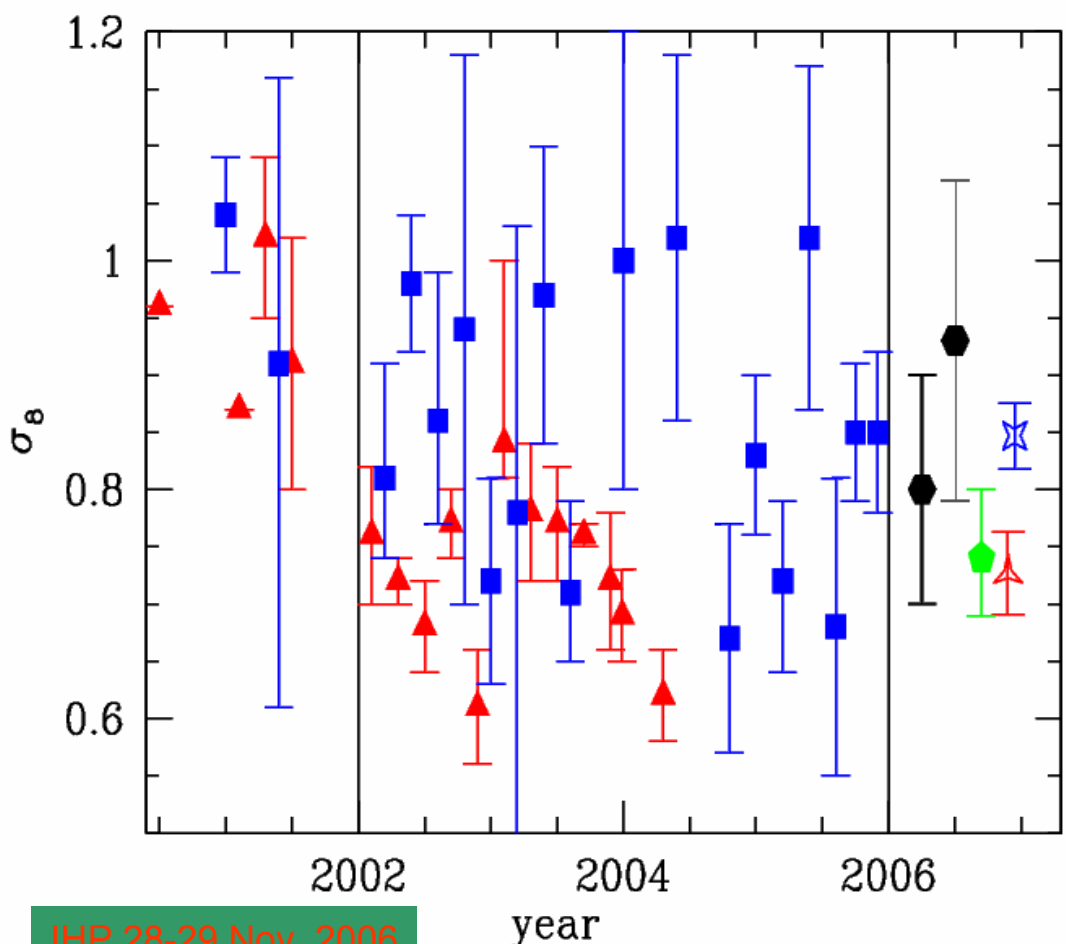
Benjamin et al 2006 In preparation

WMAP 3 year

- Virmos-Descart + CFHTLS Deep+Wide
- Much better  $n(z)$

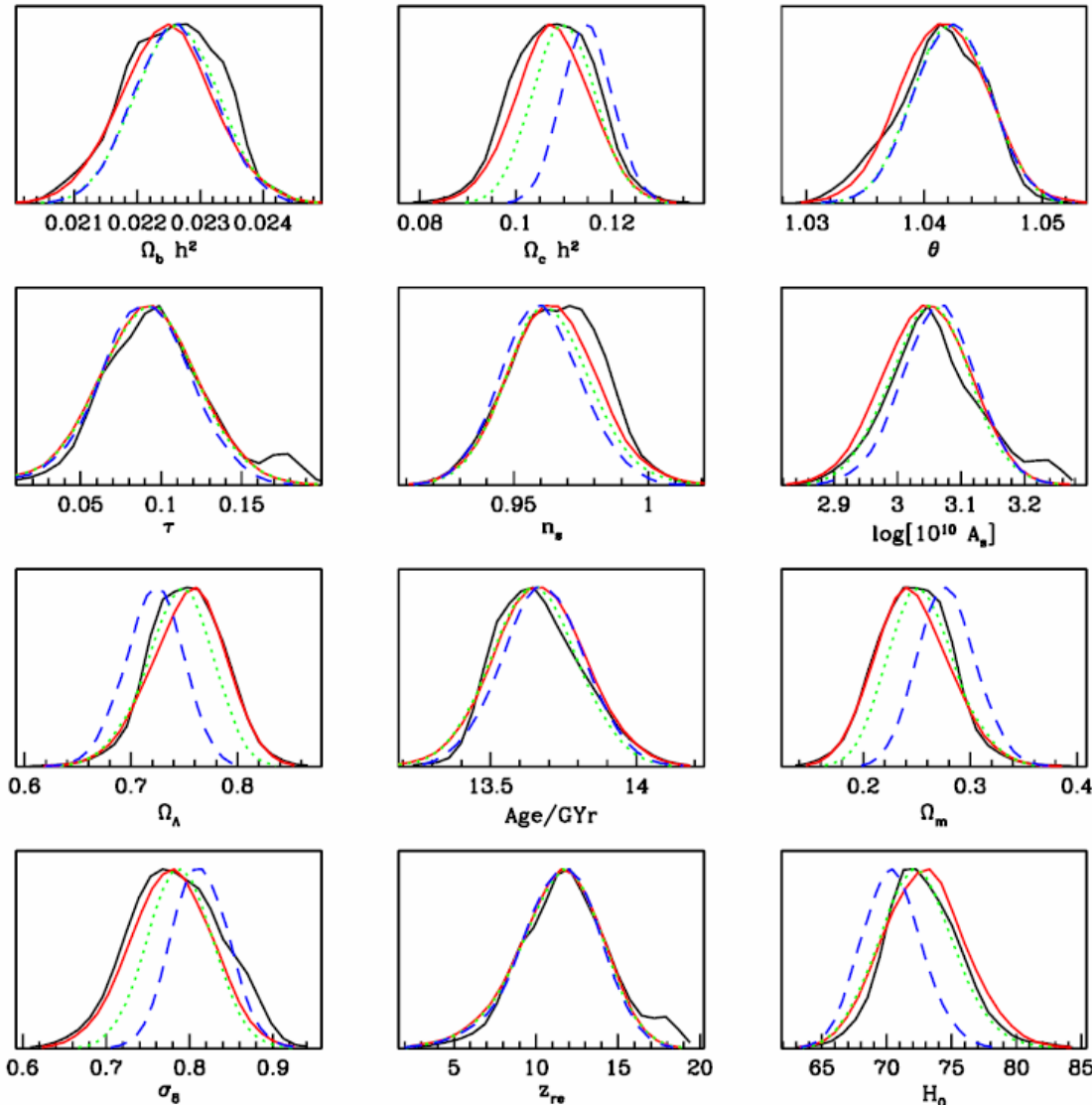
# Is WMAP-3 that accurate?

$\sigma_8$  derived from WL (blue) or clusters of galaxies (red) and Lyman-alpha forest (right)



# Is WMAP-3 that accurate?

## WMAP-3 + most recent ACBAR data



- Black: WMAP-3 only
- Red: WMAP-3+ACBAR
- Green: CMBall
- Blue: CMBall+LSS

Kuo et al 2006

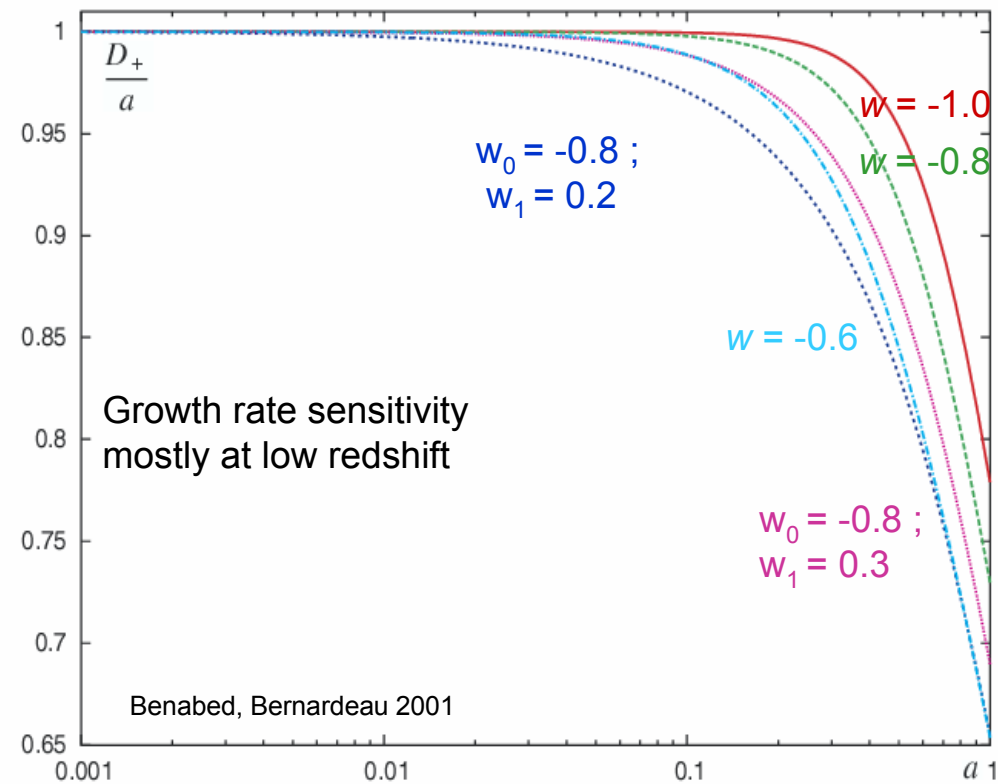
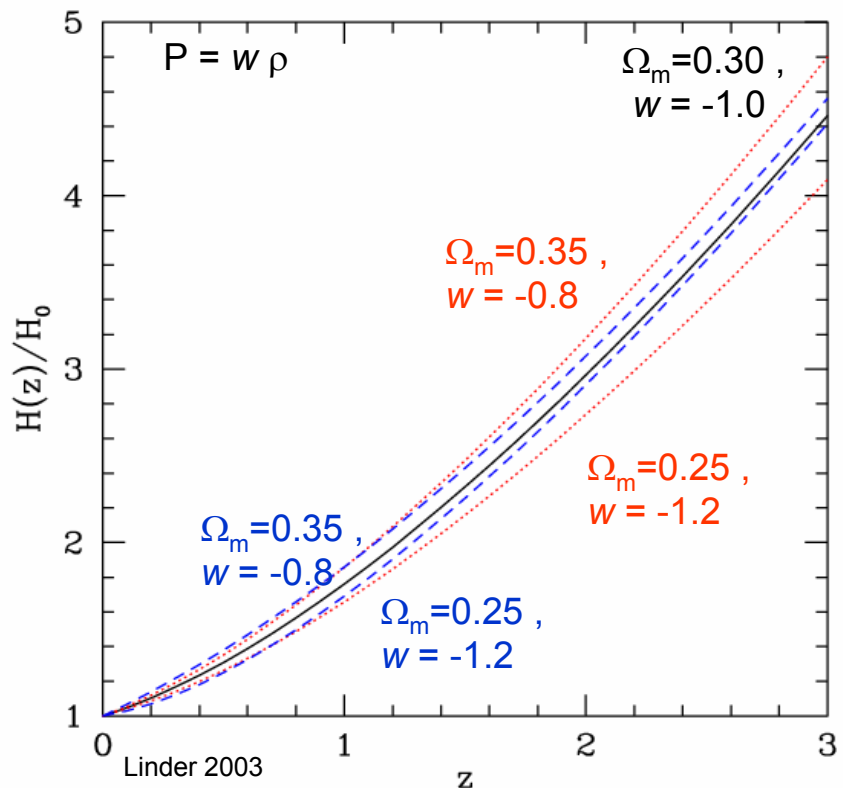
# Dark Energy

# Projected matter distribution and dark energy

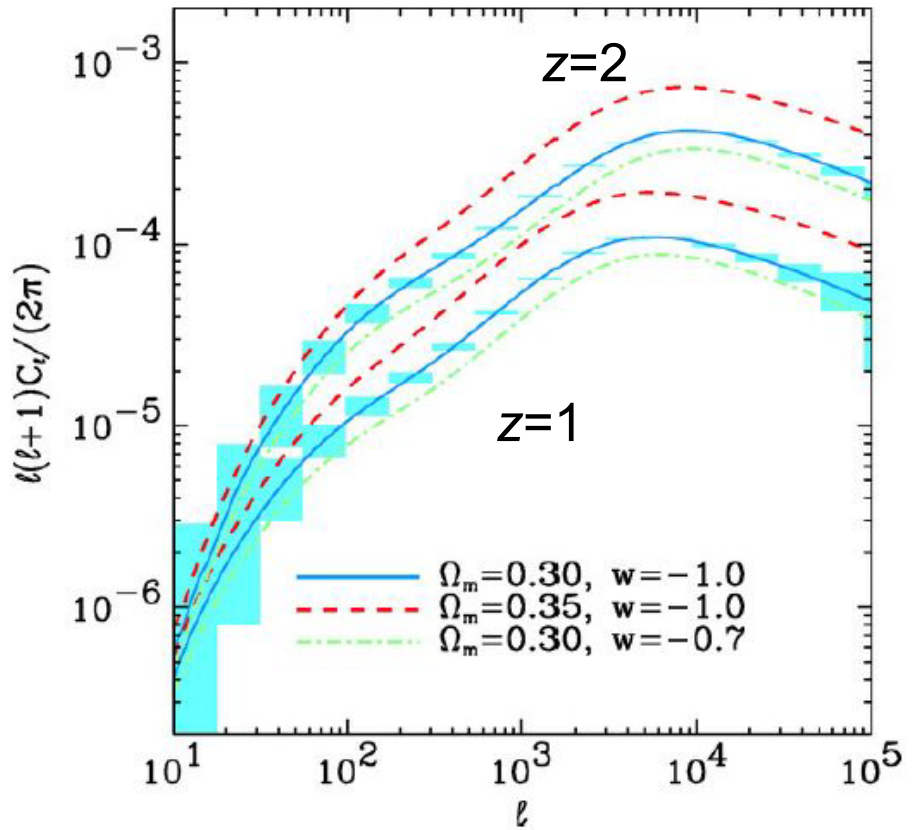
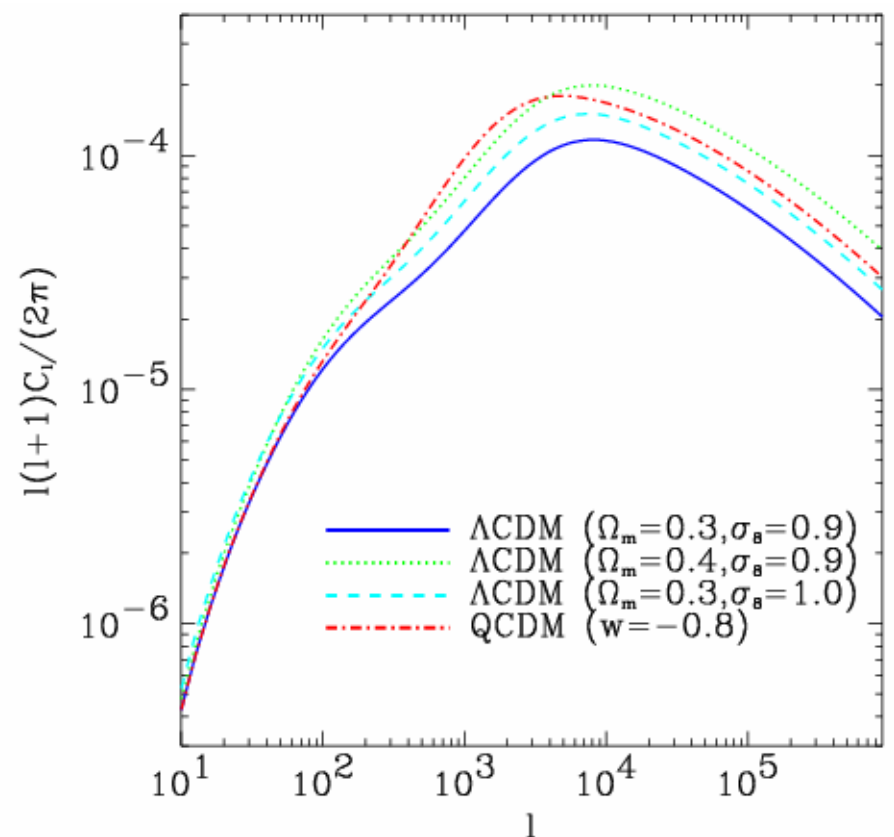
$$\kappa_{eff} = \frac{3H_0^2\Omega_0}{2c^2} \int_0^\omega \frac{f_K(\omega - \omega') f_K(\omega')}{f_K(\omega)} \frac{\delta [f_K(\omega') \theta; \omega']}{a(\omega')} d\omega'$$

Geometry                      Power spectrum,  
    growth rate of structure  $D_+$

# The Universe with Dark Energy



# Cosmic shear surveys and dark cosmological models : exploring the power spectrum



# Modeling dark energy

- Amount ?:  $\Omega_x$
- Modeling its nature :
  - equation of state :  $w$
  - theoretical dark energy model (CFHLS: see Schimdt et al 2006)
- Modeling evolution with time?

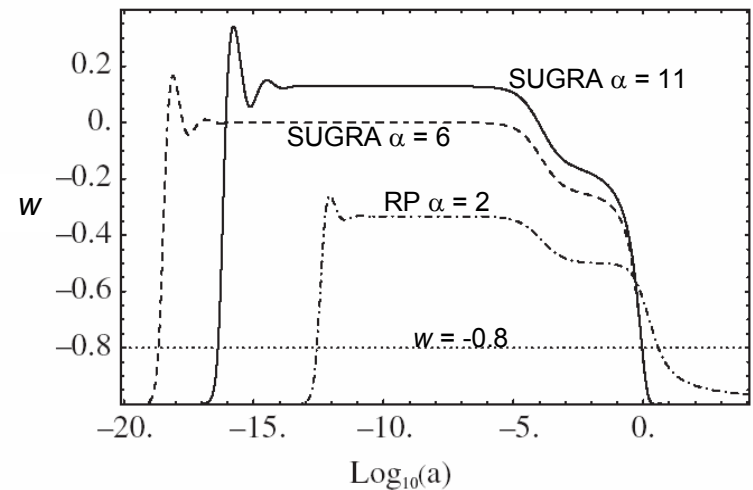
-  $w = P/\rho$  « cosmic equation of state »

- Dark energy as a scalar field with a shallow self interacting potential:  $V(\phi)$

$$V(\phi) = \frac{\Lambda^{4+\alpha}}{\phi^\alpha} \quad RP, \quad (\text{e.g. Schimd et al 2006})$$

$$V(\phi) = \frac{\Lambda^{4+\alpha}}{\phi^\alpha} \exp(4\pi G\phi^2) \quad SUGRA$$

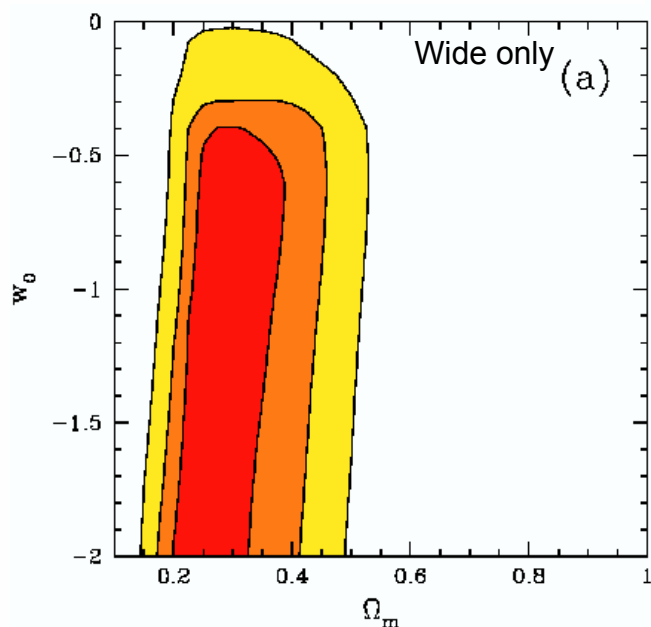
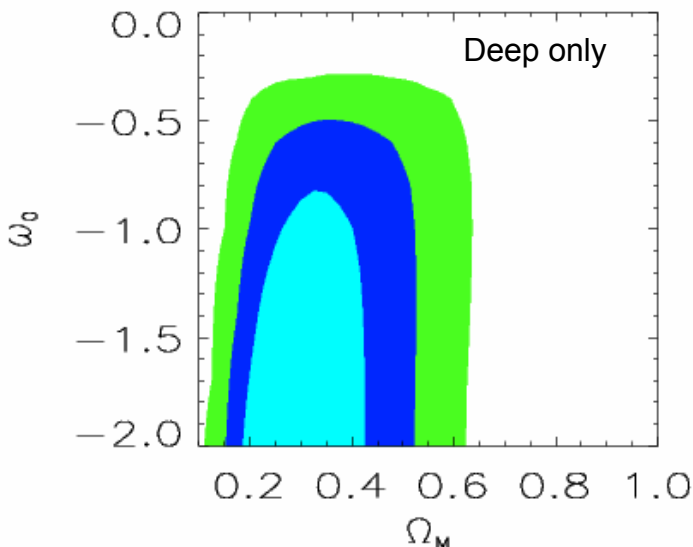
- Or a simple description:  $w = w_0 + w_1(z)$



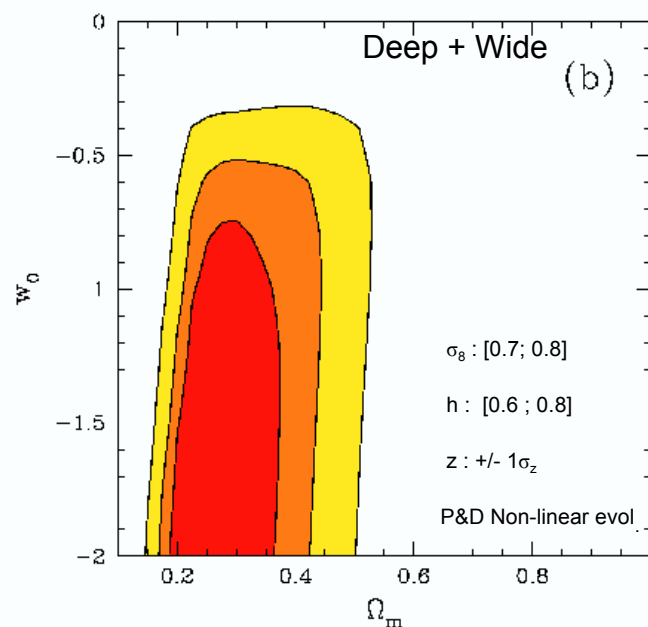
# CSLS: constraints on empirical models of Dark Energy

$$P = w_0 \rho$$

Deep + Wide :  $w_0 < -0.8$  (68%)  
 $w_0 < -0.4$  (99%)

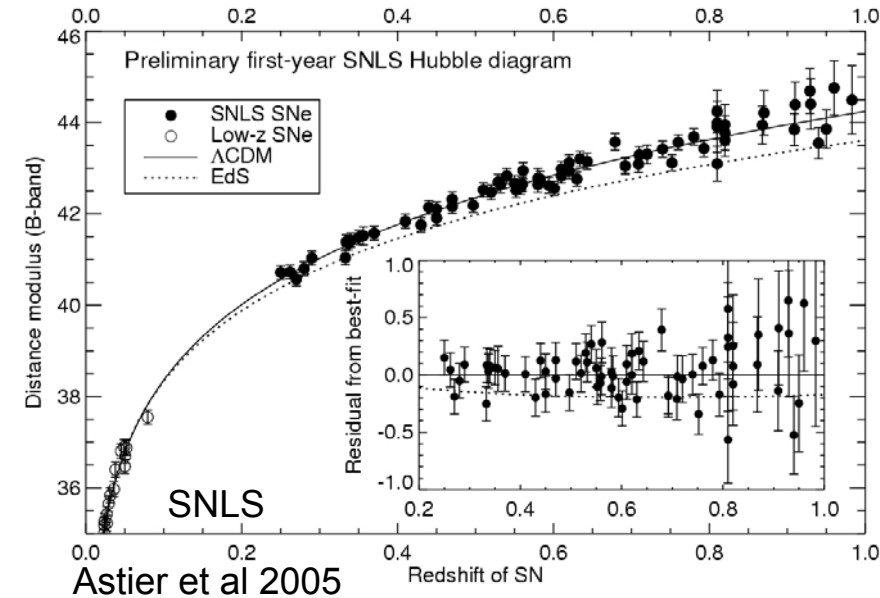


Hoekstra et al 2006 , Sembolini et al 2005



Flat universe

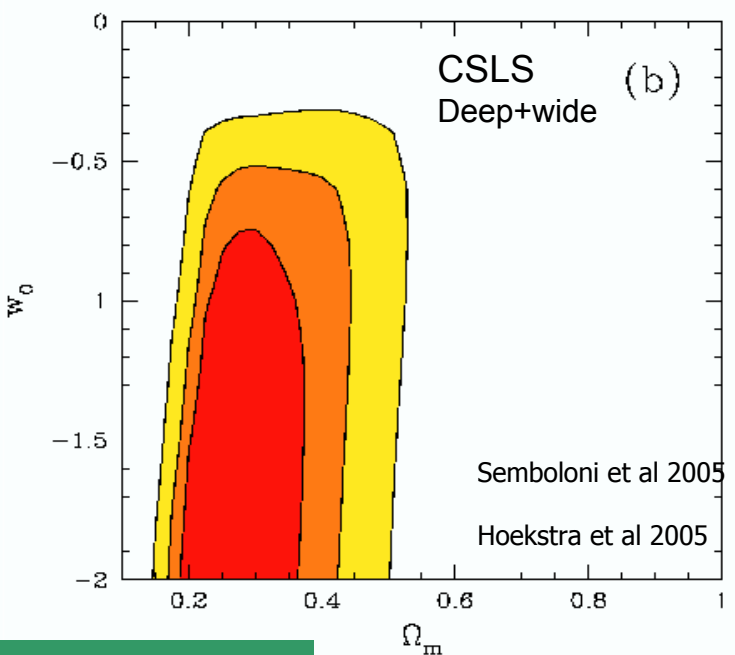
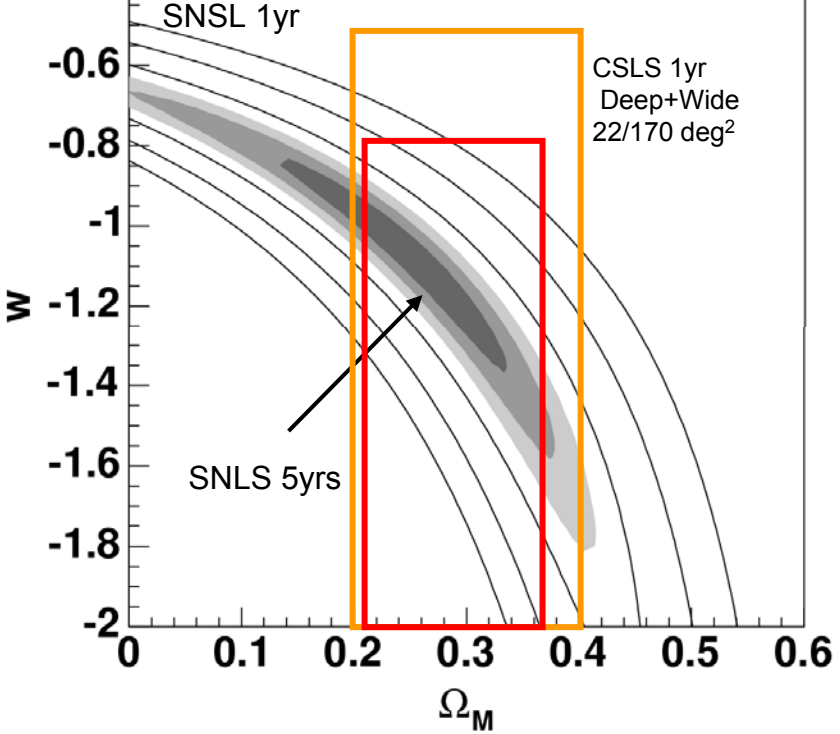
$n = 1$



# SNLS+CSLS

CSLS+SNLS

-0.4

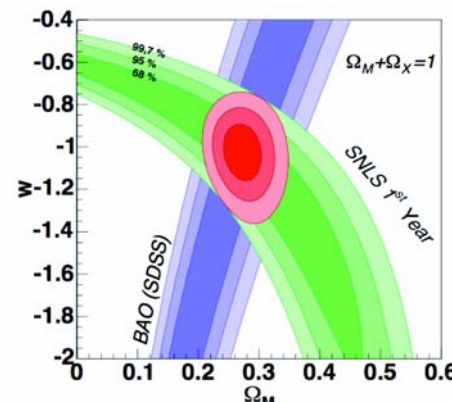
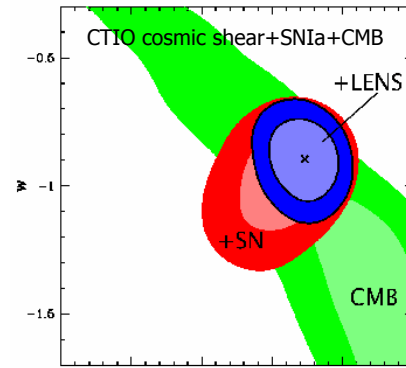
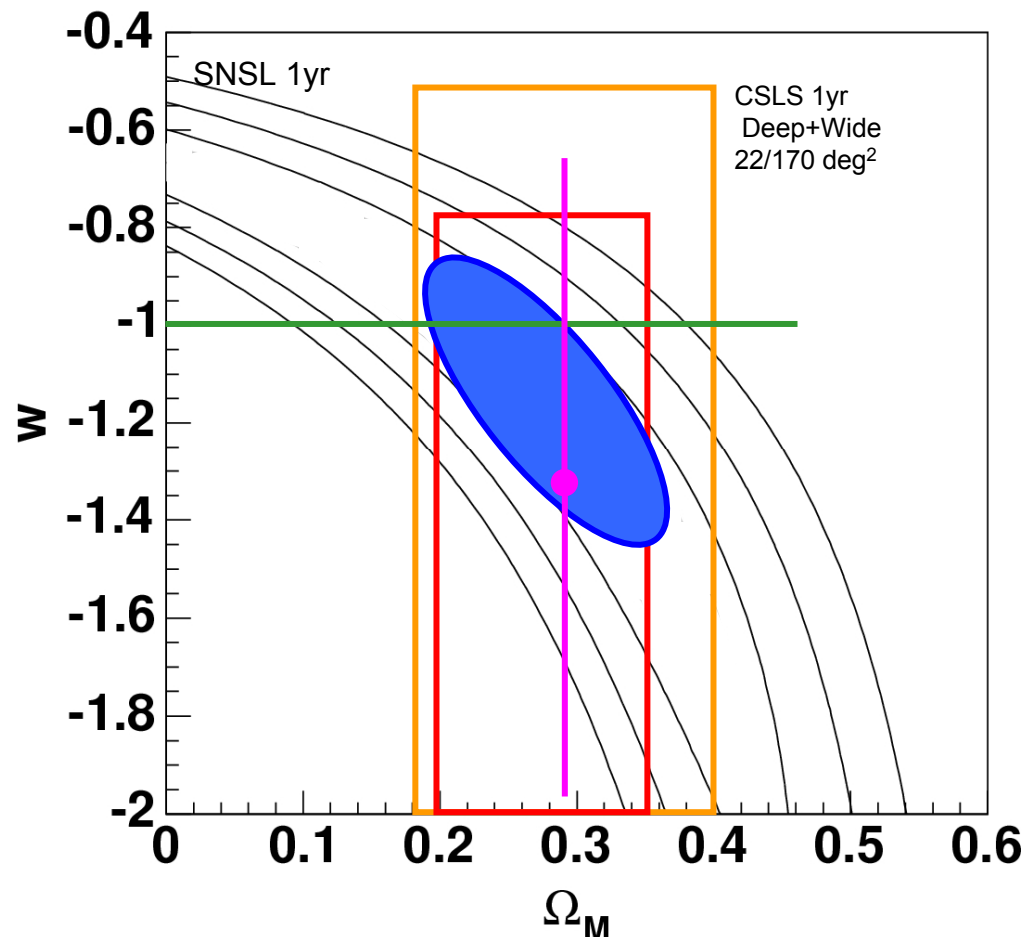


# Cosmological parameters from weak lensing surveys: present status

Survey	Telescope	Sky coverage	n gal/a min <sup>2</sup>	Mag	$\sigma_8$ ( $\Omega_m = 0.3$ )	$w_0$	Ref.
VLT-Descart	VLT	0.65 deg <sup>2</sup>	21	I <sub>AB</sub> = 24.5	1.05 ± 0.05		Maoli et al 2001
Groth Strip	HST/WFPC2	0.05 deg <sup>2</sup>	23	I=26	0.90 <sup>+0.25</sup> <sub>-0.30</sub>		Rhodes et al 2001
MDS	HST/WFPC2	0.36 deg <sup>2</sup>	23	I=27	0.94 ± 0.17		Réfrégier et al 2002
RCS	CFHT CTIO	16.4 deg <sup>2</sup> + 7.6 deg <sup>2</sup>	9	R=24	0.81 <sup>+0.14</sup> <sub>-0.19</sub>		Hoekstra et al 2002a
Virmos-Descart	CFHT	8.5 deg <sup>2</sup>	15	I <sub>AB</sub> =24.5	0.98 ± 0.06	-	van Waerbeke et al 2002
RCS	CFHT CTIO	45.4 deg <sup>2</sup> + 7.6 deg <sup>2</sup>	9	R=24	0.87 <sup>+0.09</sup> <sub>-0.12</sub>		Hoekstra et al 2002b
COMBO-17	2.2m	1.25 deg <sup>2</sup>	32	R=24.0	0.72 ± 0.09		Brown et al 2003
Keck + WHT	kECK WHT	0.6 deg <sup>2</sup> 1.0 deg <sup>2</sup>	27.5 15	R=25.8 R=23.5	0.93 ± 0.13		Bacon et al 2003
CTIO	CTIO	75 deg <sup>2</sup>	7.5	R=23	0.71 <sup>+0.06</sup> <sub>-0.08</sub>		Jarvis et al 2003
SUBARU	SUBARU	2.1 deg <sup>2</sup>	32	R=25.2	0.78 <sup>+0.55</sup> <sub>-0.25</sub>		Hamana et al 2003
COMBO-17	2.2m	1.25 deg <sup>2</sup>	R	R=24.0	0.67 ± 0.10		Heymans et al 2004
FIRST	VLA	10000 deg <sup>2</sup>	0.01	1 mJy	1.0 ± 0.2		Chang et al 2004
GEMS	HST/ ACS	0.22 deg <sup>2</sup>	60	I=27.1	0.68 ± 0.13		Heymans et al 2005
WHT + COMBO-17	WHT 2.2m	4.0 deg <sup>2</sup> + 1.25 deg <sup>2</sup>	15 32	R <sub>AB</sub> =25.8 R=24.0	1.02 ± 0.15		Massey et al 2005
Virmos-Descart	CFHT	8.5 deg <sup>2</sup>	12.5	I <sub>AB</sub> =24.5	0.83 ± 0.07	-	van Waerbeke et al 2005
CTIO	CTIO	75 deg <sup>2</sup>	7.5	R=23	0.71 <sup>+0.06</sup> <sub>-0.08</sub>	-0.89 <sup>+0.16</sup> <sub>-0.21</sub>	Jarvis et al 2006
CFHTLS Deep + Wide	CFHT	2.1 deg <sup>2</sup> + 22 deg <sup>2</sup>	22 13	i <sub>AB</sub> =25.5 i <sub>AB</sub> =24.5	0.89 ± 0.06 0.86 ± 0.05	≤ -0.80	Semboloni et al 2006 Hoekstra et al 2005
GaBoDS	2.2m	15 deg <sup>2</sup>	12.5	R=24.5	0.80 ± 0.10	-	Hetterscheidt et al 2006
ACS parallel + GEMS+GOODS	HST/STIS HST/ACS	0.018 deg <sup>2</sup> 0.027 deg <sup>2</sup>	63 96	R=27.0 ? V=27.0	0.52 <sup>+0.13</sup> <sub>-0.17</sub>		Schrabback et al 2006

# $W = -1$ ?

CSLS+SNLS +COMBO-17



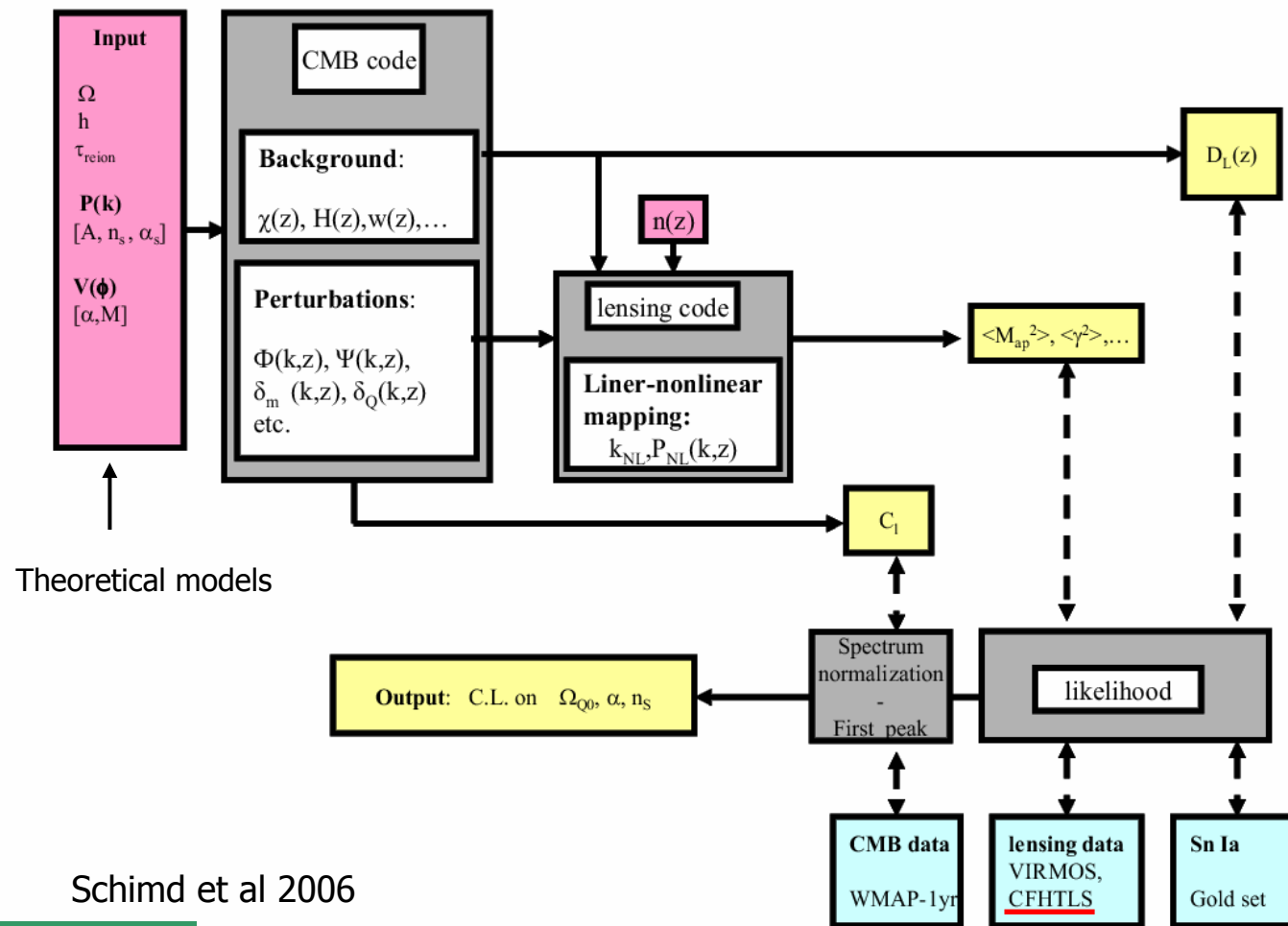
# Exploring physical models of dark energy with CFHTLS cosmic shear data: quintessence models

- Physical models:
  - Less general than the « empirical » and more conservative  $P=wp$ , but can challenge physical models to data
  - Can explore evolution with redshift. Avoid pivot redshift problems on joint data or in case  $w(z)$  evolved at high  $z$
  - Can be used in a coherent model with description of the evolution of perturbations and CMB data (normalisation , no use of  $\sigma_8$  )

PB: non linear evolution unknown for these models:

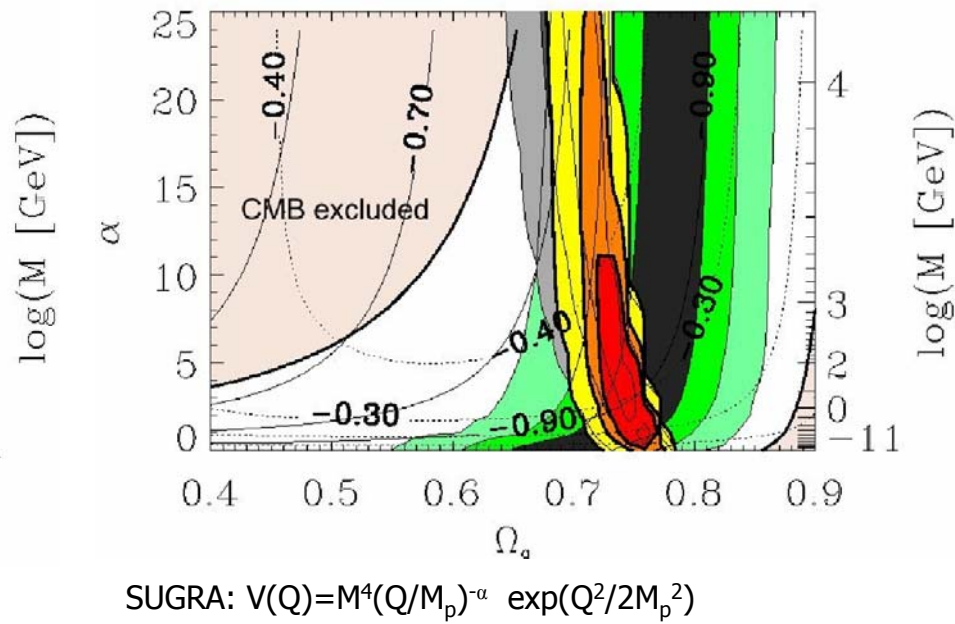
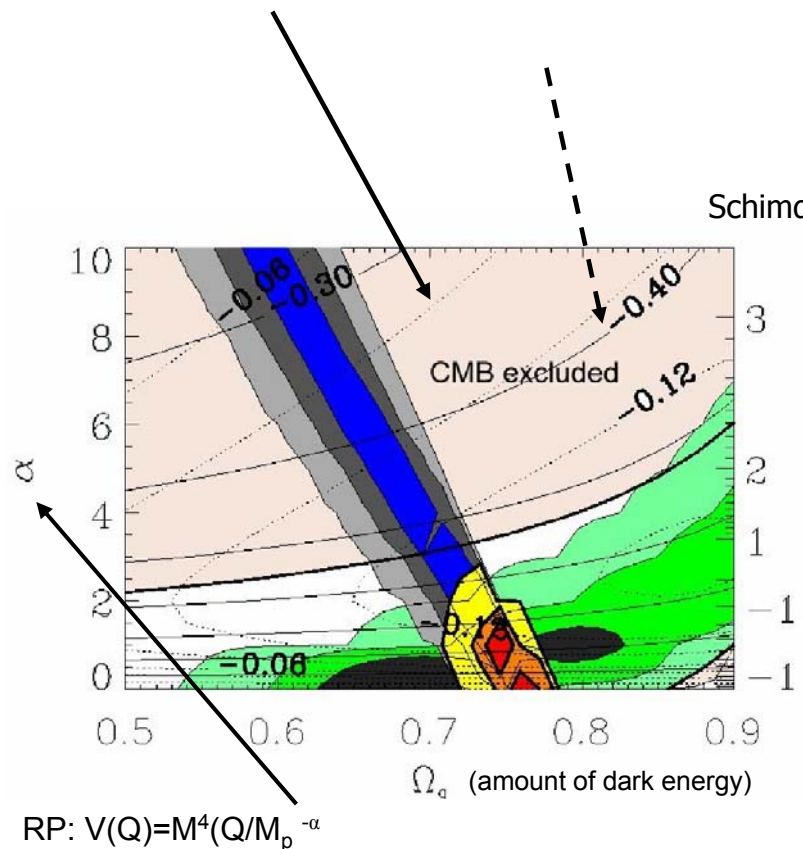
Peacock & Dodds and Halo models used

# Cosmology with physical Dark Energy models



Schimd et al 2006

# Exploring quintessence models



Ratra-Peebles

SUGRA

Cosmic shear Deep+Wide + SNIa gold set + WMAP-1

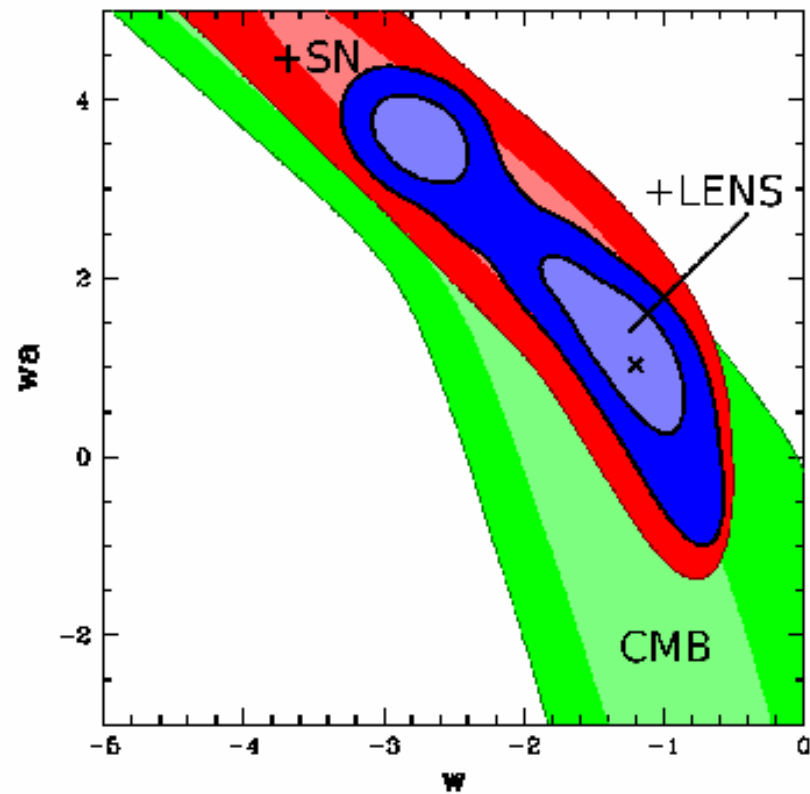
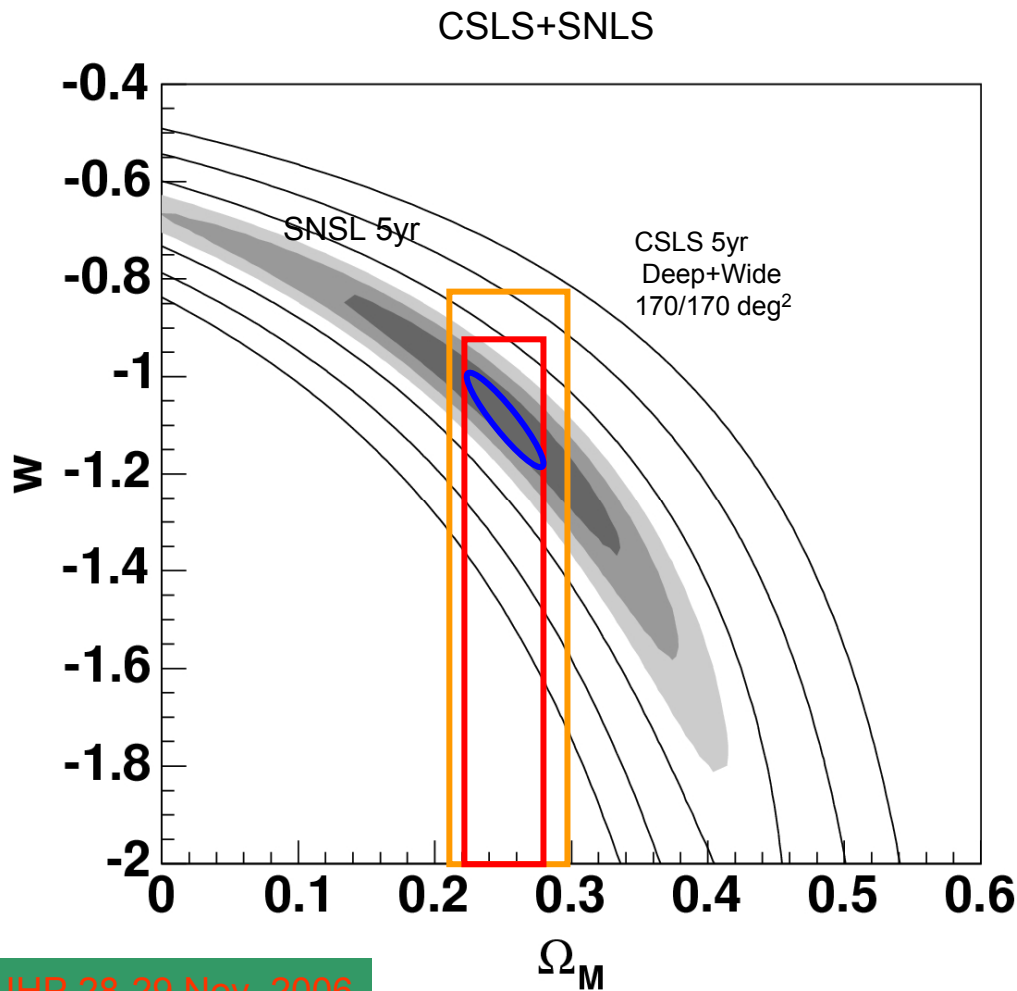
... not sure ...

This is not the end of the story

- Previous plots: assume  $w$  is constant
- Still missing precision to get a detailed description of dark energy properties
- Still concerns with systematics

# Synergy CFHTLS: SNLS+CSLS

5 years (expectations): still far from getting  $w_a$



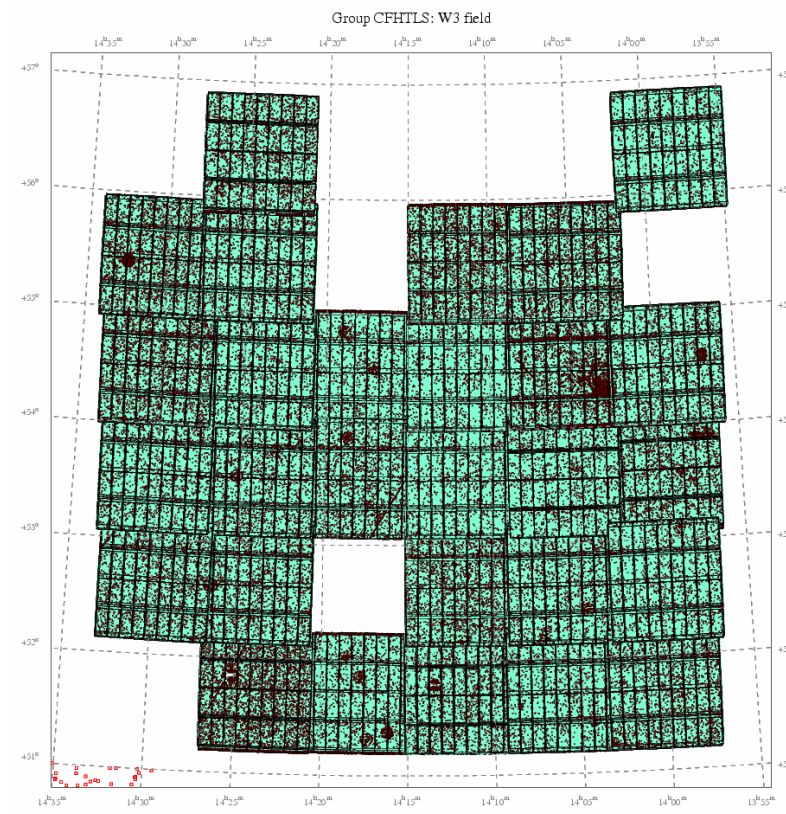
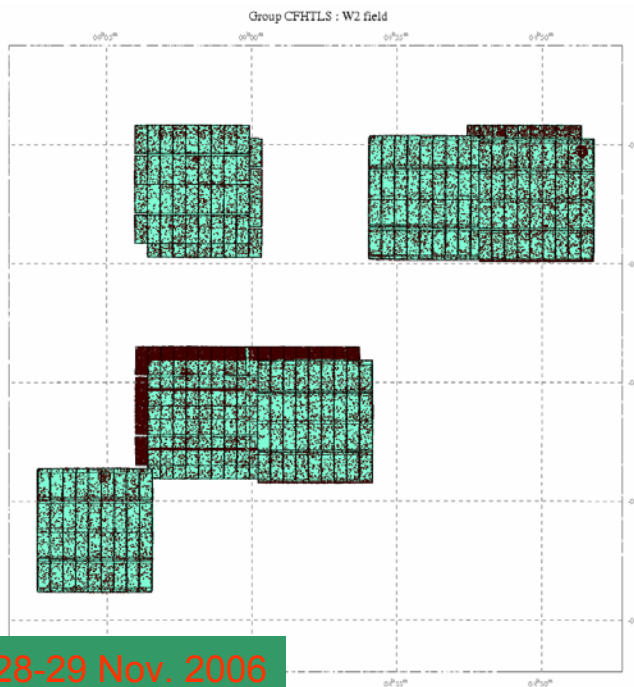
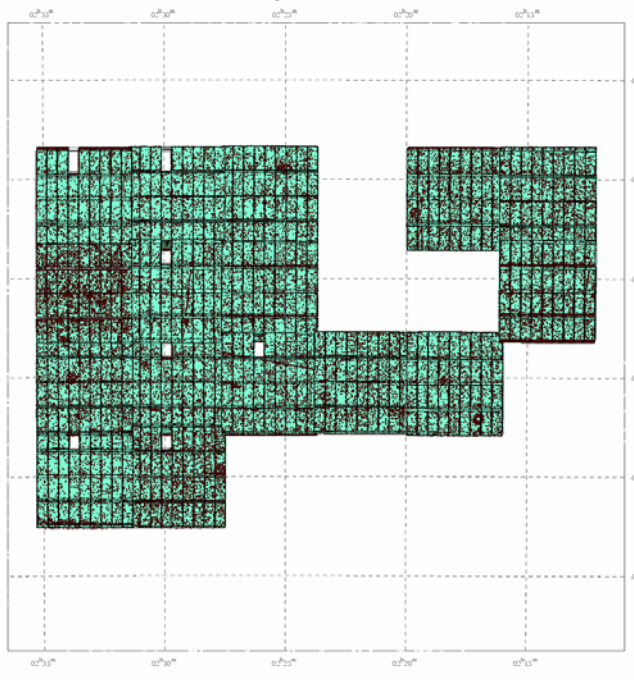
Jarvis, Jain, Bernstein, Dolney 2005

# What next ?

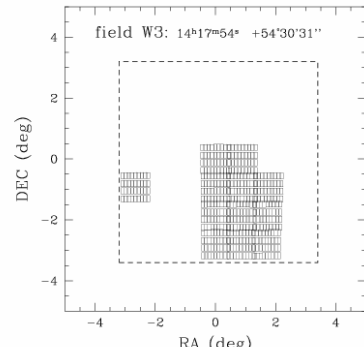
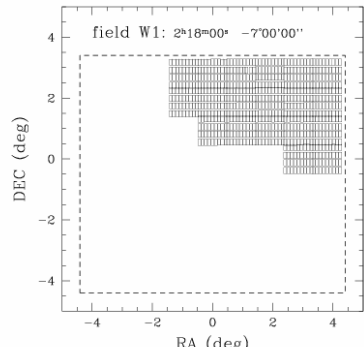
## Beyond 1 deg. angular scale:

- far beyond non-linear scales
- CFHTLS Wide field-to-field calibration
- Need to have an excellent wide field corrector for the image quality.

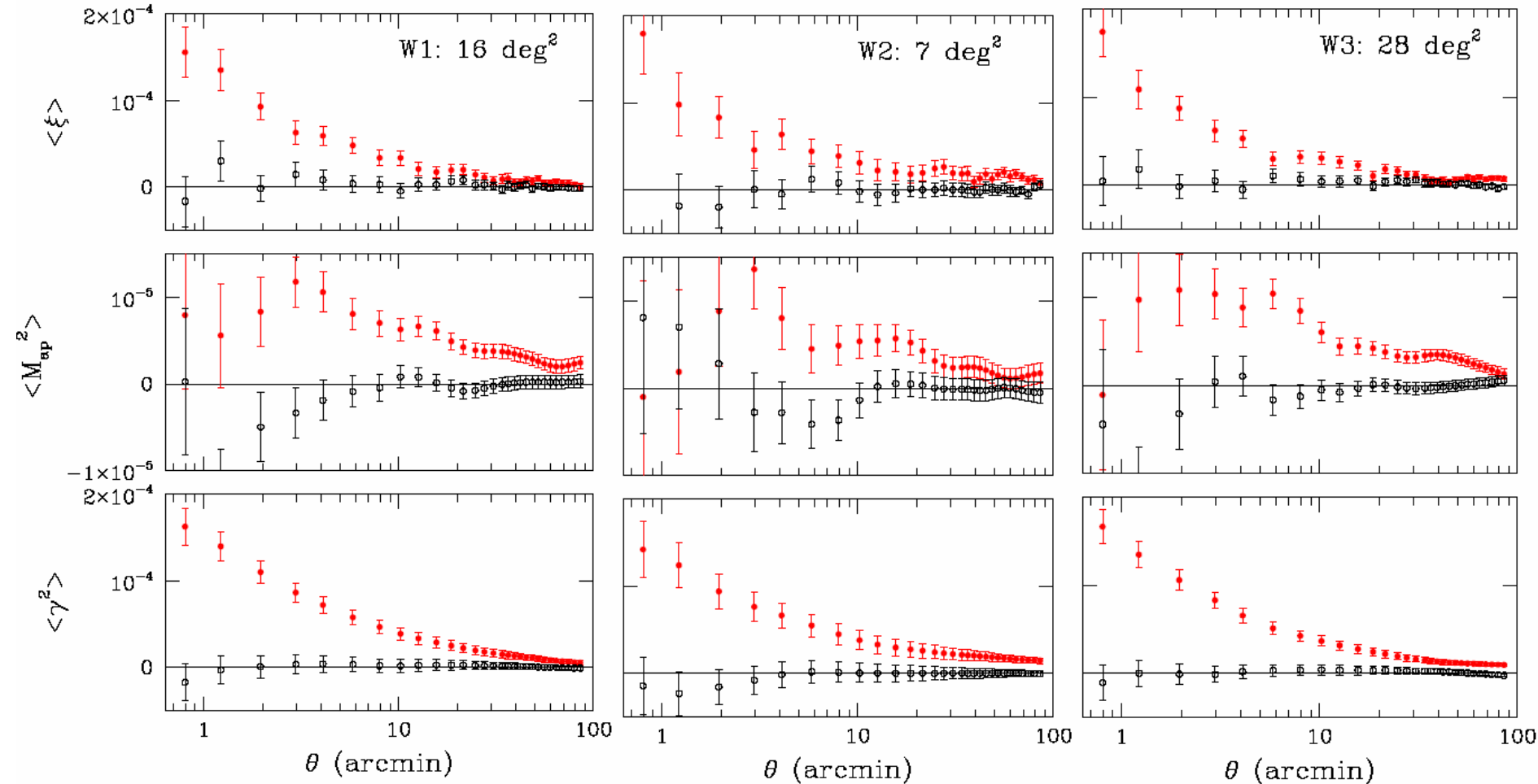
# CFHTLS CSLS second step



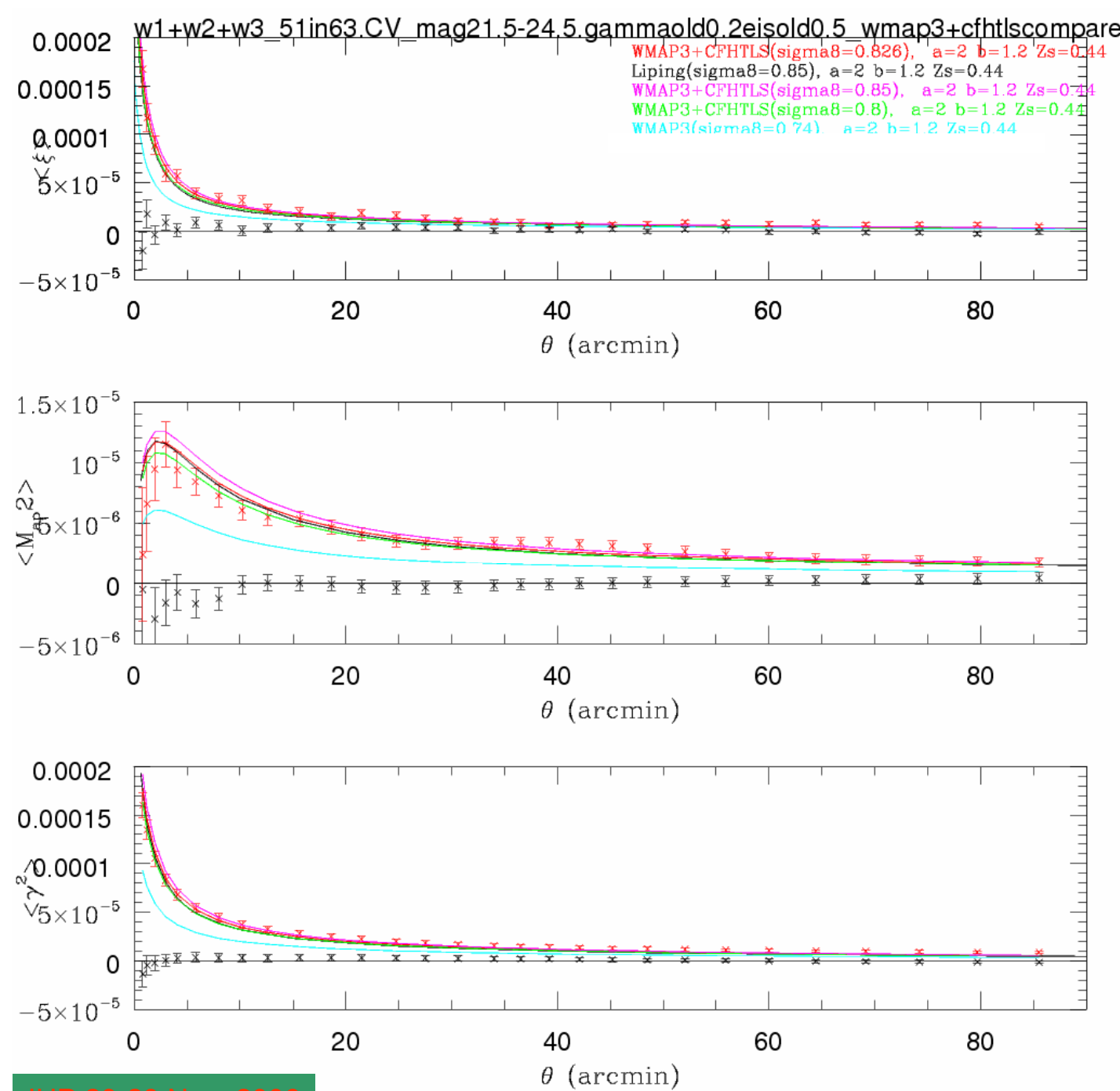
2005 data



# W1, W2, W3 (T0003): consistency



Fu et al 2006



Beyond 1 degree scale.

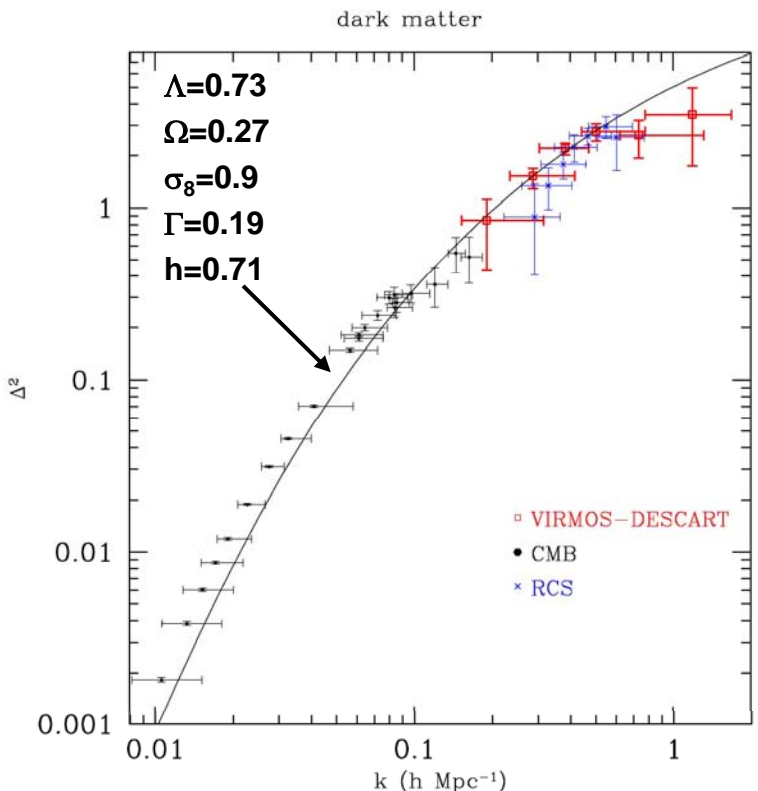
Cosmological interpretation of CFHTLS data less and less sensitive to non-linear structures

Fu et al (CSLS team) 2006

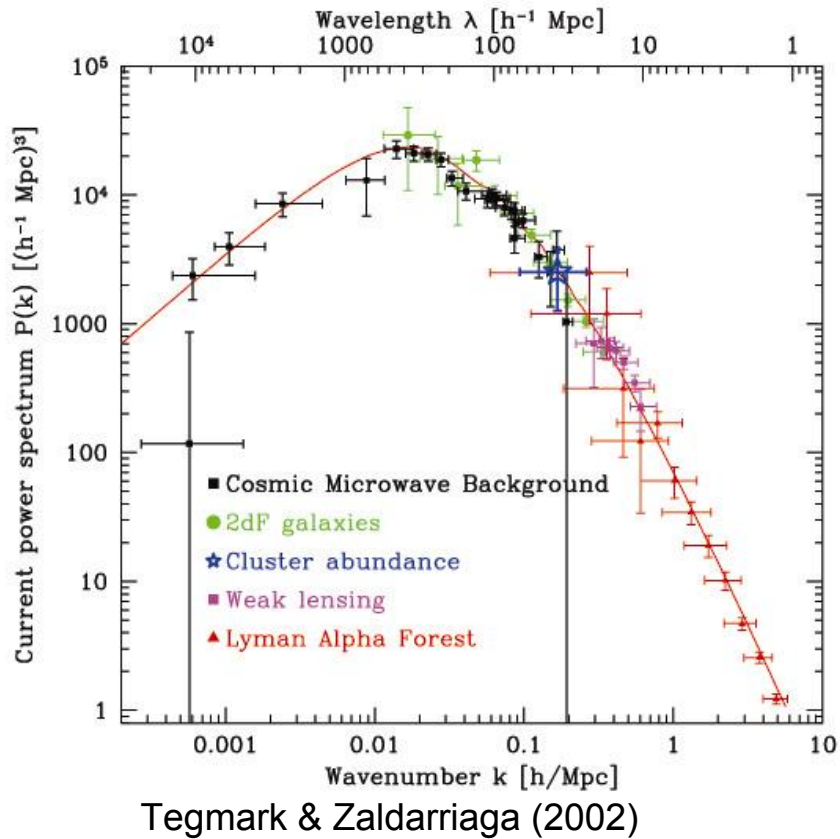
# CFHTLS cosmic shear: on-going or not done yet

- Photo-z for the full Wide survey
- 2-D/3-D power spectrum reconstruction
- Mass reconstruction and projected dark matter maps of the CFHTLS fields
- Real 3-D tomography
- Decoupling geometry and power spectrum
- Galaxy (light)-Mass-Map cross correlation: biasing
- Galaxy-galaxy lensing (Parker et al 2006)
- Exploring  $w(z)$

# 3D dark matter reconstruction



Pen, Lu, van Waerbeke, Mellier 2003

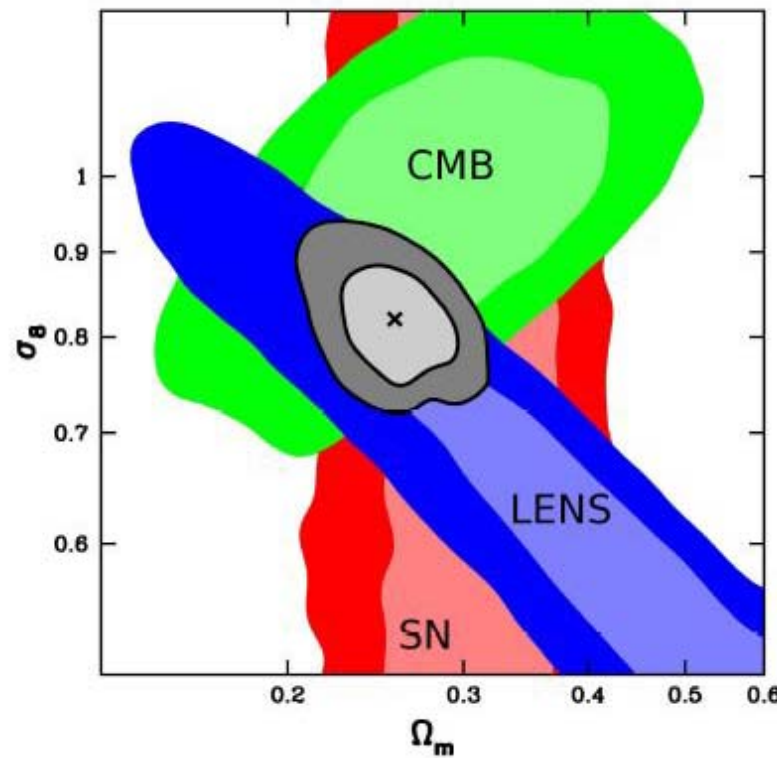


Still in a early phase, but

- Very promising for next generation surveys
- Evolution with photo-z +spectro-z likely feasible

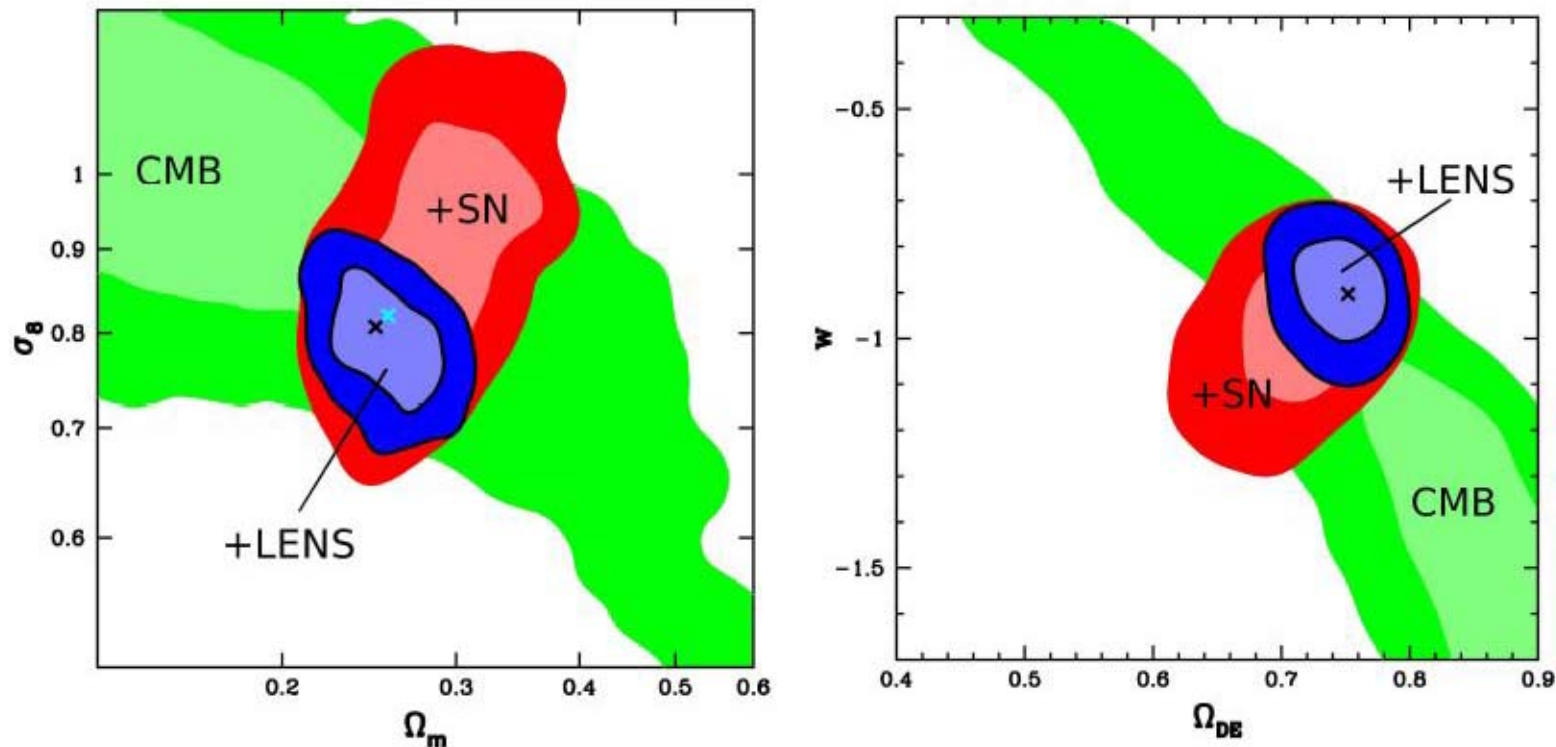
(see also, Heavens 2003, Taylor et al 2003)

# Joint Analysis



Assumed:  $w=-1$

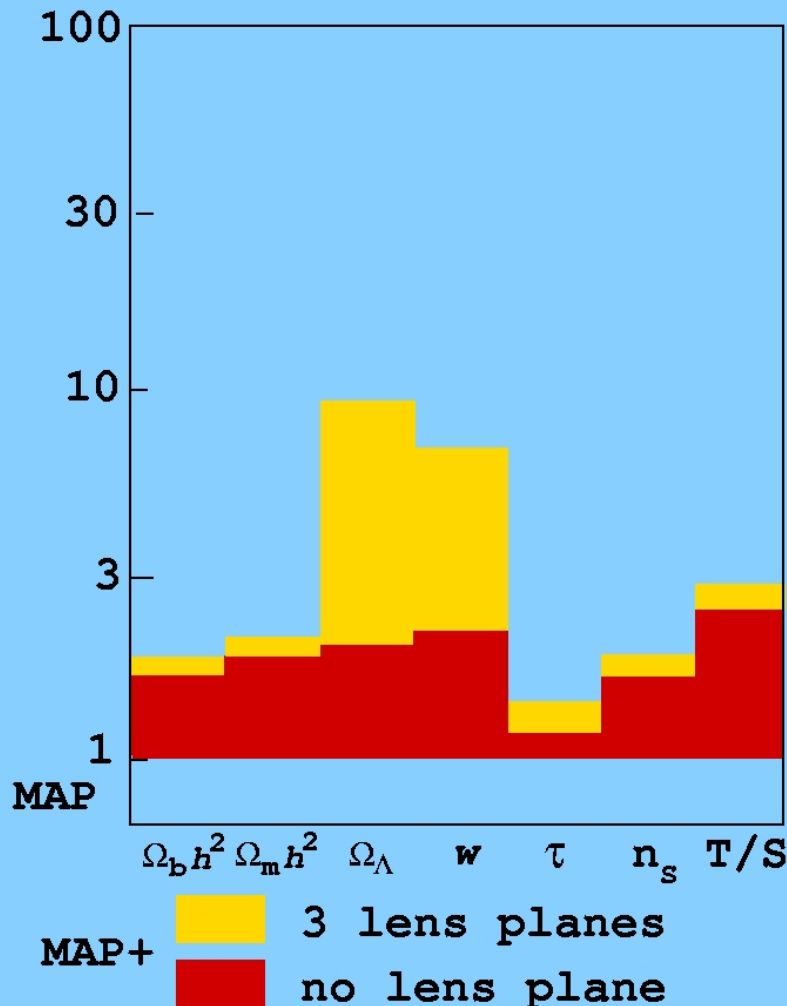
# Joint Analysis



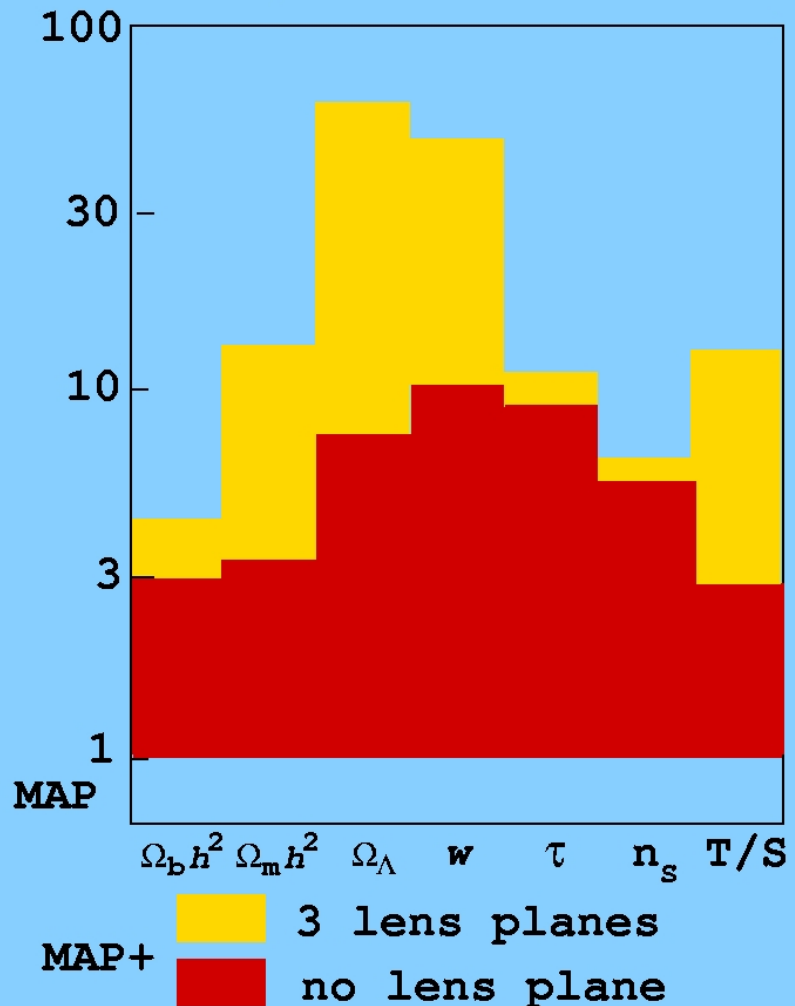
w free

# Breaking degeneracies with tomography

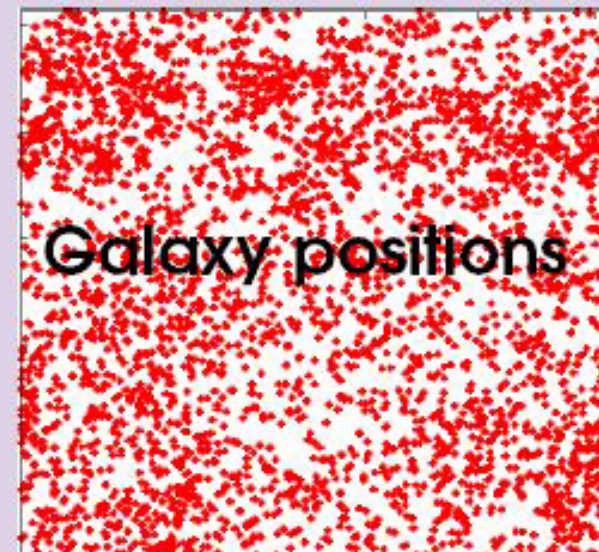
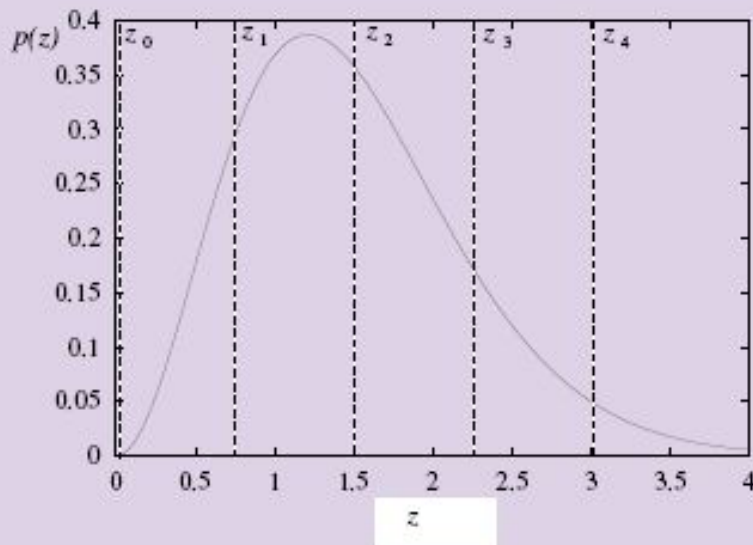
Error improvement :  $25 \text{ deg}^2$



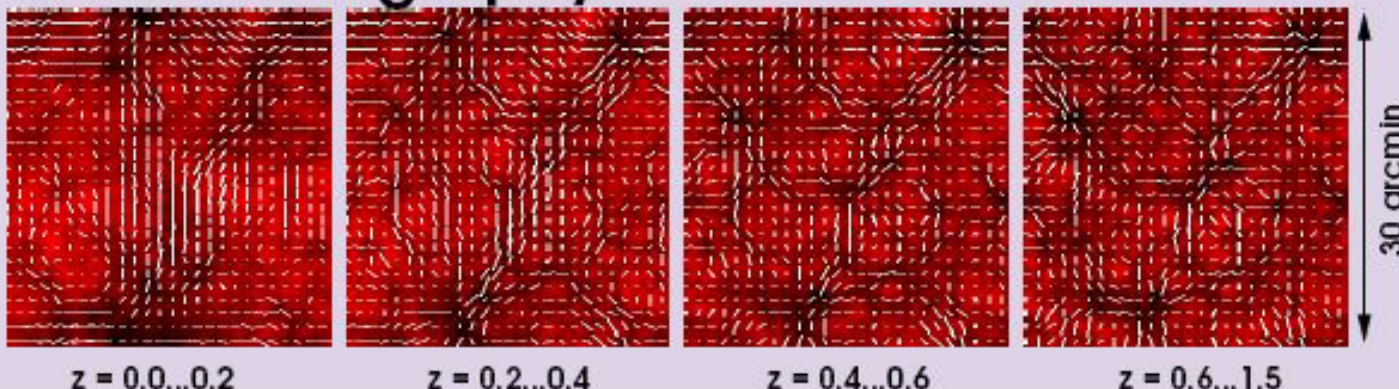
Error improvement :  $1000 \text{ deg}^2$



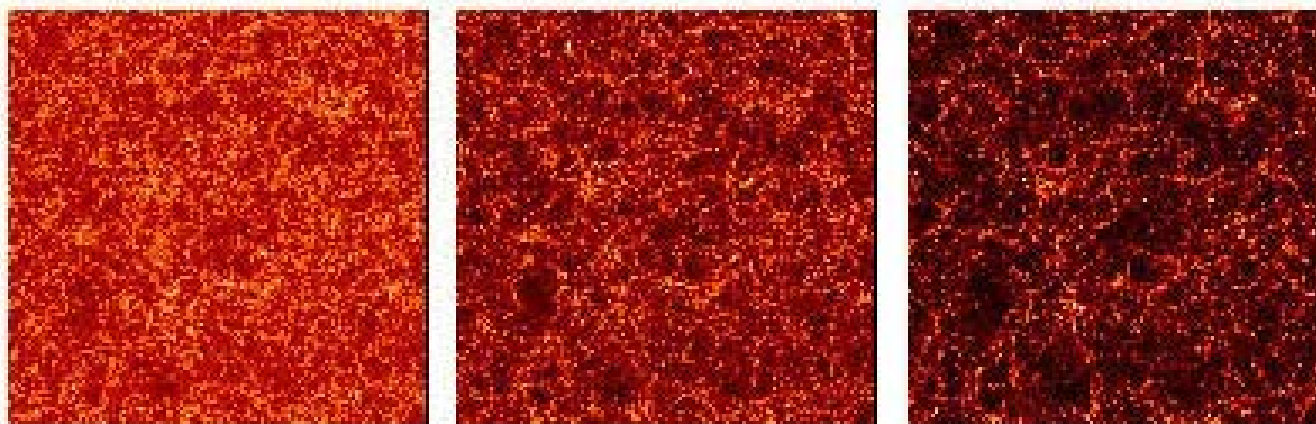
# Tomography:



**Shear tomography**

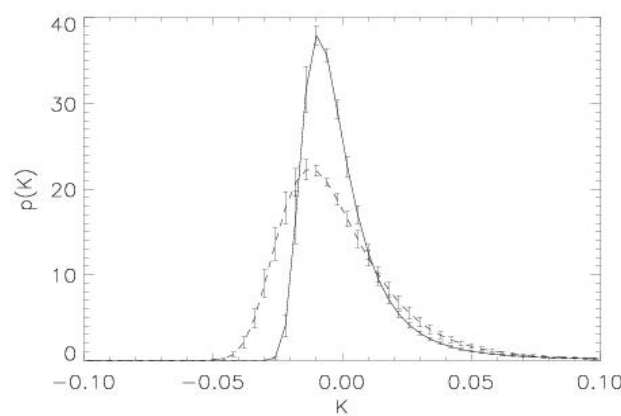


# $\Omega_m$ - $\sigma_8$ degeneracy with higher order statistics: Skewness of the convergence



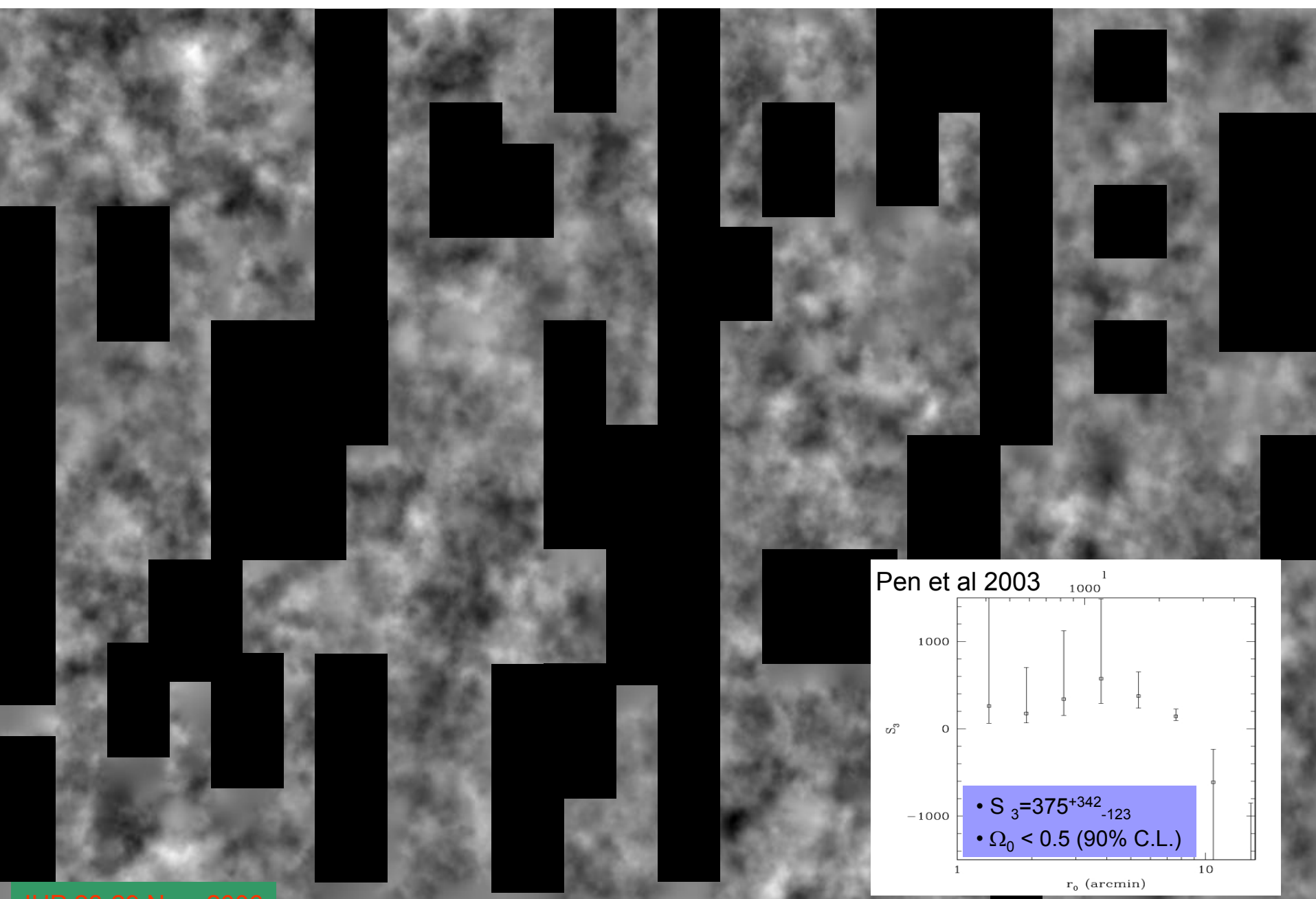
Assuming a single lens-plane and  $P(k) \propto k^n$ :

- $\langle \kappa^2(\theta) \rangle^{1/2} \approx 0.01 \sigma_8 \Omega^{0.8} \left( \frac{\theta}{1\text{deg.}} \right)^{-\frac{n+2}{2}} z_s^{0.75}$
- $\langle \kappa^2(\theta) \rangle = \langle \gamma^2(\theta) \rangle$
- $S_3(\kappa) \approx 40 \Omega^{-0.8} z_s^{-1.35}$  Jain & Seljak 1997  
Bernardeau, van Waerbeke, Mellier 1997,  
Need mass maps for skewness



- Distribution increasingly skewed by gravity that will produce non-linear structures (clusters, groups, galaxies):
- $S_3(\kappa)$  will provide a statistical description of these non-linear systems

# MASS MAP Skewness of the convergence measured in VIRIMOS-Descart data

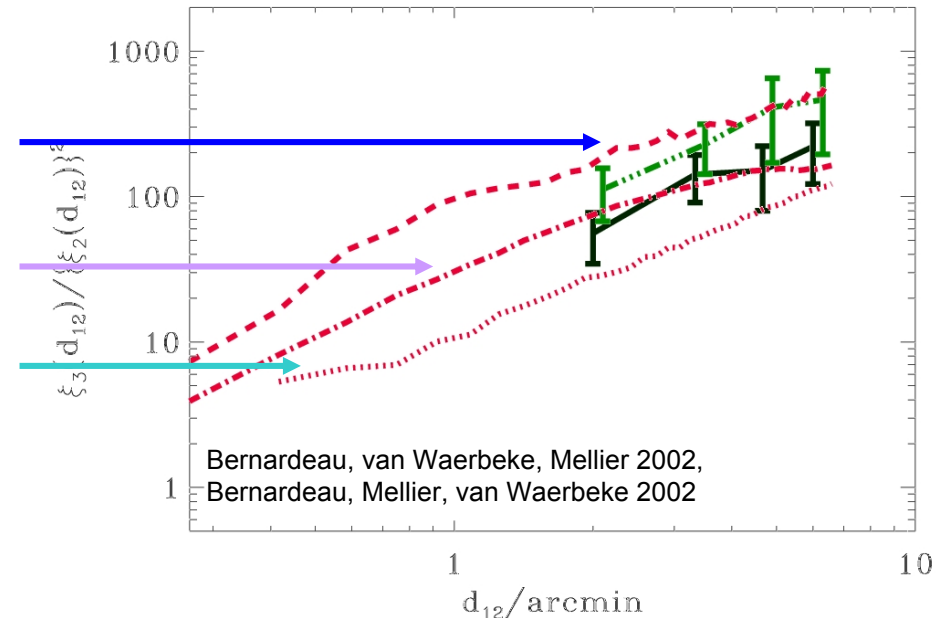


# High-order statistics: Probing non-Gaussian signatures

**OCDM:**  $\Omega_m=0.3; \Lambda=0.0; \sigma_8=0.85; H_0=70$

**$\Lambda$ CDM:**  $\Omega_m=0.3; \Lambda=0.7; \sigma_8=0.85; H_0=70$

**$\tau$ CDM:**  $\Omega_m=1.0; \Lambda=0.0; \sigma_8=0.6; H_0=50.$

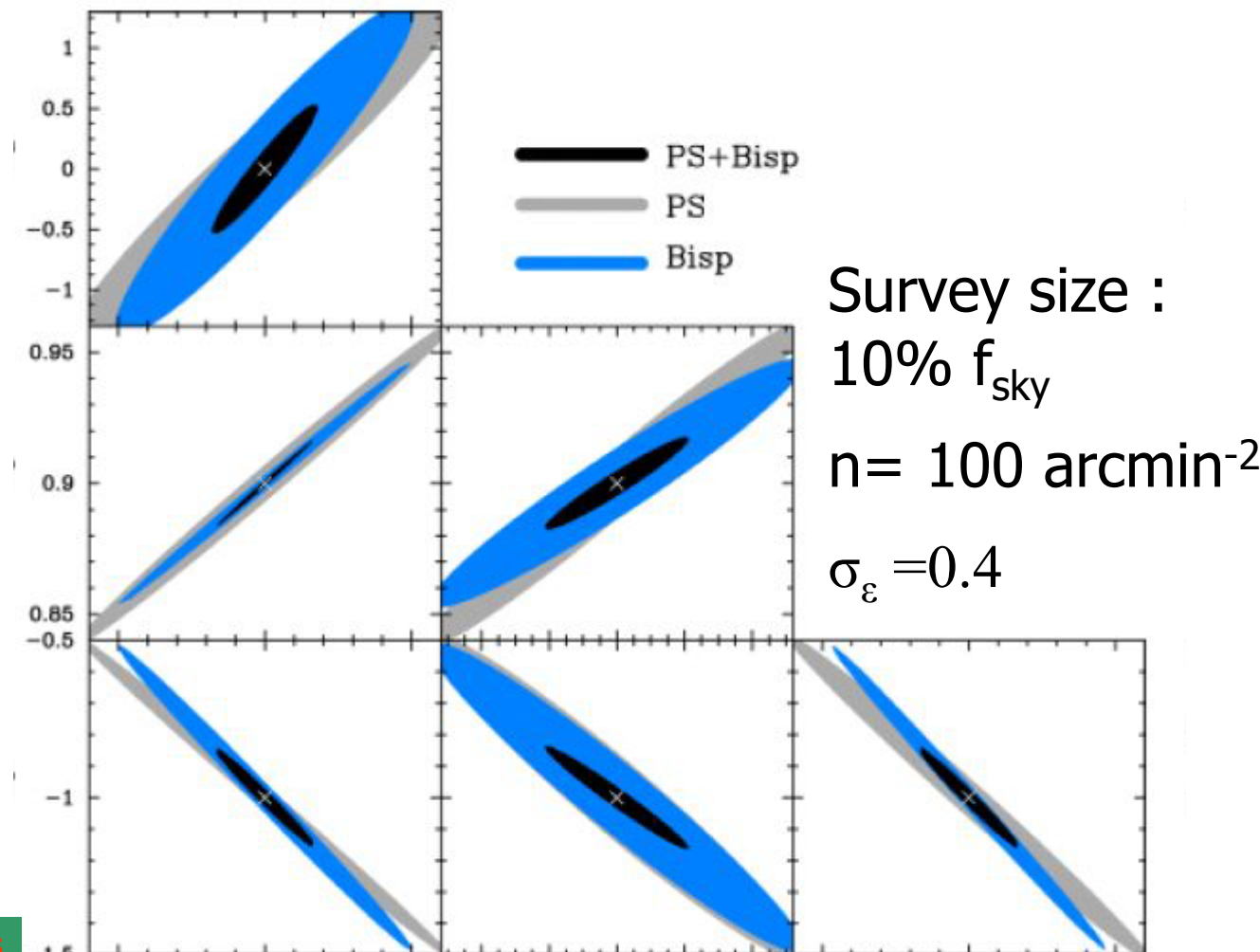


- At least: confirm the signal is of cosmological nature with CDM + gravitational instability model
- But still too noisy to separate cosmological models
- Need to get E/B modes

Alternative ?

- kurtosis? (Takada & Jain 2002)
- Skewness of  $M_{ap}$ ? (Schneider et al 1998)
- 3PCF of the shear field

# Using high-order statistics and 2 redshift bins



# Decoupling geometry and power spectrum:

$$\kappa_{eff} = \frac{3H_0^2\Omega_0}{2c^2} \int_0^\omega \frac{f_K(\omega - \omega') f_K(\omega')}{f_K(\omega)} \frac{\delta [f_K(\omega') \theta; \omega']}{a(\omega')} d\omega'$$

Distances

Power spectrum,  
growth rate of structure

The diagram illustrates the decoupling of geometry and the power spectrum. It shows the integral expression for the effective deflection angle  $\kappa_{eff}$ . The term  $f_K(\omega - \omega') f_K(\omega') / f_K(\omega)$  is highlighted with a red oval and labeled "Distances", representing the geometric part. The term  $\delta [f_K(\omega') \theta; \omega'] / a(\omega')$  is highlighted with a green oval and labeled "Power spectrum, growth rate of structure", representing the physical part.

# Decoupling geometry and power spectrum

$$P_{g\gamma}(\ell; f, b) = \frac{3\Omega_{m0}H_0^2}{2c^2} \int \frac{d\chi_f}{a(\chi_f)} W_f(\chi_f) \int d\chi_b W_b(\chi_b) \\ \times \frac{\chi_b - \chi_f}{\chi_b \chi_f} P_{ff}(\frac{\ell}{\chi_f}, \chi_f) \Theta(\chi_b - \chi_f)$$

$$P_{\gamma\gamma}(\ell; f, b) = \left( \frac{3\Omega_{m0}H_0^2}{2c^2} \right)^2 \\ \times \int d\chi_f W_f(\chi_f) \int d\chi_b W_b(\chi_b) \\ \times \int \frac{d\chi}{a(\chi)^2} \frac{\chi_b - \chi}{\chi_b} \frac{\chi_f - \chi}{\chi_f} P_{ff}(\frac{\ell}{\chi}, \chi) \Theta(\chi_b - \chi) \Theta(\chi_f - \chi).$$

$f$ = foreground ;  $b$ =background

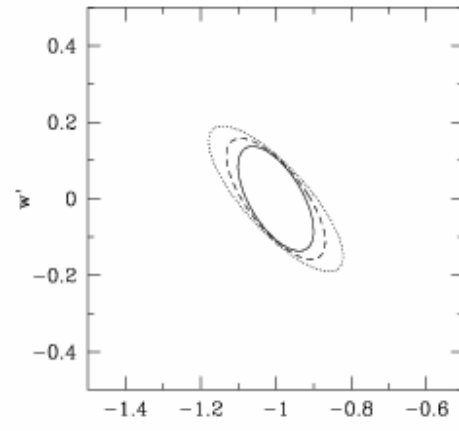
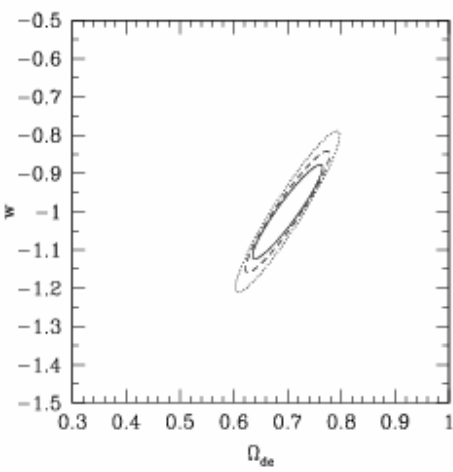
If overlap between the 2 population is small:

$$P_{g\gamma}(\ell; f, b) \approx F(\ell; f) + G(\ell; f)/\chi_{\text{eff}}(b)$$

$$P_{\gamma\gamma}(\ell; f, b) \approx A(\ell; f) + B(\ell; f)/\chi_{\text{eff}}(b)$$

Scaling of lensing signal independent of the power spectrum but only depends on geometry

$$\frac{P(\ell; f, b) - P(\ell; f, b')}{P(\ell; f, b'') - P(\ell; f, b''')} = \frac{\chi_{\text{eff}}(b)^{-1} - \chi_{\text{eff}}(b')^{-1}}{\chi_{\text{eff}}(b'')^{-1} - \chi_{\text{eff}}(b''')^{-1}}$$



Need at least 3 source planes

Zhang, Hui, Stebbins 2003:  
4000 deg<sup>2</sup>  
Error on photo-z: 0.01, 0.02, 0.05

# Next Generation Cosmic Shear Surveys

Goal: dark energy properties known to 5%-1% (50%-20% today)

Larger field of view

Multiple lens planes (tomography)

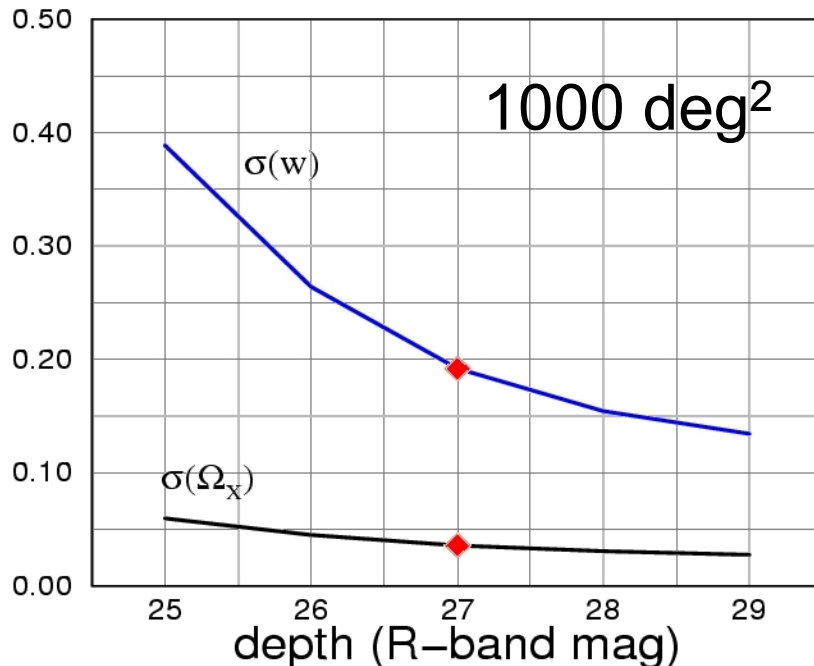
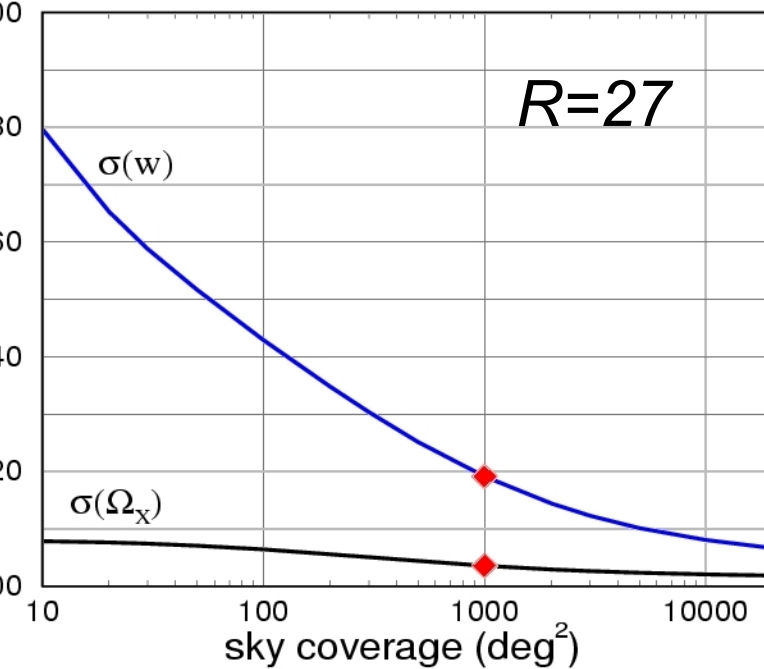
Accurate 3D positions of lensed galaxies and lenses

Better accuracy on galaxy shape measurements

# Future Progress

KIDS + CFHTLS Wide + CFHTLS Deep: 3 lens planes

Survey	Sq. Degrees	Filters	Depth	Dates	Status
CTIO	75	1	shallow		published
VIRMOS	9	1	moderate		published
COSMOS	2 (space)	1	moderate		complete
DLS (NOAO)	36	4	deep		complete
Subaru	30?	1?	deep	2005?	observing
CFH Legacy	170	5	moderate	2004-2008	observing
RCS2 (CFH)	830	3	shallow	2005-2007	approved
VST/KIDS/ VISTA/VIKING	1700	4+5	moderate	2007-2010?	50% approved
DES (NOAO)	5000	4	moderate	2008-2012?	proposed
Pan-STARRS	~10,000?	5?	moderate	2006-2012?	~funded
LSST	15,000?	5?	deep	2010-2020?	proposed
JDEM/SNAP	1000+ (space)	9	deep	2013-2018?	proposed
VST/VISTA	5000?	4+5	moderate	2010-2015?	proposed
DUNE	20000? (space)	2+1?	moderate	2012-2015?	proposed

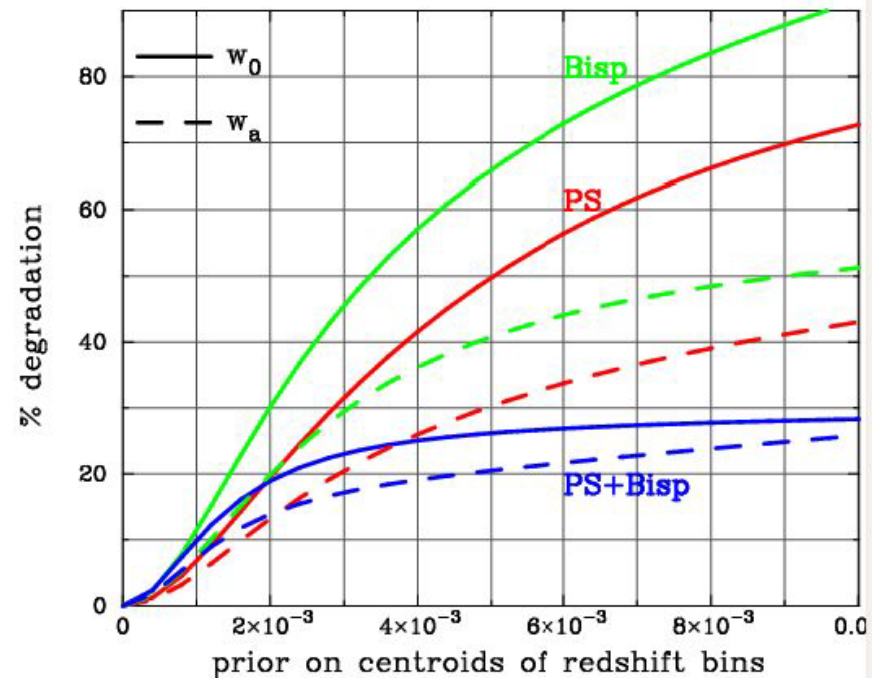
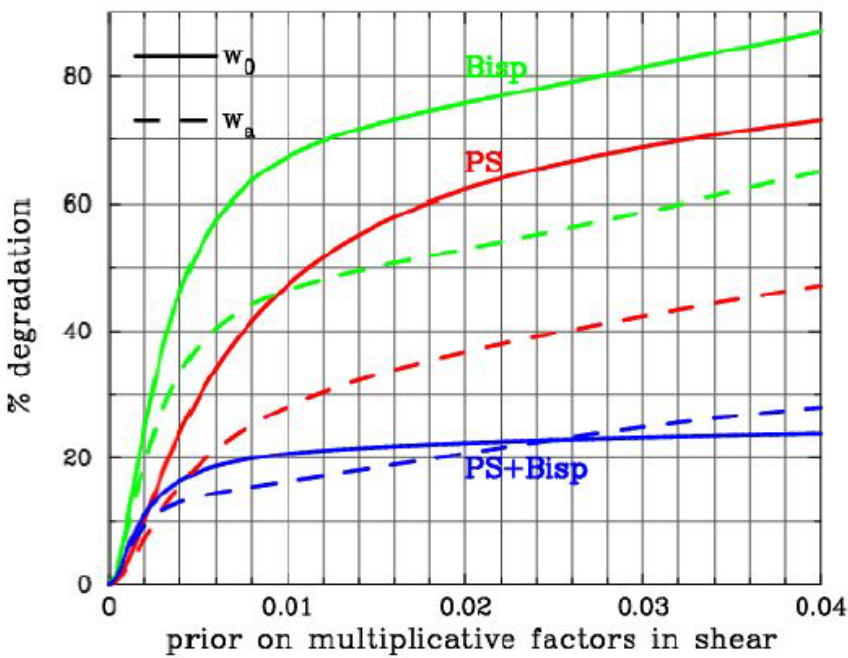


## Sky coverage and depth (Assuming NO lens planes)

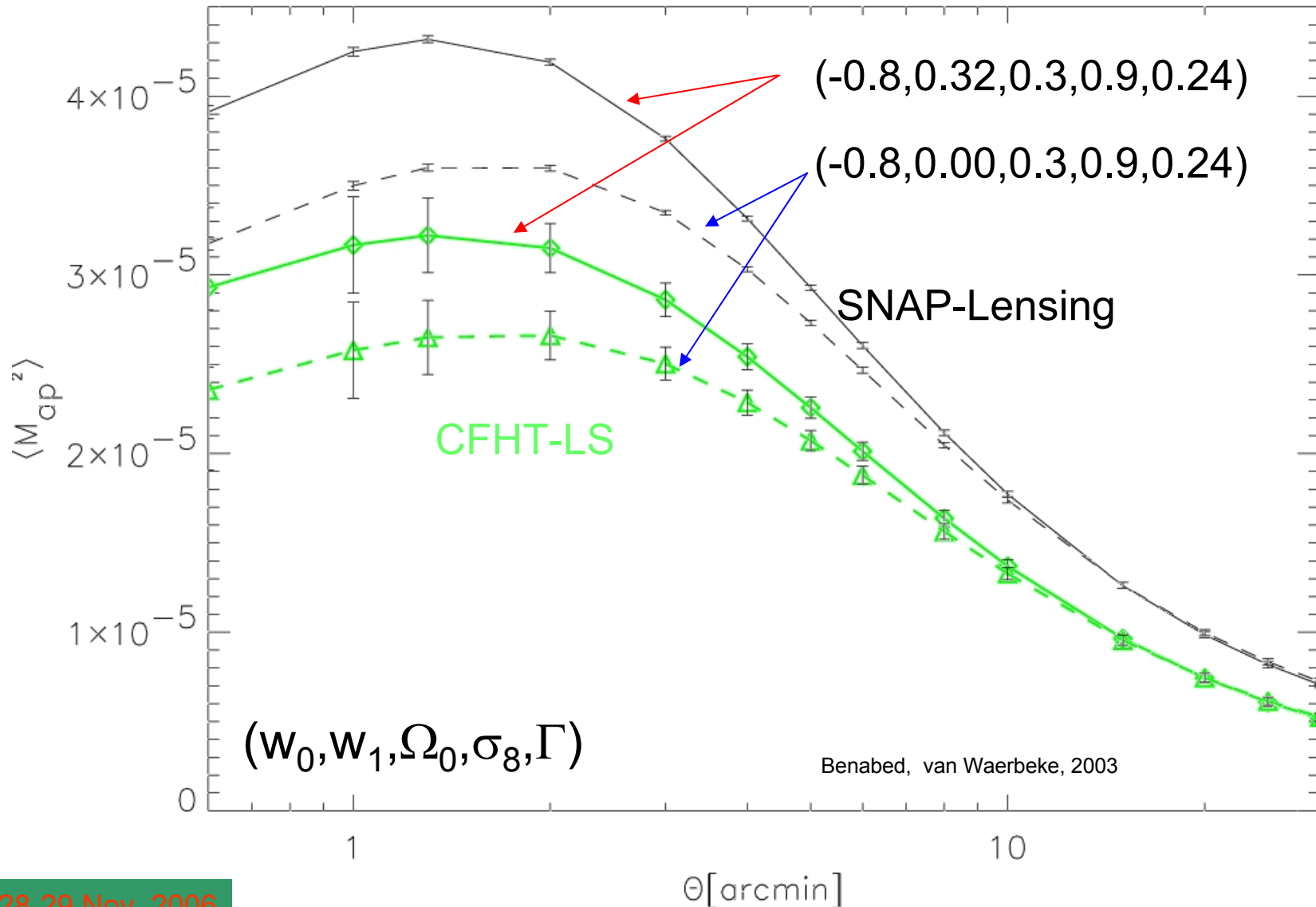
Gains:

- A factor of 2 on  $\sigma(w)$  from 100 to 1000 deg $^2$
- Another factor of 2 from 1000 to 5000 deg $^2$
- A factor of 2 on  $\sigma(\Omega_x)$  from 100 to 1000 deg $^2$ ; few beyond.
- A factor of 2 on  $\sigma(w)$  from  $R=25$  (present survey) to  $R=27$ ; few beyond.

# Sensitivity to critical parameters: shear calibration and z-calibration



# $M_{ap}$ for CFHT-LS and SNAP-Lensing



## Baseline:

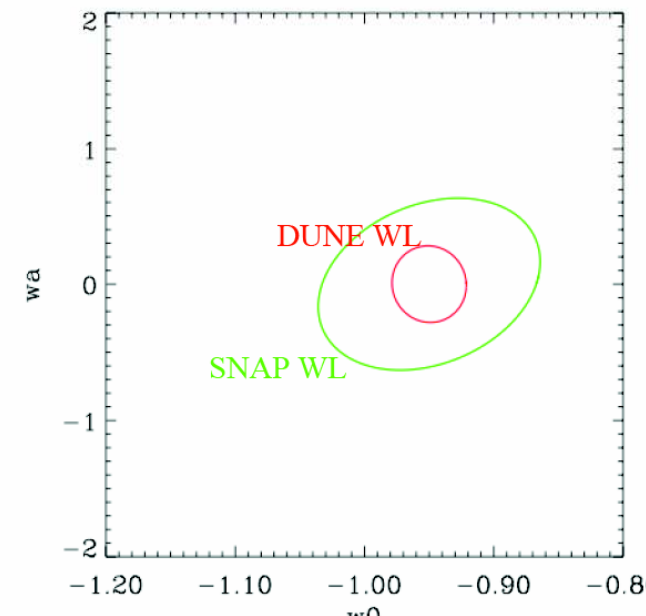
- 1.2m telescope
- FOV 0.5 deg<sup>2</sup>
- WL survey: 20000 deg<sup>2</sup> in 1 red broad band, 35 galaxies/amin<sup>2</sup> with median z~1, ground based follow-up for photo-z's
- SNe survey: 2×60 deg<sup>2</sup>, observed for 9 months each every 4 days in 6 bands, 10000 SNe out to z~1
- launch target: 2012

Unique synergy  
Space+Ground:

Need ground based  
follow up  
DarkCam+VISTA is an  
option

ESA proposal: study  
phase for a 1.5m + vei  
red/NIR filters added

dapnia  
cea



By Amara et al.

Dark energy evolution:  $w(a)=w_0+(a_n-a)w_a$ ,  $a_n=0.6$  assume a flat universe

# DUNE

## Dark UNiverse Explorer

PI: Réfréaier

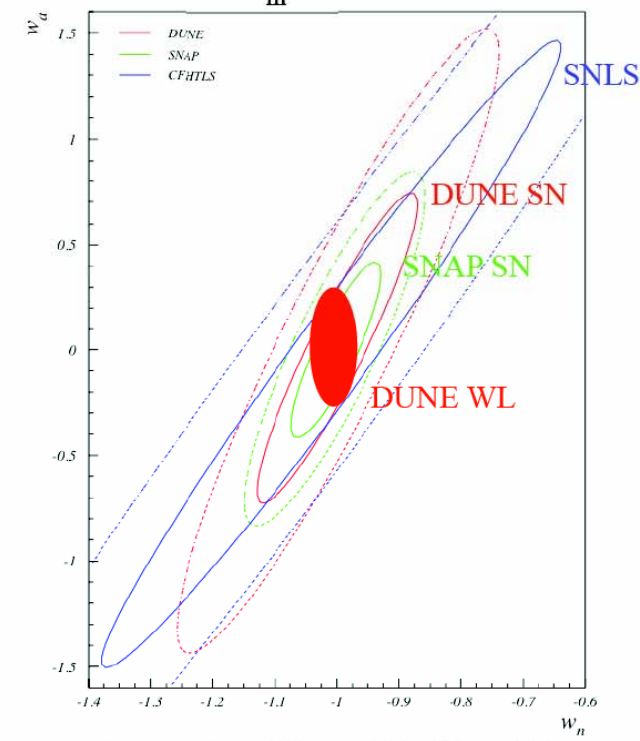


### Constraints on Dark Energy (II)

#### Weak Lensing:

- C<sub>l</sub> measurement in 3 z-bins
- Photo-z errors of Δz=0.1
- No priors

- Supernovae:  
Prior:  $\Delta\Omega_m=0.03$



By Pain, Kroely, Astier, Antilogus , Barrelet et al.

# The ultimate step ?

